ISSN 2217-8139 (Print)
ISSN 2334-0229 (Online)

UDK: 06.055.2:62-03+620.1+624.001.5(497.1)=861

DIMK

2017.
GODINA
LX

GRAĐEVINSKI MATERIJALI I KONSTRUKCIJE

2

BUILDING MATERIALS AND STRUCTURES

ČASOPIS ZA ISTRAŽIVANJA U OBLASTI MATERIJALA I KONSTRUKCIJA
JOURNAL FOR RESEARCH OF MATERIALS AND STRUCTURES

DRUŠTVO ZA ISPITIVANJE I ISTRAŽIVANJE MATERIJALA I KONSTRUKCIJA SRBIJE
SOCIETY FOR MATERIALS AND STRUCTURES TESTING OF SERBIA

DRUŠTVO ZA ISPITIVANJE I ISTRAŽIVANJE MATERIJALA I KONSTRUKCIJA SRBIJE
SOCIETY FOR MATERIALS AND STRUCTURES TESTING OF SERBIA

GRAĐEVINSKI MATERIJALI I KONSTRUKCIJE

BUILDING MATERIALS AND STRUCTURES

ČASOPIS ZA ISTRAŽIVANJA U OBLASTI MATERIJALA I KONSTRUKCIJA
JOURNAL FOR RESEARCH IN THE FIELD OF MATERIALS AND STRUCTURES

PUBLISHER

Society for Materials and Structures Testing of Serbia, 11000 Belgrade, Kneza Milosa 9
Telephone: 381 11/3242-589; e-mail:dimk@ptt.rs, veb sajt: www.dimk.rs

REVIEWERS: All papers were reviewed

KORICE: Postavka ispitivanja za određivanje prigušenja udarnog opterećenja
COVER: Test arrangement for determination of attenuation of impact loads

Financial supports: Mnistry of Scientific and Technological Development of the Republic of Serbia

ISSN 2217-8139 (Print)
ISSN 2334-0229 (Online)

GODINA LX - 2017.

DRUŠTVO ZA ISPITIVANJE I ISTRAŽIVANJE MATERIJALA I KONSTRUKCIJA SRBIJE
SOCIETY FOR MATERIALS AND STRUCTURES TESTING OF SERBIA

GRAĐEVINSKI MATERIJALI I KONSTRUKCIJE

BUILDING MATERIALS AND STRUCTURES

ČASOPIS ZA ISTRAŽIVANJA U OBLASTI MATERIJALA I KONSTRUKCIJA
JOURNAL FOR RESEARCH IN THE FIELD OF MATERIALS AND STRUCTURES

SADRŽAJ

CIP - Каталогизација у публикацији
Народна библиотека Србије, Београд

620.1

GRAĐEVINSKI materijali i konstrukcije : časopis za istraživanja u oblasti materijala i konstrukcija = Building Materials and Structures : journal for research of materials and structures / editor-in-chief Radomir Folić. - God. 54, br. 1 (2011)- - Beograd (Kneza Miloša 9) : Društvo za ispitivanje i istraživanje materijala i konstrukcija Srbije, 2011- (Novi Beograd : Hektor print). - 30 cm

Tromesečno. - Je nastavak: Materijali i konstrukcije = ISSN 0543-0798
ISSN 2217-8139 = Građevinski materijali i konstrukcije
COBISS.SR-ID 188695820

CONTENTS

COMPARATIVE ANALYSIS OF THE INFLUENCE OF CREEP OF CONCRETE COMPOSITE BEAMS OF STEEL - CONCRETE MODEL BASED ON VOLTERRA INTEGRAL EQUATION

KOMPARATIVNA ANALIZA UTICAJA TEČENJA BETONA SPREGNUTE GREDE ČELIK – BETON MODELIMA ZASNOVANIM NA INTEGRALNOJ JEDNAČINI VOLTERRA

Doncho PARTOV
Vesselin KANTCHEV

ORIGINALNI NAUČNI RAD
ORIGINAL SCIENTIFIC PAPER
UDK: 624.044:539.42
doi:10.5937/grmk1702003P

INTRODUCTION

Steel-concrete composite beams are widely spread form of construction in both buildings and bridges, (Cosenza and Zandonini 1999; Dujmović, Androić, and Lukačević, 2015; Folić and Zenuvović 2009; Johnson 2004; Oehlers and Bradford 1999; Vayas and Iliopoulos 2014, Wang 2002). The time-varying behaviour of composite steel-concrete members under sustained service loads drawn the attention of engineers who were dealing with the problems of their design more than 60 years. Creep has a considerable impact upon the performance of composite beams, causing increased deflection as well as affecting stress distribution. Creep in concrete represents dimensional change in the material under the influence of sustained loading. Failure to include creep effects in the analysis of the composite steel-concrete beams may lead to excessive deformation and cause significant redistribution of stress between concrete plate and steel beam. In general, time-dependent deformation of concrete regarding creep phenomena may severely affect the serviceability, durability and stability of structures. Creep analysis of composite structures is normally performed on the basis of the linear theory of viscoelasticity for aging materials.

A large number of practical problems concerning the influence of creep effect on the reliability and durability of concrete and composite structures can be solved exactly through four fundamental theorems of this theory, as demonstrated by (Chiorino et al. 2010). These compact formulations are particularly suitable for codes and technical guidance documents (CEN 2004a, CEN 2004b), and helpful in the global assessment of creep induced structural effect in the preliminary design stages, as well as in the control of the output of the detailed numerical investigations and safety checks.

In this paper we try to make the comparison in results, obtained from Eurocode 2(Comité Européen de Normalisation[CEN], 2004a), ACI209-R2(ACI Committee 209, 2008), and G&L(Gardner and Lockman 2001), models in numerical creep analysis of composite steel - concrete beams. Before that we try to introduce the fundamentals of linear viscoelasticity of aging materials applied to concrete in the light of the great international school of hereditary mechanics of: Northwest University in USA present of (Bažant et al. 1975, 1993, 2000), Politecnico of Turin present of (Chiorino et al. 2007) and ČVUT in Prague present of (Křistek 1988).

RESEARCH SIGNIFICANCE

The investigation of creep effect in composite steel-concrete beams has been an important task for engineers since the first formulation of the mathematical model of linear viscoelasticity (Bažant 1975). The mechanic-mathematical model and design equations for describing the creep effect of composite sections are

Corresponding author, Professor Dr. Doncho Partov**,** of structural mechanics at the University of Structural Engineering and Architecture "L.Karavelov" in Sofia, Bulgaria
[2]Dr. Vesselin Kantchev**,** Associate professor of mathematics at the University of Structural Engineering and Architecture "L.Karavelov" in Sofia, Bulgaria

based on the integral equations of Volterra of second kind. The paper discusses the problem concerned with the development of computer program for the automatic computation (both numerical and graphical) of the entire set of functions that are of interest for creep analysis of composite - concrete structures, on the basis of the physical parameters characterizing the structural problem under consideration, and with reference to three prevailing creep prediction models. The paper analyzes the time dependent behaviour of composite steel-concrete beam with respect to rheological properties of concrete according to world code provisions: Eurocode2 (Comité Européen de Normalisation [CEN] 2004a, ACI209R-92 (ACI Committee 209, 2008), and GL2000 (Gardner and Lockman 2001).

FUNDAMENTALS OF LINEAR VISCOELASTICITY OF AGING MATERIALS APPLIED TO CONCRETE

Concrete is considered to comply with the linear theory of viscoelasticity for aging materials (Bažant et al. 1975, 1993, 2000), (Chiorino et al. 2007), and (Křistek 1988). Introducing the creep (compliance) function *J(t,t)* and summing the responses to all uniaxial stress increments introduced at times t, the following integral relations are obtained to model the responses at time *t* to sustained variable imposed stresses.

$$e_{cs}(t) = \int_{t_0}^{t} \frac{ds}{dt} J(t,t)dt \qquad (1)$$

where: $e_{cs} = e_c(t) - e_{cn}(t) =$ stress - dependent strain; $e_c(t) =$ total strain at time t ; $e_{cn}(t) =$stress independent strain. Here the hereditary integrals must be intended as Stieltjes integrals in order to admit discontinuous stress histories *s(t)*.If the law of variation of the imposed stress is considered continuous after an initial finite step, the ordinary Rieman definition of the integral applies and eqs.(1) may be written in the form:

$$e_{cs}(t) = s(t_0)J(t,t_0) + \int_{t_0}^{t} \frac{ds}{dt} J(t,t)dt \ ; \qquad (2)$$

Equation (1) can be written in the operator form: $e_{cs} = Js$, where J represent the unaxial creep operators according to (Bažant 1975).

The compliance function *J(t,t)* is normally separated, on the basis of some convention, into an initial strain *J(t+D ,t)* with D = *t* - t small, which is treated as instantaneous and elastic (nominal elastic strain) introducing a corresponding elastic modulus for the concrete $E_c(t)$, and a creep strain *C(t,t)*, i.e:

$$J(t+\Delta,t) \cong J(t,t) = 1/E_c(t); \qquad (3)$$

$$J(t,t) = 1/E_c(t) + C(t,t); \qquad (4)$$

A creep coefficient f is normally introduced representing the ratio between the creep strain *C(t ,t)* and the initial strain at *t* =t (e.g. in B3 model), or at a conventional age t at loading (e.g. in CEB MC90 model, with t = 28 days), i.e.:

$$J(t,t) = \frac{1}{E_c(t)} + \frac{f(t,t)}{E_c(t)}; \qquad (5)$$

$$J(t,t) = \frac{1}{E_c(t)} + \frac{f_{28}(t,t)}{E_{c28}(t)}; \qquad (6)$$

It must be noted that for structural analysis the compliance function *J(t,t)* is very important. The conventional separation adopted in eq. (3) and the value of D in eq. (2) have no influence on the result of the analysis, except in the definition of the “initial” (nominally elastic) state of deformation or of stress due to a sudden application of actions (respectively forces or imposed deformations). Such a state is in effect by itself a matter of convention depending on the procedures in the application of the actions at $t = t_0$ on the structure, on the initial time $t_0 + D$ of observation of the effect and on measuring procedures.

Time-dependent properties of concrete are fully characterized by *J(t,t).* For realistic forms of *J(t,t)* eq. (1) cannot be integrated analytically, and numerical integration is mandatory.

In this respect, it must be considered that creep of concrete is a very complex phenomenon involving several interacting physical mechanisms at different scales of microstructure, which are influenced by many factors; physical mechanisms and modelling criteria are still being debated (Bažant, 1993, 2000). Hence, a relatively high degree of sophistication in a realistic creep prediction model is unavoidable. A further cause of complexity of creep models to be used in structural analysis is the need to provide the average creep properties of the cross section for traditional simplified one-dimensional analysis of beams and frames. Such properties are characterized by non-uniform creep and shrinkage developing within the section, due to the drying process, and are influenced by the cross section geometry and stress distribution. As a consequence, the algebraic expressions for the prediction of compliance function *J(t,t)* for the average creep properties of the concrete cross section in drying conditions are inevitably rather complex (and less accurate than the constitutive law for a material point) in all the prevailing creep prediction models presented in recent literature (Bažant, 1993, 2000), and/or considered by international associations [CEB (1993), ACI (2004)]. Standard numerical procedures for the solution of integral equation of Volterra have been developed by Bažant (Jirasek&Bažant 2002), and they have been incorporated in manuals design by (Chiorino 2010), bringing to an end a line of research, that has been investigated for more than fifty years. It has been in fact practically demonstrated that no formulation for *J(t,t)* can be found that is sufficiently accurate and allows at the same time the precisely solution of the creep problem in the structures. The problem of the creep induced stress redistribution in the composite steel-concrete beams is dealt with within the theory of linear viscoelasticity for aging materials, which is normally considered appropriate for the creep analysis of structures (Bažant 1975, 1993, 2000) and (Chiorino

2007, 2010). Recent progresses of the theory of linear viscoelasticity, extended to materials like concrete showing a complex creep behaviour, allow a rational interpretation of any kind of creep induced structural effects through very compact formulations on the basis of integral equations of Volterra. For this purpose, proper design aids, to be inserted in manuals of bridge practice, can be offered to designers by a numerical solution of the Volterra integral equation, performed once for ever for the above mentioned creep prediction models suggested by international civil engineering associations, or of a powerful numerical solution for the automatic immediate calculation of development of internal forces in the time t from any given compliance function *J(t,t0)*. This paper focuses on the development of these numerical solutions and theoretically consistent procedures, and of the corresponding design aids, for the evaluation of the creep induced stress redistribution in composite steel-concrete sections and on their application to steel-concrete bridges.

BASIC EQUATIONS FOR DETERMINING CREEP COEFFICIENT ACCORDING TO VARIOUS CREEP MODELS AND PROVISIONS

Eurocode 2 model

The creep (compliance) function proposed by the 1990 CEB Model Code ("CEB-FIP"1991) is given by the relationship: $J(t,t_0)=\frac{1}{E_c(t_0)}+\frac{f(t,t_0)}{E_c}$, where $j(t,t_0)$= the creep coefficient; and $E_c(t_0)$ and E_c = modulus of elasticity at the age of t_0 and 28 days, respectively[1]. The creep coefficient is evaluated with the following formula: $f(t,t_0)=f_{RH}\,b(f_{cm})\,b(t_0)\,b_c(t-t_0)$ where $f_{RH}=1+\frac{1-RH/100}{0.46(h_0/100)^{0.33}}$ - is a factor to allow for the effect of relative humidity on the notional creep coefficient. RH is the relative humidity of the ambient environment in % $b(f_{cm})=\frac{5.3}{(f_{cm}/10)^{0.5}}$ - is a factor to allow for the effect of concrete strength on the notional creep coefficient. $b(t_0)=\frac{1}{0.1+(t_0)^{0.2}}$ - is a factor to allow for the effect of concrete age at loading on the notional creep coefficient (the function is considered for continuous process).

$b(t)=\frac{1}{0.1+(t)^{0.2}}$ is a function of aging, depending on the age of concrete and it characterizes the process of aging. $b_c(t-t_0)=\left[\frac{t-t_0}{b_H+(t-t_0)}\right]^{0.3}$ is a function to describe the development of creep with time after loading. $b_H=150\left[1+\left(1.2\frac{RH}{100}\right)^{18}\right]\frac{h_0}{100}+250\le 1{,}500$ coefficient depending on the relative humidity (*RH* in %) and notional member size (h_0 in mm), where $f_{cm}=f_{ck}+8=$ the mean compressive strength of concrete at the age of 28 days (MPa); and $h_0=\frac{2A_c}{u}=$ the notional size of member (mm) (A_c = the cross section; and *u* = the perimeter of member in contact with the atmosphere). Constant Young's modulus is given by $E_c=10^4(f_{cm})^{\frac{1}{3}}$. Variable Young's modulus is given by: $E_c(t)=b_{cc}^{0.5}E_c$, where $E_c=10^4(f_{cm})^{\frac{1}{3}}$ and $b_{cc}=\exp\left[s\left(1-5.3/t^{0.5}\right)\right]$, where *s* = 0.25 for normal and rapid hardening cements. So $E_c(t)=336190e^{0.5\left[0.25\left(1-\frac{5.3}{\sqrt{t}}\right)\right]}$, $f_0=f_{RH}\,b(f_{cm})b(t_0)$ is a final creep.

ACI 209R-92 model

This is an empirical model developed by (Branson and Christiason 1977), with minor modification introduced in ACI 209R-92(ACI Committee 209, 2008). The shape of the curve and ultimate value depend on several factors such as curing conditions, age of application of load, mixture proportioning, ambient temperature and humidity. Correction factors are applied to ultimate values. Since the linear function of the ultimate values is creep equation for any period, the correction factors in this procedure may be applied to short –term creep. The creep function proposed by the ACI 209R-92 model, that presents the total stress-dependent strain by unit stress is given by the relationship: $J(t,t_0)=\frac{1}{E_{cmt0}}+\frac{f(t,t_0)}{E_{cmt0}}=\frac{1+f(t,t_0)}{E_{cmt0}}$, where

- $f(t,t_0)$ is the creep coefficient as the ratio of the creep strain to the elastic strain at the start of loading at the age t_0 (days) and E_{cmt0} is the modulus of elasticity at the time of loading t_0 (MPa or psi), respectively. The creep model proposed by ACI 209R-92 has two components that determine the ultimate asymptotic value and the time development of creep. The predicted parameter is not creep strain, but creep coefficient $f(t,t_0)$, (defined as the ratio of the creep strain to the initial elastic strain). The creep coefficient is evaluated with the following formula: $f(t,t_0)=f_u\,b_c(t-t_0)$, where: $f(t,t_0)$ is the creep coefficient at the concrete age t due to a load applied at the age t_0 ;($t-t_0$) is the time since application of load; f_u is the ultimate creep coefficient. For standard conditions in the absence of specific creep date for local aggregates and conditions, the average value proposed for the ultimate creep coefficient f_u is equal to 2,35. For conditions

other than standard conditions the value of the ultimate creep coefficient $f_u = 2.35$ should be modified by six correction factors, depending on particular conditions: where: $f_u = 2.35 g_c$; and: $g_c = g_{c,t0} g_{c,RH} g_{c,vs} g_{c,s} g_{c,y} g_{c,a}$; $g_{c,t0} = 1.25 t_0^{-0.118}$ - corresponds to $b(t_0)$ in CEB MC90, is a function of aging, depending on the age of concrete and it characterizes the process of aging; $g_{c,RH} = 1.27 - 0.67h$ for $h \geq 0.40$ is the ambient humidity factor, where the relative humidity *h* is in decimal -correspond to f_{RH} CEB MC90 ; $g_{c,vs} = \frac{2}{3}\left(1 + 1.13 e^{\{-0.0213(V/S)\}}\right)$ (corresponds to b_H in CEB MC90), where V is the specimen volume in mm^3 and S the specimen surface area in mm^2, allows to consider the size of member in terms of the volume-surface ratio; $g_{c,s} = 0.82 + 0.00624s$ is slump factor, where $s = 75\ mm$ is the slump of fresh concrete; $g_{c,y} = 0.88 + 0.0024y$ is fine aggregate factor, where $y = 40$ is the ratio of fine aggregate to total aggregate by weight expressed as percentage; $g_{c,a} = 0.46 + 0.09a \geq 1$ is air content factor, where $a = 2$ is the air content in percentage. $b_c(t - t_0) = \left[\frac{(t-t_0)^{0.6}}{10 + (t-t_0)^{0.6}}\right]$- is a function to describe the development of creep with time after loading. The secant modulus of elasticity of concrete E_{cmt0} at any time t_0 of loading is given by $E_{mct0} = 0,043 r_c^{1,5} \sqrt{f_{cmt0}}$ MPa; where r_c is the unit weight of concrete (kg/m^3) and f_{cmt0} is the mean concrete compressive strength at the time of loading (MPa).The general equation for predicting compressive strength at an time t is given by $f_{cmt} = \left[\frac{t}{a + bt}\right] f_{cm28}$,where f_{cm28} is the concrete mean compressive strength of 28 days in MPa; a (in days) and b are constant and t is the age of the concrete.

Gardner&Lockman 2000 model

It is a modified Atlanta 97 model 1993(Gardner and Lockman 2001, which itself was influenced by CEB MC90-99. The compliance expression is based on the modulus of elasticity at 28 days, instead of the modulus of elasticity at age of loading. This model includes a term for drying before loading, which applies to both basic and drying creep. Required parameters: Age of concrete when drying starts, usually taken as the age at the end of moist curing (days); Age of concrete at loading (days); Concrete mean compressive strength at 28 days (MPa or psi); Concrete means a compressive strength at loading (MPa or psi); Modulus of elasticity of concrete at 28 days (MPa or psi); Modulus of elasticity of concrete at loading (MPa or psi); Relative humidity expressed as a decimal; and Volume-surface ratio (mm or in.); The creep (compliance) function proposed by the (Gardner and Lockkman 2001), is composed of the elastic and creep strains. The elastic strain is reciprocal of the modulus of elasticity at the age of loading E_{cmto} and the creep strain is the 28 day creep coefficient $f_{28}(t,t_0)$ divided by the modulus of elasticity at 28 days E_{cm28}.The creep coefficient $f_{28}(t,t_0)$ is the ratio of the creep strain to the elastic strain due to the load applied at the age of 28 days. So: $J(t,t_0) = \frac{1}{E_{cmt0}(t_0)} + \frac{f_{28}(t,t_0)}{E_{cm28}}$; where: E_{cmt0} is the modulus of elasticity of concrete at the time of loading t_0; E_{cm28} -is the mean modulus of elasticity concrete at 28 days (MPa); $1/E_{cmt0}$ - represents the initial strain per unit stress at loading. $f(t,t_0)$ gives the ratio of the creep strain since the start of loading at the age t_0 to the elastic strain due to a constant stress applied at a concrete age of 28 days; The 28-day creep coefficient $f_{28}(t,t_0)$ calculated using the next formulae:

$$f_{28}(t,t_o) = \Phi(t_c)\left[2\frac{(t-t_o)^{0,3}}{(t-t_o)^{0,3}+14} + (\frac{7}{t_0})^{0,5}(\frac{(t-t_o)}{(t-t_o)+7})^{0,5} + \right.$$
$$\left. + 2,5(1-1,086h^2)(\frac{(t-t_o)}{(t-t_o)+0,12(V/S)^2})^{0,5}\right].$$

The creep coefficient includes three terms. The first two terms are required to calculate the basic creep, and the third term is for the drying creep. At a relative humidity of 0.96 there is only basic creep. There is no drying creep. $\Phi_{(t_c)}$ is the correction term for the effect of drying before loading. If $t_o = t_c; \Phi(t_c) = 1$; When:

$t_0 > t_c$

$$\Phi(t_c) = \left[1 - \left(\frac{(t_0 - t_c)}{(t_0 - t_c) + 0,12(V/S)^2}\right)^{0,5}\right]^{0,5};$$

t_o = age of concrete at loading, (days); t_c = age of concrete when drying starts at the end of moist curing, (days).

To calculate relaxation, $\Phi(t_c)$ remains constant at the initial value throughout the relaxation period. For creep recovery calculation, $\Phi(t_c)$ remains constant at the value at the age of loading. If experimental values are unavailable the modulus of elasticity E_{cmt} at any time *t* is given by : $E_{cmt} = 3500 + 4300\sqrt{f_{cmt}}$, where the strength development in time can be calculated from the compressive strength using the equation

: $f_{cmt} = b_e^2 . f_{cm28}$. This equation is a modification of the CEB strength-development relationship. So $b_e = \exp\left[\frac{s}{2}(1-\sqrt{\frac{28}{t}}\right]$; where s =0,4 is CEB(1993) style strength – development parameter and b_e relates strength development to cement type. Relationship between specified and mean compressive strength of concrete can be estimated from the equation: $f_{cm28} = 1{,}1 f_c^{/} + 5{,}0$ .This equation is a compromise between recommended equation of ACI Committee 209 (1982) and ACI Committee 363 (1992). It can be noted that this equation fails to include any effects for aggregate stiffness or concrete density. Instead of making an allowance for density of the concrete, it is preferable to measure the modulus of elasticity.

Due to further justify the present model, it is desirable to clarify the differences from other models, which are presented in this paper. According to (Bažant&Baweja 1993, 2000), many basic features of model GL are questionable on the basis of the current understanding of the mechanics and physics of concrete shrinkage and creep, and violate the guidelines published by a RILEM Committee. Some of them are as follows: disagreement with diffusion theory, the effect of age on creep according to this model is far too weak and too short-lived, the creep coefficient for the additional creep due to drying is given in this model by a curve that does not have a bounded final value, the creep recovery curve calculated according to the principle of superposition is violated by the GL model (Bažant&Baweja 2000).

BASIC ASSUPTION AND MATERIAL CONSTITUTIVE RELATIONSHIP

The hypotheses essentially based on those introduced in last studies of (Partov and Kantchev 2014) in the elastic analysis of composite steel-concrete sections with stiff (rigid) shear connectors are assumed as following:

a) Bernoulli's concerning plane strain of cross-sections (Preservation of the plane cross section for the two elements considered compositely).

b) No vertical separation between parts, in other words identical vertical displacement at the slab-beam interface is assumed.

c) The connection system is distributed continuously along the axis of the beam.

d) The cross sections are free to deform (because they belong to statically determinate structures)

e) Concrete is not cracked $s_c \le (0.4 \div 0.5) R_c$.

f) For the service load analysis of these cross sections the stress levels are small and, therefore , linear elastic behaviour may be assumed for the steel beam, i.e. Hooke's law applies to steel as well as to concrete under short-time loads.

g) Moreover, for the concrete part, if the dependence of strains and stresses upon histories of water content and temperature is disregarded, with the exclusion of large strain reversals, and under normal environment conditions, the strain can be considered as a linear function of the previous stress history alone. This linearity implies the principle of superposition, which states that strain response due to stress increments applied at different times may be added.

h) In the range of service ability loads concrete behaves in a way allowing to be treated as a linear viscoelastic body. On the basis of our assumptions for the purpose of structure analysis the total strain for concrete subjected to initial loading at time t_0 with a stress $s(t_0)$ and subjected to subsequent stress variations $\Delta s(t_i)$ at time t_i may be expressed as follows:

$$e_{tot}(t,t_0) - e^{sh}(t,t_0) = s(t_0) J(t,t_0) + \int_{t_0}^{t} \frac{ds(t)}{dt} J(t,t)dt$$

, where t is the time elapsed from casting of concrete; $e_{tot}(t,t_0)$ - total axial strain; $e^{sh}(t,t_0)$ - strain due to shrinkage, i.e. an elastic strain. Then the stress-strain behaviour of concrete can be described with sufficient accuracy by the integral equations (1) by Bolztmann-Volterra

$$e_c(t) = \frac{s_c(t_0)}{E_c(t_0)}\left[1+f(t-t_0)\right] + \int_{t_0}^{t} \frac{ds_c(t)}{dt} \frac{1}{E_c(t)}\left[1+f(t-t)\right]dt$$

i) According to our proposal, the influence of the development of the bending moment $M_{c,r}(t)$ in the concrete member upon the redistribution of the normal force of concrete $N_{c,r}(t)$ can be neglected.

j) For the service load analysis no slip and uplift effects occur between the steel and concrete.

k) A single theory of interaction ignoring shear lag effects is considered. Thus, shear lag phenomenon of the deck slab is considered by using the appropriate effective slab width.

BASIC EQUATION OF EQUILIBRIUM

It is known that while in steel beam, under the effect of the serviceability loads, elastic deformations can be seen in the concrete plate during the time significant inelastic deformation take place as a consequence of creep of concrete. These inelastic strains in the concrete deck cause redistribution of stress and significant increases in deformation. Let us denote both the normal forces and the bending moments in the cross-section of the plate and the girder after the loading in the time t = 0 with $N_{c,0}$, $M_{c,0}$, $N_{a,0}$, $M_{a,0}$ and with $N_{c,r}(t)$, $M_{c,r}(t)$, $N_{a,r}(t)$, $M_{a,r}(t)$ a new group of normal forces and bending moments, arising due to creep and shrinkage of concrete (Fig.1). For a composite bridge girder with $J_c = \frac{A_c(nI_c)n}{A_s I_s} \le 0.2$, according to the suggestion of (Partov and Kantchev, 2009), the equilibrium conditions in time t are the following:

$$N(t) = 0; \quad N_{c,r}(t) = N_{a,r}(t); \qquad (7a)$$

$$\sum M(t) = 0; \quad M_{c,r}(t) + N_{c,r}(t) r = M_{a,r}(t); \qquad (7b)$$

Due to the fact that the problem is a twice internally statically indeterminate system, the equilibrium equations (7a & 7b) are insufficient to solve it. It is necessary to produce two additional equations in the sense of compatibility of deformations of both steel girder and concrete slab in time *t* (Fig. 1).

DERIVING THE FUNDAMENTAL INTEGRAL EQUATIONS OF VOLTERRA OF SECOND KIND FOR DETERMINING $N_{c,r}(t)$, $M_{c,r}(t)$, $N_{a,r}(t)$ AND $M_{a,r}(t)$

The following Volterra type linear integral equations which hold for the determination of a new group of normal forces $N_{c,r}(t)$, $N_{a,r}(t)$ and bending moments $M_{c,r}(t)$, $M_{a,r}(t)$, arising due to creep of concrete, are derived.

Analysis according to EC 2

Strain compatibility on the contact surfaces between the concrete and steel members of composite girder:

For constant elasticity module of concrete strain compatibility on the contact surfaces between the concrete and steel members of composite girder is:

$$e_{sh}(t_0)\, f(t-t_0) + \frac{N_{c,0}}{E_c(t_0)\,A_c}\left[1 + f_{RH}\, b(f_{cm})\, b(t_0)\, b_c(t-t_0)\right] -$$

$$- \frac{1}{E_c(t_0)\,A_c}\int_{t_0}^{t} \frac{dN_{c,r}(t)}{dt}\left[1 + f_{RH}\, b(f_{cm})\, b(t)\, b_c(t-t)\right] dt +$$

$$+ \frac{N_{a,0}}{E_a A_a} - \frac{1}{E_a A_a}\int_{t_0}^{t} \frac{dN_{a,r}(t)}{dt}\, dt = \frac{M_{a,0}}{E_a I_a}\, r + r\,\frac{1}{E_a I_a}\int_{t_0}^{t} \frac{dM_{a,r}(t)}{dt}\, dt$$

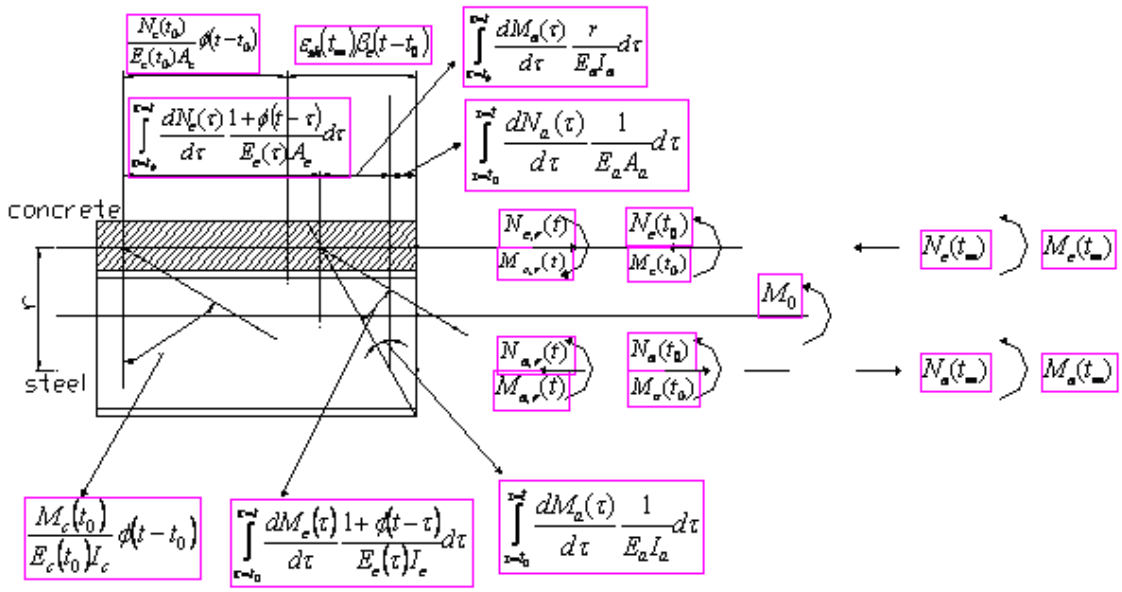

Figure 1. Mechanic-Mathematical model for deformations in cross-section, regarding creep of the concrete

Compatibility of Curvatures when $t = t$ is

$$\frac{M_{c,0}}{E_c(t_0)I_c}\left[1+f_{RH}b(f_{cm})b(t_0)b_c(t-t_0)\right]-$$
$$-\frac{1}{E_c(t_0)I_c}\int_{t_0}^{t}\frac{dM_{c,r}(t)}{dt}\left[1+f_{RH}b(f_{cm})b(t)b_c(t-t)\right]dt =$$
$$=\frac{M_{a,0}}{E_aI_a}+\frac{1}{E_aI_a}\int_{t_0}^{t}\frac{dM_{a,r}(t)}{dt}dt$$

After integrating the two equations by parts and using the (7a and 7b) for assessment of normal forces $N_{c,r}(t)$ and bending moment $M_{c,r}(t)$ two linear integral Volterra equations of the second kind are derived.

$$N_{c,r}(t)=\lambda_N\int_{t_0}^{t}N_{c,r}(\tau)\frac{d}{d\tau}\left[1+\varphi\phi_{RH}\beta(f_{cm})\beta(\tau)\beta(t-\tau)\right]d\tau+$$
$$+\lambda_N N_{c,0}\phi_{RH}\beta(f_{cm})\beta(t_0)\beta_c(t-t_0)+\lambda_N N_{sh}\beta_c(t-t_0) \quad (8)$$

$$M_{c,r}(t)=\lambda_M\int_{t_0}^{t}M_{c,r}(\tau)\frac{d}{d\tau}\left[1+\phi_{RH}\beta(f_{cm})\beta(\tau)\beta_c(t-\tau)\right]d\tau+$$
$$+\lambda_M M_{c,0}\phi_{RH}\beta(f_{cm})\beta(t_0)\beta_c(t-t_0)-\lambda_M\frac{E_cI_c}{E_aI_a}N_{c,r}(t)r \quad (9)$$

where:

$$l_N=\left[1+\frac{E_cA_c}{E_aA_a}\left(1+\frac{A_ar^2}{I_a}\right)\right]^{-1},\ l_M=\left[1+\frac{E_cI_c}{E_aI_a}\right]^{-1}.$$

Analysis according to ACI 209R-92

Using the above mentioned approach, for constant elasticity module of concrete for assessment of normal forces $N_{c,r}(t)$ and bending moment $M_{c,r}(t)$ two linear integral Volterra equations of the second kind are derived.

$$N_{c,r}(t)=l_N\int_{t_0}^{t}N_{c,r}(t)\frac{d}{dt}\left[1+2,35g_{c5}b(t)b_c(t-t)\right]dt+$$
$$+l_N N_{c,0}2,35g_{c5}b(t_0)b_c(t-t_0) \quad (10)$$

$$M_{c,r}(t)=l_M\int_{t_0}^{t}M_{c,r}(t)\frac{d}{dt}\left[1+2,35g_{c5}b(t)b_c(t-t)\right]dt+$$
$$+l_M M_{c,0}2,35g_cb(t_0)b_c(t-t_0)-l_M\frac{E_cI_c}{E_aI_a}N_{c,r}(t)r, \quad (11)$$

Analysis according to Gardner& Lockman model

Using the above mentioned approach for constant elasticity module of concrete for assessment of normal forces $N_{c,r}(t)$ and bending moment $M_{c,r}(t)$ two linear integral Volterra equations of the second kind are derived.

$$N_{c,r}(t)=l_N\int_{t_0}^{t}N_{c,r}(t)\frac{d}{dt}\left[1+\Phi(t_c)b_c(t-t)\right]dt+$$
$$+l_N N_{c,0}\Phi(t_c)b_c(t-t_0) \quad (12)$$

$$M_{c,r}(t)=l_M\int_{t_0}^{t}M_{c,r}(t)\frac{d}{dt}\left[1+\Phi(t_c)b_c(t-t)\right]dt+$$
$$+l_M M_{c,0}\Phi(t_c)b_c(t-t_0)-l_M\frac{E_cI_c}{E_aI_a}N_{c,r}(t)r \quad (13)$$

NUMERICAL METHOD

The solutions of structural creep problems, resp. the aforementioned integral equations of Volterra, with realistic compliance function, such as in EC2, ACI209R-92, and G&L models for creep of concrete provisions, cannot be performed analytically and require a deep knowledge in the higher level of mathematics theory, such as integral equations of Volterra of the second kind, and its numerical solutions, using formulae for the approximation of the integrals with finite sums (quadratures) - such as: Simpson, Chebyshev, Gaus, Euler-Gregory-Macloren, rectangle and trapezoidal rules (Atkinson,1997). The last option allows a quicker solution and usually leads to acceptable approximations if the number of time steps is not too small. However, computation time is insignificant even when adopting the trapezoidal rule.

The integral equations (8-13) are weakly singular Volterra integral equation of the second kind:

$$y(t)=g(t)+\lambda\int_{t_0}^{t}\mathrm{K}(t,\tau)y(\tau)d\tau$$
$$t\in[t_0,\ T],\ 0<t_0<T<\infty, \quad (14)$$

So, in our case discontinuous kernel function $\mathrm{K}(t,t)$ has an infinite singularity of type $(t-t)^{g-1}, g>0$.

In order to solve (14), the idea of product integration is used by considering the special case of:

$$y(t)=g(t)+\lambda\int_{t_0}^{t}L(t,\tau)(t-\tau)^{\gamma-1}y(\tau)d\tau$$
$$t\in[t_0,\ T],\ 0<t_0<T<\infty, \quad (15)$$

where the given functions $g(t)$ and $L(t,t)$ are sufficiently smooth which guarantee the existence and uniqueness of the solution $y(t)\in C_{[t_0,T]}$ (Atkinson 1997).

To solve (15) the method called product trapezoidal rule is used.

Let $n\geq 1$ be an integer and points $\{t_j=t_0+jh\}_{j=0}^{n}\in[t_0,T]$. Then for general $y(t)\in C_{[t_0,T]}$ we define

$$\left(L(t,\tau)\,y(\tau)\right)_n = \frac{1}{h}\Big[\left(t_j-\tau\right)L\left(t,t_{j-1}\right)y\left(t_{j-1}\right)+$$
$$\left(L(t,\tau)\,y(\tau)\right)_n = +\left(\tau-t_{j-1}\right)L\left(t,t_j\right)y\left(t_j\right)\Big] \quad (16)$$

for $t_{j-1} \le t \le t_j \quad t \in [t_0,\ T]$

This is piecewise linear in t and it interpolates $L(t,t)y(t)$ at $t = t_0, \mathbf{K}, t_n$. Using numerical approximation (16) the following method for solving the integral equation (15) is obtained:

$$\tilde{y}_n(t_i) = g(t_i) + l\sum_{j=0}^{i} w_{n,j}(t_i)\left[L\left(t_i,t_j\right)\tilde{y}_n\left(t_j\right)\right] \quad (17)$$

for $i = 0,1,\mathbf{K},n$,

with weights

$$w_{n,0}(t_i) = \frac{1}{h}\int_{t_0}^{t_1}(t_1-t)(t_i-t)^{g-1}\,dt$$

$$w_{n,n}(t_n) = \frac{1}{h}\int_{t_{n-1}}^{t_n}(t-t_{n-1})(t_n-t)^{g-1}\,dt$$

$$\omega_{n,j}(t_i) = \frac{1}{h}\int_{t_{j-1}}^{t_j}(\tau-t_{j-1})(t_i-\tau)^{\gamma-1}\,d\tau +$$
$$+\frac{1}{h}\int_{t_j}^{t_{j+1}}(t_{j+1}-\tau)(t_i-\tau)^{\gamma-1}\,d\tau$$

for $i = 0,1,\mathbf{K},n$.

Calculating analytically the weights, the approximate solution values $y_n(t_i)$ are computed from the system (17).

Theorem 1 Consider the numerical approximation defined with piecewise linear interpolation (11). Then for all sufficiently large n, the equation (9) is uniquely solvable and moreover if $y(t) \in C^2_{[t_0,T]}$, then there is

$$\|y - y_n\| \le \frac{ch^2}{8}\max_{t_0\le t,t\le T}\left|\frac{\partial^2 L(t,t)y(t)}{\partial^2 t}\right|. \quad (18)$$

Since $L(t,.) \in C^2_{[t_0,T]},\ t_0 \le t \le T$ the estimate (12) is an immediate consequence of theorem 4.2.1 in Atkinson 1997.

EQUIVALENT CONDITIONS FOR A COMPARISON OF MODELS

For a comparison of the predictions of different models, equivalent conditions must be established setting the same values or equivalent parameters. Therefore, the *"Guide for Modelling and Calculating Shrinkage and Creep in Harden Concrete"*(ACI 209.2R-08)," ACI Committee 209, 2008, American Concrete Institute, Farmington Hills, MI, 45pp was strictly followed.

NUMERICAL ANALYSIS

The method presented in the previous paragraph is now applied to a simply supported beam, subjected to a uniform load, whose cross section is shown in fig. 2.

On the base of numerous solved examples the optimal step of one day for solving the integral equations is found. The elapsed time for solving the problem for the period of twenty years (7300 days) is about up to ten minutes. For the period of about forty years (12028 - 12730 days - as in our case) the elapsed time increases up to forty minutes.

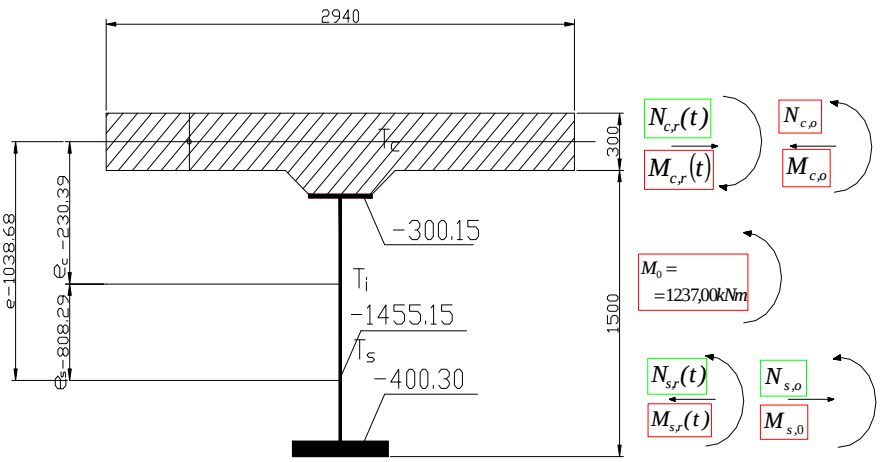

Figure 2. Composite beam with cross-section characteristic
(Note: Dimensions in mm;1 mm=0,0397 in.; 1kNm=8851 lbf.in

The following parameters are according to EUROCODE 2 model

$E_c = 3.2.10^4\ MPa\,(4,640,000\,psi)$,

$E_a = 2.1.10^5\ MPa\,(30,450,000\,psi)$,

$A_c = 8820\,cm^2\,(1367 in^2)$,

$A_a = 383.25\,cm^2\,(59,40 in^2)$,

$n = \frac{E_a}{E_c} = 6,56,\ I_c = 661,500\,cm^4\,(15,876 in^4)$,

$I_a = 1,217,963.7\,cm^4\,(29,231 in^4)$,

$r_c = 23.039\,cm\,(9,070 in)$,

$r_a = 80.829\,cm\,(31,823 in)$,

$r = 103.868\,cm\,(40,893 in)$,

$A_i = 1727.762\,cm^2\,(371,637 in^2)$,

$I_i = 4,536,360.758\ cm^4\,(108,873 in^4)$,

$M_0 = 1237\,kNm\,(10,948,687 lbf.in)$,

$N_{c,o} = 846.60\,kN\,(190,315 lbf)$,

$M_{c,o} = 27.56\,kNm\,(243,933 lbf.in)$,

$M_{a,o} = 330.13 kNm\,(2,921,980 lbf.in)$,

$$l_N = \left[1+\frac{E_c A_c}{E_a A_a}\left(1+\frac{A_a r^2}{I_a}\right)\right]^{-1} = 0.060545358,$$

$$l_M = \left[1+\frac{E_c I_c}{E_a I_a}\right]^{-1} = 0.922950026$$

$RH = 80\%(humidity)$

$h_0 = 2AC/u = 300\ mm\,(11.811 in)$;

$b_H = 150\left[1+(1.2*80/100)^{18}\right]h_0/100 +$

$+250 = 915,82 < 1500$;

$$b(f_{cm}) = \left.\frac{5.3}{(f_{cm}/10)^{0.5}}\right|_{f_{cm}=30} = 3.06;$$

$$b(t_0) = \left.\frac{1}{0.1+(t_0)^{0.2}}\right|_{t_0=60} = 0,4223;$$

$$f_{RH} = 1+\left.\frac{1-RH/100}{0.46\ \sqrt[3]{(h_0/100)}}\right|_{RH=80,h_0=300} = 1,3014;$$

$f_0 = f_{RH}\,b(f_{cm})b(t_0)$=**1,6817;**

$b_c(36500-60) = 0,9925811$;

$f_{t=36500} = f_0 b_c(36500-60) = 1,669242$;

$RH = 80\%(humidity)$

The following parameters are according to ACE 209R-92 model

$E_c = 2.8178.10^4\ MPa\,(4,85,810\,psi)$,

$E_a = 2.1.10^5\ MPa\,(30,450,000\,psi)$,

$A_c = 8820\,cm^2\,(1367 in^2)$,

$A_a = 383.25\,cm^2\,(59.40 in^2)$,

$n = \frac{E_a}{E_c} = 7,452,$

$I_c = 661,500\,cm^4\,(15,876 in^4)$,

$I_a = 1,217,963.7\,cm^4\,(29,231 in^4)$,

$r_c = 25.407\,cm\,(10.002 in)$,

$r_a = 78.463 cm\,(30.891 in)$,

$r = 103.870\,cm\,(40.893 in)$,

$A_i = 1566.82\,cm^2\,(237.37 in^2)$,

$I_i = 4,420,140.76\ cm^4\,(106,084 in^4)$,

$M_0 = 1237\,kNm\,(10,948,687 lbf.in)$,

$N_{c,o} = 837.286\,kN\,(188,222 lbf)$,

$M_{c,o} = 24.716\,kNm\,(218,802 lbfin)$

$M_{a,o} = 338.05 kNm\,(2,992,080 lbf.in)$,

$$l_N = \left[1+\frac{E_c A_c}{E_a A_a}\left(1+\frac{A_a r^2}{I_a}\right)\right]^{-1} = 0.068220902,$$

$$l_M = \left[1+\frac{E_c I_c}{E_a I_a}\right] = 0.93155$$

$g_{c,t0} = 1.25 t_0^{-0.118}$ corresponds to $b(t_0)$ = 0,61684 for t=60 days;

$g_{c,RH} = 1.27 - 0.67h$ for $h = 0,80$ =0,734;

$g_{c,vs} = \frac{2}{3}\left(1+1.13e^{\{-0.0213(V/S)\}}\right)$=0,6975,

where V/S=150;

$g_{c,s} = 0.82 + 0.00624s$ =1,018;

where $s = 75\ mm\,(2.95275 in)$;

$g_{c,y} = 0.88 + 0.0024y$ = 0,976; where $y = 40$;

$g_{c,a} = 0.46 + 0.09a \geq 1$; is air content factor, where;

$a = 2$, $g_{c,a} = 1$; $b_c(36500-60) = 0,982004$.

$RH = 80\%(humidity)$

The following parameters are according to Gardner&Lockman model

$E_c = 2.8014.10^4\ \ MPa\,(4,060,590\,psi)$,

$E_a = 2.1.10^5\ \ MPa\,(30,450,000\,psi)$,

$A_c = 8820\,cm^2\ \ (1367\ in^2)$,

$A_a = 383.25\,cm^2\ \ (59.40\,in^2)$,

$n = \dfrac{E_a}{E_c} = 7,496$

$I_c = 661,500\,cm^4\,(15,876\ in^4)$,

$I_a = 1,217,963.7\,cm^4\ (29,231\ in^4)$,

$r_c = 25.50\,cm\,(10.039\,in)$,

$r_a = 78.37\,cm\,(30.854in)$,

$r = 103.870\,cm\,(40.893in)$,

$A_i = 1560.82\,cm^2\ (236.464\,in^2)$,

$I_i = 4,415,813.859\ \ cm^4\ (105,979\,in^4)$,

$M_0 = 1237\,kNm\,(10,948,687\,lbf\,.in)$,

$N_{c,o} = 840,50kN\ (188,944\,lbf\,)$,

$M_{c,o} = 24,7206\,kNm\ \ (218,802\,lbf\,.in)$;

$M_{a,o} = 338.386kNm\,(2,995,054lbf\,.in)$,

$$l_N = \left[1+\frac{E_c A_c}{E_a A_a}\left(1+\frac{A_a r^2}{I_a}\right)\right]^{-1} = 0,068593645,\ ;$$

$$l_M = \left[1+\frac{E_c I_c}{E_a I_a}\right]^{-1} = 0,931921295$$

$RH = 80\%(humidity)$.

COMPARISONS OF THE RESULTS OBTAINED FROM DIFFERENT MODELS

When looking at the figures from 3 to 26 the difference between the results obtain according the world standards: EC2, ACI209-R2 and G/L2000 for evaluation of creep of concrete can be seen.

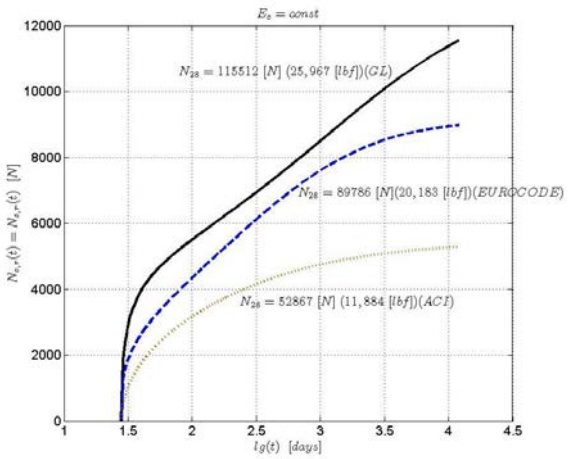

Figure 3. Normal forces $N_{c,r}(t) = N_{a,r}(t)$ *in time* $t = 12028$ *days* $(t_0 = 28)$. *(Note:1N=0.2248lbf.)*

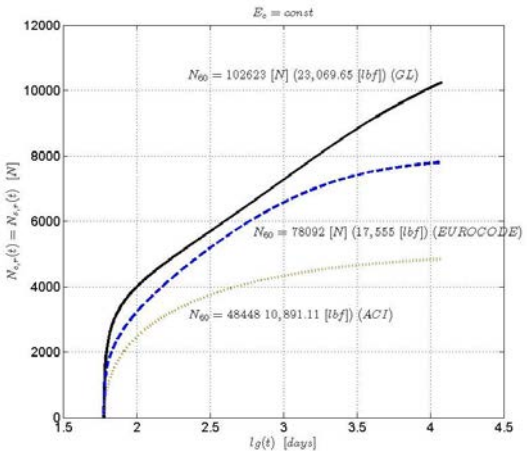

Figure 4. Normal forces $N_{c,r}(t) = N_{a,r}(t)$ *in time* $t = 12060$ *days* $(t_0 = 60)$. *(Note:1N=0.2248lbf.)*

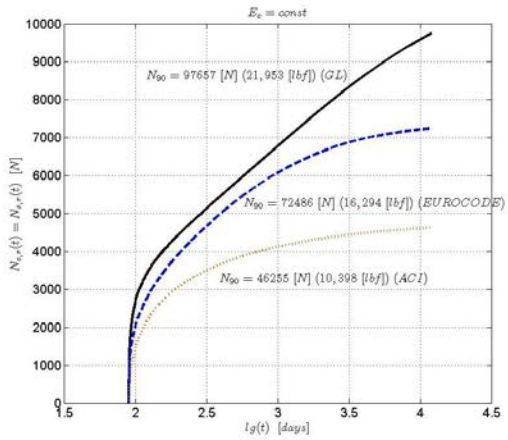

Figure 5. Normal forces $N_{c,r}(t) = N_{a,r}(t)$ *in time* $t = 12090$ *days* $(t_0 = 90)$. *(Note: 1N=0.2248lbf)*

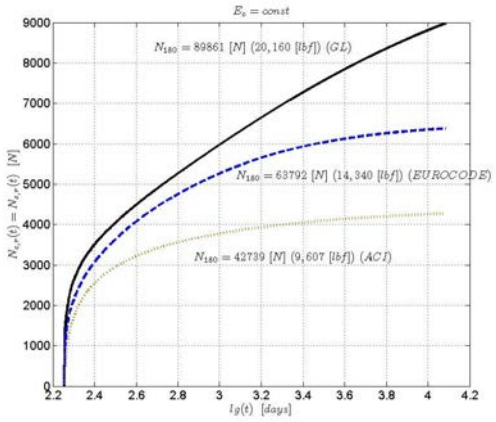

Figure 6. Normal forces $N_{c,r}(t) = N_{a,r}(t)$ *in time* $t = 12180$ *days* $(t_0 = 180)$. *(Note: 1N=0.2248lbf)*

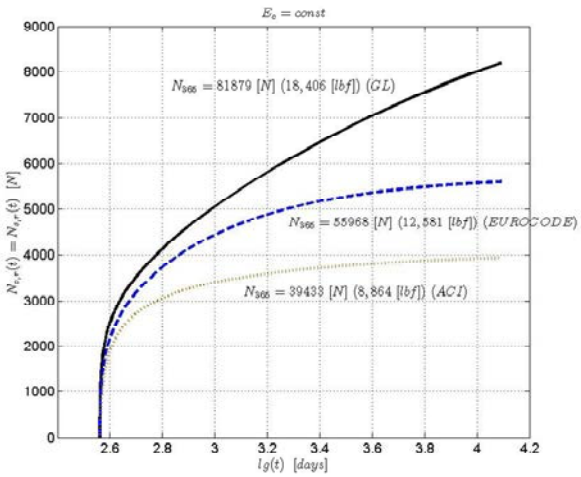

Figure 7. Normal forces $N_{c,r}(t) = N_{a,r}(t)$ *in time* $t = 12365$ *days* $(t_0 = 365)$. *(Note: 1N=0.2248lbf)*

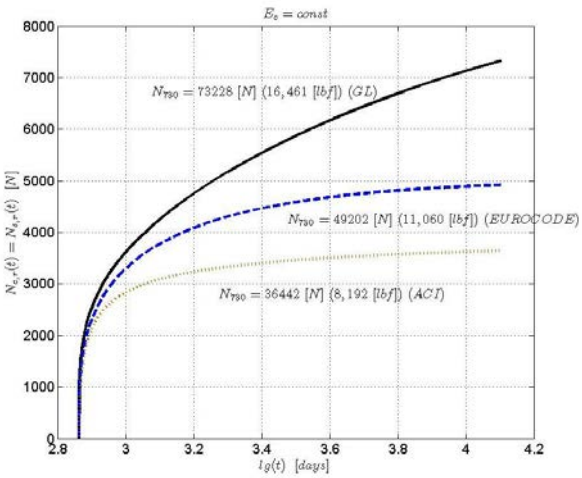

Figure 8. Normal forces $N_{c,r}(t) = N_{a,r}(t)$ *in time* $t = 12730$ *days* $(t_0 = 730)$. *(Note: 1N=0.2248lbf)*

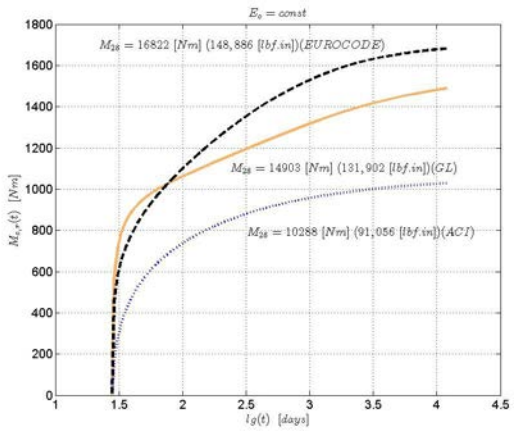

Figure 9. Bending moments $M_{c,r}(t)$ *in time* $t = 12028$ *days* $(t_0 = 28)$ *.(Note:1Nm=8.8507lbf.in.)*

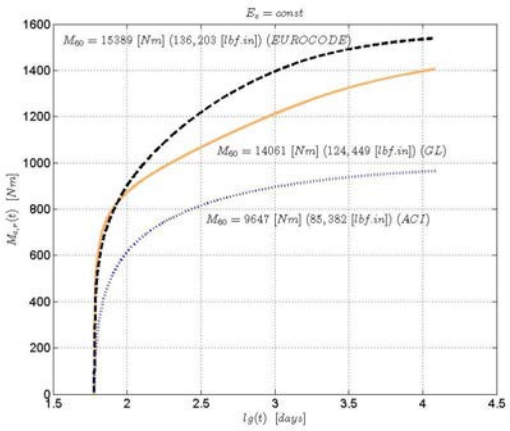

Figure 10. Bending moments $M_{c,r}(t)$ *in time* $t = 12060$ *days* $(t_0 = 60)$. *(Note:1 Nm=8.8507lbf.in.)*

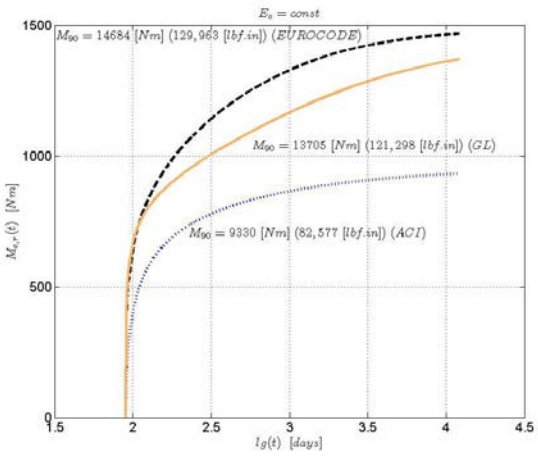

Figure 11. Bending moments $M_{c,r}(t)$ *in time* $t = 12090$ *days* $(t_0 = 90)$. *(*1 Nm=8.8507 lbf.in.*)*

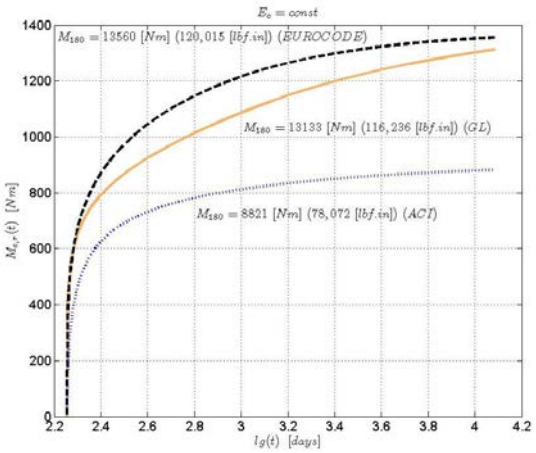

Figure 12. Bending moments $M_{c,r}(t)$ *in time* $t = 12180$ *days* $(t_0 = 180)$ *.(* 1 Nm=8.8507 lbf.in.*)*

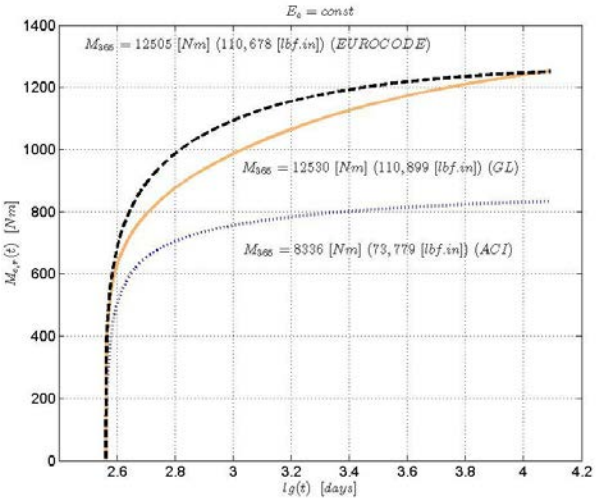

Figure 13. Bending moments $M_{c,r}(t)$ *in time* $t = 12365$ *days* $(t_0 = 365)$ *.(Note:* 1 Nm=8.8507 lbf.in.*)*

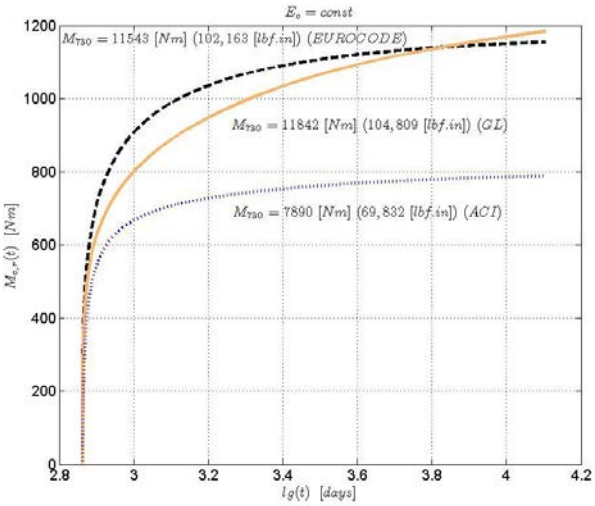

Figure 14. Bending moments $M_{c,r}(t)$ *in time* $t = 12730$ *days* $(t_0 = 730)$ *.(Note:* 1 Nm=8.8507 bf.in.*)*

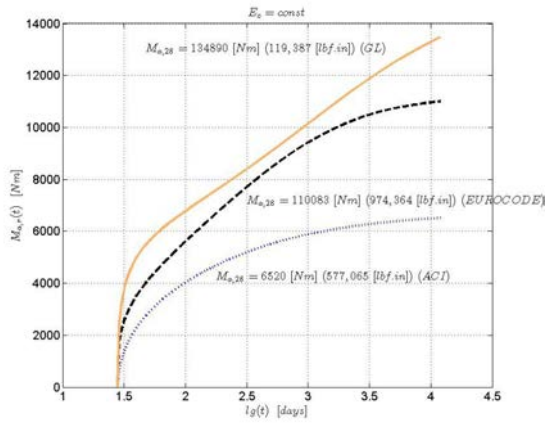

Figure 15. Bending moments $M_{a,r}(t)$ *in time* $t = 12028$ *days* $(t_0 = 28)$ *.(Note:* 1 Nm=8.8507lbf.in.*)*

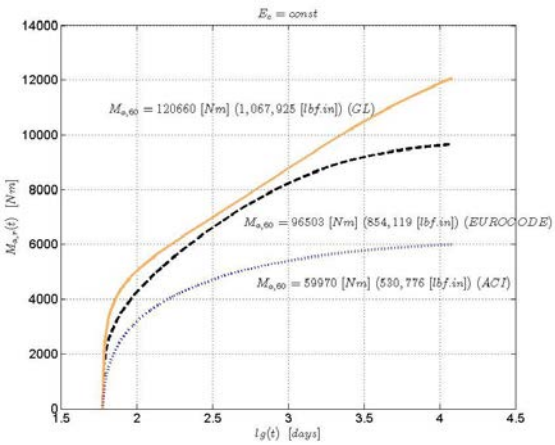

Figure 16. Bending moments $M_{a,r}(t)$ *in time* $t = 12060$ *days* $(t_0 = 60)$ *.(Note:* 1 Nm=8.8507 lbf.in.*)*

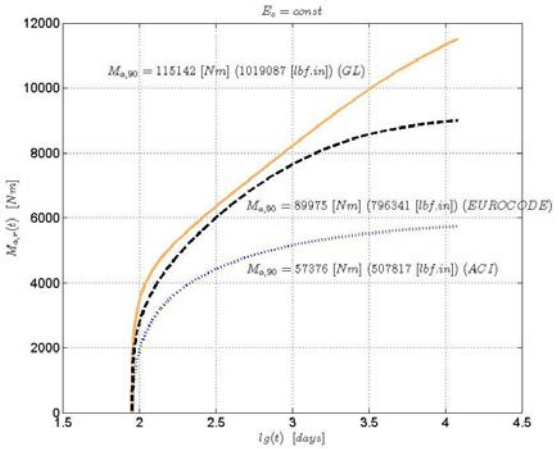

Figure 17. Bending moments $M_{a,r}(t)$ *in time* $t = 12090$ *days* $(t_0 = 90)$ *.(Note:1 Nm=8.8507 lbf.in.)*

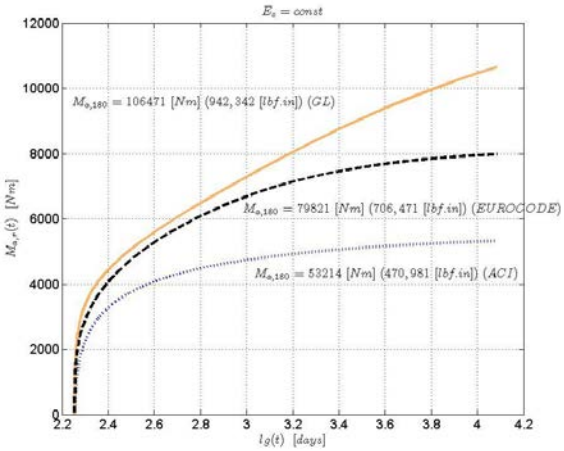

Figure 18. Bending moments $M_{a,r}(t)$ *in time* $t = 12180$ *days* $(t_0 = 180)$ *.(Note:1 Nm=8.8507 bf.in.)*

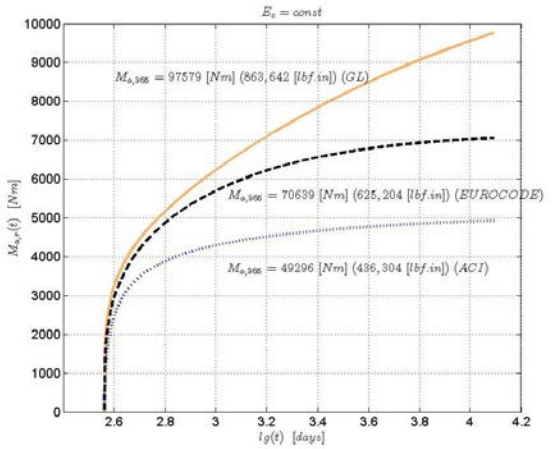

Figure 19. Bending moments $M_{a,r}(t)$ *in time* $t = 12365$ *days* $(t_0 = 365)$ *.(Note: 1 m=8.8507lbf.in.)*

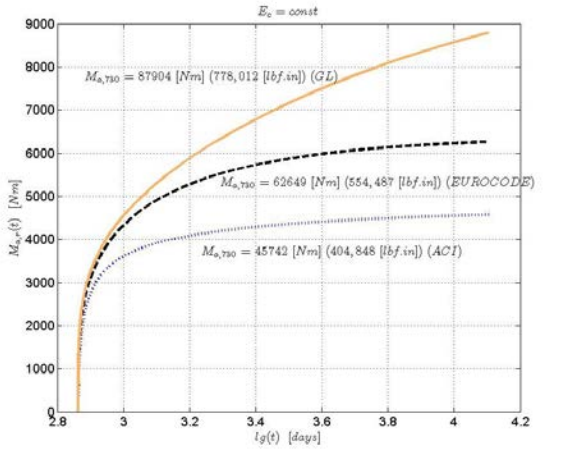

Figure 20. Bending moments $M_{a,r}(t)$ *in time* $t = 12730$ *days* $(t_0 = 730)$ *.(Note: 1 Nm=8.8507 lbf.in.)*

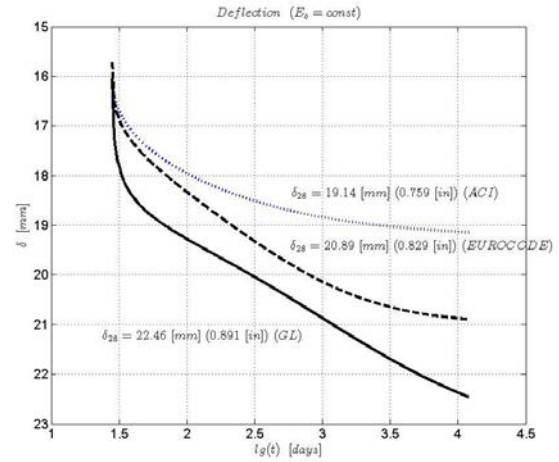

Figure 21. Deflection of steel girder (composite steel-concrete) $d(t)$ *in time* $t = 12028$ *days* $(t_0 = 28)$ *(Note:1 mm=0,0397 in).*

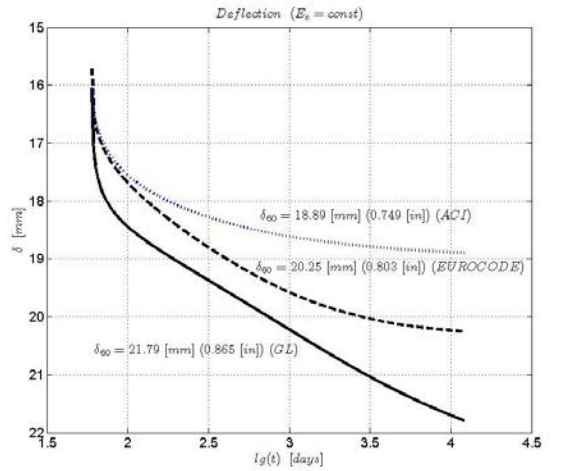

Figure 22. Deflection of steel girder (composite steel-concrete) $d(t)$ *in time* $t = 12060$ *days* $(t_0 = 60)$ *(Note:1 mm=0,0397 in).*

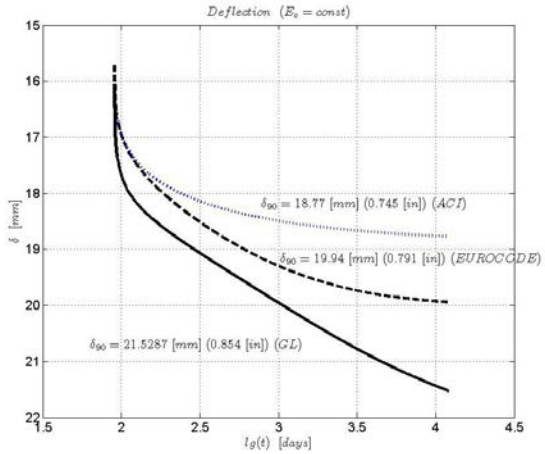

Figure 23. Deflection of steel girder (composite steel-concrete) $d(t)$ *in time* $t = 12090$ *days* $(t_0 = 90)$ *(Note:1 mm=0,0397 in).*

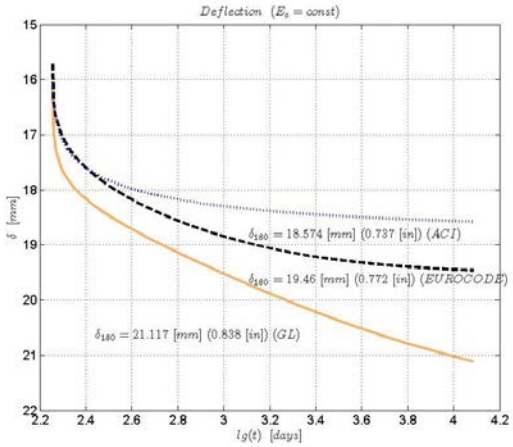

Figure 24. Deflection of steel girder (composite steel-concrete) $d(t)$ *in time* $t = 12180$ *days* $(t_0 = 180)$ *(Note:1 mm=0,0397 in).*

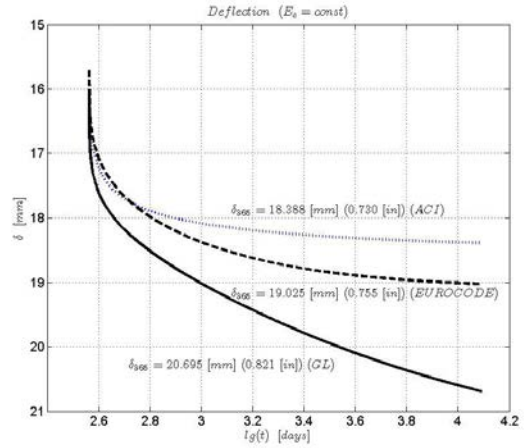

Figure 25. Deflection of steel girder (composite steel-concrete) $d(t)$ *in time* $t = 12365$ *days* $(t_0 = 365)$ *(Note:1 mm=0,0397 in).*

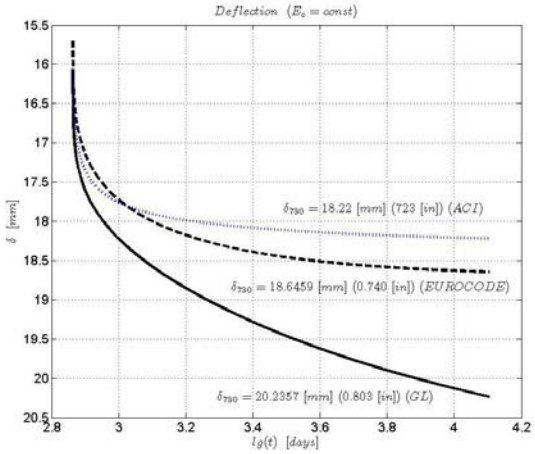

Figure 26. Deflection of steel girder (composite steel-concrete) $d(t)$ *in time* $t = 12730$ *days* $(t_0 = 730)$ *(Note:1 mm=0,0397 in).*

ANALYSIS OF THE RESULTS OBTAINED FROM DIFFERENT MODELS

Although the reliability of creep prediction models must be evaluated with respect to their agreement with the available experimental results essentially concerning the compliance function $J(t,t')$, a comparison between the predictions of different models is not devoid of interest. In fact, it has been observed (Chiorino, 2010) that in spite of good ratings-depending on the adopted statistical criteria and indicators attributed in the recent literature (Bažant, 2000) to all three considered models with regard to their agreement with the data bank, considerable difference can be observed between the predictions of different models. These differences concern both the shapes of the families of curves, and their long-term values, for all the basic functions. In fact, the influence of both long elapsed times $t = 12028(12730)days$, (e.g. for time ranges of the order of magnitude of the service life of a structure, that largely exceed the extension of any experimental collection of date), and of almost the entire range of ages $t_0 = 28(730)days$ at the loading, is evaluated in significantly different ways by all three type of models. This can be clearly observed in the set of Figures from 3 to 26. These differences and their impact on design strategies as well as on formulation of code provisions, will be discussed in the future paper.

CONCLUSIONS

The general approach of creep analysis of composite structures based on the linear theory of viscoelasticity and on the extended use of the integral equations of Volterra of the second kind leads to precisely and theoretically correct solutions for steel-concrete composite beams with rigid shear connectors.

In this perspective the paper has presented a powerful design tool, conceived for researches and designers, consisting of a software application for a quick automatic calculation of three basic principle creep models presently considered by international civil engineering societies. For a good accuracy of the time values, the numerical results are presented on logarithmic time scales. The choice of the length of time step of the proposed numerical algorithm is based on numerous numerical experiments with different steps (seven, three and one days). Therefore, it can be concluded that good results can be achieved from practical point of view with one day step. For our purpose we consider a period of about 33-35 years.

Our mathematical model was derived using a Stieltjes hereditary integral, which represents time loading history. It would be very interesting to investigate models with short time steps for early ages which are increased afterwards. A numerical method for time-dependent analysis of composite steel-concrete sections, according to the three following models has been considered: CEB MC 90, ACI209R-92 and G/L2000. Using MATLAB code a numerical algorithm was developed and subsequently applied to a simple supported beam. These numerical procedures, suited to a PC, are employed to better understand the influence of the creep of the concrete in time-dependent behaviour of composite section. The computer program has been designed for easy use and to allow control on all the parameters involved by prediction models. It has a powerful graphic module for handling and printing charts. To allow a large distribution of this design, web pages will be created in future with the aim of developing further automatic tools devoted to the creep structural analysis of composite beams. From this web page the software can be easily downloaded.

For the service load analysis, the proposed numerical method makes it possible to follow with great precision the migration of stresses from the concrete slab to the steel beam, which occurs gradually during the time as a result of the creep of the concrete.

The parametric analysis results are characterized by the following effects:

– the state of stress in the concrete slab depends on the age of the concrete at loading time t_0 ;

– the stress in the top flange of the steel section increases strongly with time;

– the stress in the bottom flange undergoes small variations;

– the stress increases more for young concrete and little for old one.

From Figures from 3 to 26 it can be clearly seen that according to the proposed method according to GL2000, the forces $N_{c,r}$, $N_{a,r}$ and $M_{a,r}$ are much greater (between 25 % -30 %) than the same ones in the CEB MC90-99 method. It reminds the differences obtained from the results, when solving the same task using the methods based on the theory of viscoelastic body and the theory of aging of Dischinger or modified theory of aging of Rüsch-Jungwirth. Then, we explained these facts through the assumptions of the viscoelastic body theory. According to this theory, which takes into account the delayed elastic strain developing in constrained conditions, it leads to appearance of recovery of stresses. They themselves decrease the relaxation of stresses in concrete of composite beams. That is why this fact leads to lower $N_{c,r}$ and respectively $M_{a,r}$. Therefore, according to the theory of viscoelastic body there is less stress in the steel beam, which leads to the more economic design of composite beam. To our opinion neglecting the “reversal of the creep recovery curves obtained from the GL2000 model according to the principle of superposition” denoted from Bažant in (Bažant and Baweja 2000), can be the reason for significant differences between the results obtained with the GL2000 and CEB MC90-99 methods. It means, that in the light of theory of viscoelastic body, the relaxation process in the concrete plate will be essentially greater compared with the results when the creep recovery is taken into account correctly according to CEB FIP model. (ENV 1992-I-I: 1991, ENV 1994-I-I: 1994). It is observed from figure 3-26 that ACI 209 code provisions in comparison with CEB FIB model code-1990 underestimate, to our opinion, the influence of creep on time dependent behaviour of composite steel-concrete beams.

According to our results based on numerous practical examples it can be stated that about 90-92% of the maximum values of the stressed in concrete or steel in time t_∞ are reached after about three years. Besides that 98% are reached after about twenty years in comparison with the period of hundred years obtained by the EMM Method (Partov and Kantchev 2014).

The results between internal forces obtained by numerical methods according to GL2000 model, ACI 209 code and CEB MC90-99 provision are incomparable with each other. It is observed from figure 3-24 that GL2000 model in comparison with CEB MC90-99 provision overestimate, to our opinion, the influence of creep on time dependent behaviour of composite steel-concrete beams. Finally, the creep effect must be carefully evaluated in order to fully understand the behaviour of the structure.

In this paper it is made an attempt to analyze the time dependent behaviour of composite steel-concrete beam with respect to rheological properties of concrete according to world code provisions GL2000, ACI209-R2 and CEB MC 90-99. All three methods lead to deferent results in practical point of view.

The most important conclusion of our investigation is that considering the creep effect, using the integral equations (8,9), (10,11) and (12,13) a universal numerical method has been elaborated for statically determinate bridge composite plate girder according to CEB MC 90-99, ACI 209R-92 and GL2000 models. This method allows the use of a perfect linear theory of concrete creep i. e. the theory of the viscoelastic body of Boltzman-Volttera-Maslov-Arutyunyan-Trost- Bažant.

The age-adjusted effective method (AAMM) (Jirasek and Bažant 2002) and effective modulus method (EMM) mentioned above will be used in our future works as reference approximate method for comparison with our numerical solutions. Besides CEB MC90-99, ACI 209 2R-08 and GL2000 prediction models, also model Bažant – Baweja(B3), (Jirasek&Bažant 2002) will be considered in the examples in future paper.

ACKNOWLEDGEMENT

This article is dedicated to the scientific heritage of the great Italian mathematician Vito Volterra (1860-1940).

REFERENCES

[1] ACI Committee 209, 2008, *"Guide for Modelling and Calculating Shrinkage and Creep in Harden Concrete"*(ACI 209.2R-08)," American Concrete Institute, Farmington Hills, MI, 45pp.

[2] Atkinson, E. K.,1997, *The Numerical Solution of Integral Equations of the Second Kind,* Cambridge University Press, Cambridge, UK, 572 pp.

[3] Bažant Z. P., 1975, "*Theory of Creep and Shrinkage in Concrete Structures: A Précis of Recent Developments"*, Mechanics Today, Vol.2, Pergamon Press, New York, 1975, pp. 1-93.

[4] Bažant, Z. P.; Xi, Y. P.; Baweja, S., and Carol, I., 1993, "Preliminary guidelines and recommendations for characterizing creep and shrinkage in structural design codes", *Proceedings. of the 5th International RILEM Symposium on Creep and Shrinkage of Concrete* (Barcelona), Z. P.Bažant and I. Carol eds., E&FN Spon, London, UK, pp.805-829.

[5] Bažant, Z. P. and Baweja, S., 2000, "Creep and Shrinkage Prediction Model for Analysis and Design of Concrete Structures: Model B3", *Adam Nevile Simposium: Creep and Shrinkage – Structural design Effects,* SP-194, A. Al-Manasereer, ed., American Concrete Institute, Farmington Hills, MI, pp.1-84.

[6] Bažant, Z. P., 2000, "Criteria for Rational Prediction of Creep and Shrinkage of Concrete"*, Adam Neville Symposium: Creep and Shrinkage – Structural Design Effects*, SP-194*,* A. Al-Manaseer ed., American Concrete Institute, Farmington Hills, MI, pp. 237-260.

[7] Branson, D. E., 1977, *Deformation of Concrete Structures*, McGraw Hill Book Co., New York, 546 pp.

[8] Chiorino, M., Sassone, M., Bigaran, D. and Casalegno, C., 2007, "Effects of Creep and Shrinkage on the Serviceability Limit State*", Proceedings of Symposium, Concrete Sructures-Stimulators of Development*, Dubrovnik, May, pp.623-632.

[9] Chiorino, M. A., 2010,"An Internationally harmonized Format for Time dependent Analysis of Concrete Structures", *Proceedings IABSE-FIP Conference,* Dubrovnik, May, V.1, pp.473-480.

[10] Comité Européen de Normalisation (CEN), 2004a "Eurocode 2: Design of Concrete Structures-Part 1-1: General Rules and Rules for Buildings", European Standard BS EN 1992-1-1: 2004, European Committee for Standardization (CEN), Brussels, Belgium, 227 pp.

[11] Comité Européen de Normalisation (CEN), 2004b "Eurocode 4: Design of Composite Steel and Concrete Strucures-Part 1-1:General Rules and Rules for Buildings", European Standard BS EN 1994-1-1: 1994, European Committee for Standardization (CEN), Brussels, Belgium, 118 pp.

[12] Cosenza, E., and Zandonini, R. 1999, *Composite Construction. Structural Engineering Handbook*, C. Wai-Fah, ed., CRC Press, Boca Raton, FL., pp. 1-122.

[13] Dujmović, D.; Androić, B., and Lukačević,I., 2015, "*Composite structures according to Eurocode 4",* Wilhelm Ernst & Sohn Verlag fur Architektur und Technische Wissenschaften, GmbH& Co. KG, Berlin, Germany, 890 pp.

[14] Folić, R., and Zenuvović, D., 2009, "*Composite Structures of Steel and Concrete,* Faculty of Technical Sciences, Novi Sad, Serbija, 362 pp.

[15] Gardner, N. G., and Lockman, M. J., 2001, "Design Provisions for Drying Shrinkage and Creep of Normal Strength Concrete", *ACI Materials Journal*, March-April, pp. 159- 167.

[16] Jirasek, M., and Bažant, Z. P., 2002, *Inelastic Analysis of Structures*, Wiley and Sohns, LTD,

[17] Hoboken, NJ, 732 pp.

[18] Johnson, R.P., 2004, *Composite Structures of Steel and Concrete*, Blackwell, Oxford, UK, 230 pp…..

[19] Oehlers, D., and Bradford, M., 1999, *Elementary behavior of composite steel and concrete stucrural members,* Oxford, Butterworth-Heinemann, 279 pp.

[20] Partov, D., and Kantchev, V., 2009,"Time-dependent analysis of composite steel-concrete beams using integral equation of Volterra, according EUROCODE-4", *Engineering Mechanics,* V. 16, No 5, pp. 367-392*.*

[21] Partov, D., and Kantchev, V., 2011a, "Numerical analysis of composite steel-concrete section using integral equation of Volterra", *Central. European Journal of Engineering,* V.1, No.3, pp. 316-331.

[22] Partov, D., and Kantchev, V., 2011b,"Level of creep sensitivity in composite steel-concrete beams, according to ACI 209R-92 model, comparison with EUROCODE-4(CEB MC90-99)", *Engineering Mechanics*, V. 18, No. 2, pp. 91-116.

[23] Partov, D., and Kantchev, V., 2014,"Gardner and Lockman model in Creep analysis of composite steel-concrete section ", *ACI Structural Journal*, Vol.111, No. 1,(January-February),, pp. 59-69.

[24] Šmerda, Z., and Křistek, Vl., 1988*, Creep and Shrinkage of Concrete Elements and Structures*, Elsevier, New York, 296 pp.

[25] Vayas, I., and Iliopoulos, A., 2014, *"Design of steel-concrete Composite Bridge to Eurocodes",*

[26] CRC Press, Taylor&Francis Group, Boca Raton, FL., 576 pp.

[27] Wang, C. Y., 2002, *Steel and Composite Structures*, *Behavior and Design for Fire Safety*, Taylor and Francis Group, London, UK, 352 pp.

Conversation factors for the units

1 mm = 0.03937 in,
1 N = 0.2248 lbf.
1 kPa = 0.145 lbf/in^2
1 Mpa = 145 psi
1 Nm=8.8507 lbf.in.
1 kN=224.8 lbf.

SUMMARY

COMPARATIVE ANALYSIS OF THE INFLUENCE OF CREEP OF CONCRETE COMPOSITE BEAMS OF STEEL - CONCRETE MODEL BASED ON VOLTERRA INTEGRAL EQUATION

Doncho PARTOV
Vesselin KANTCHEV

The paper presents analysis of the stress-strain behaviour and deflection changes due to creep in statically determinate composite steel-concrete beam according to EUROCODE 2, ACI209R-92 and Gardner&Lockman models. The mathematical model involves the equation of equilibrium, compatibility and constitutive relationship, i.e. an elastic law for the steel part and an integral-type creep law of Boltzmann – Volterra for the concrete part considering the above mentioned models. On the basis of the theory of viscoelastic body of Maslov-Arutyunian–Trost-Zerna-Bažant for determining the redistribution of stresses in beam section between concrete plate and steel beam with respect to time "t", two independent Volterra integral equations of the second kind have been derived. Numerical method based on linear approximation of the singular kernel function in the integral equation is presented. Example with the model proposed is investigated.

Key words: steel-concrete section, integral equations, rheology, creep of concrete, redistribution of stresses, numerical method

REZIME

KOMPARATIVNA ANALIZA UTICAJA TEČENJA BETONA SPREGNUTE GREDE ČELIK – BETON MODELIMA ZASNOVANIM NA INTEGRALNOJ JEDNAČINI VOLTERRA

Doncho PARTOV
Vesselin KANTCHEV

U radu je prikazana analiza odnosa napon-dilatacija i promene ugiba statički određene spregnuta grede čelik – beton prema EVROCODU 2, ACI209R-92 i Gardner&Lockman modelu. Razvijen j matematički model koji uključuje jednačine ravnoteže, kompatibilnosti i konstitutivne veze. Za čelični deo usvojeno je elastično ponašanje, a za betonski integralna veza saglasno zakonu Boltzmann – Volterra uvodeći u analizu napred pomenute modele. Na bazi Teorije visko-elastičnog tela i predloga autora: Maslov-Arutyunian–Trost-Zerna-Bažant, za određivanje preraspodela napona između betona i čelika, u presecima spregnute grede čelik – beton tokom vremena "*t*". Formulisan je matematički model zasnovan na dve nezavisne integralne jednačine Volterra druge vrste. U numeričkom modelu koristi se linearna aproksimacija funkcije jezgra integralne jednačine. Primena modela je ilustrovana kroz primer i primenu predloženog modela.

Ključne reči: spregnuti presek čelik – beton, integralne jednačine, veza napon – dilatacija, reologija, tečenje betona, numerička metoda

PRIMENA METODE DINAMIČKE KRUTOSTI U NUMERIČKOJ ANALIZI SLOBODNIH VIBRACIJA PLOČA SA UKRUĆENJIMA

APPLICATION OF DYNAMIC STIFFNESS METHOD IN NUMERICAL FREE VIBRATION ANALYSIS OF STIFFENED PLATES

Emilija DAMNJANOVIĆ
Miroslav MARJANOVIĆ
Marija NEFOVSKA-DANILOVIĆ
Miloš JOČKOVIĆ
Nevenka KOLAREVIĆ

ORIGINALNI NAUČNI RAD
ORIGINAL SCIENTIFIC PAPER
UDK: 624.073.042.3:534.53
doi:10.5937/grmk1702021D

1 UVOD

Primena građevinskih materijala visokih mehaničkih karakteristika, pre svega čelika, dovodi do smanjenja dimenzija (debljine) konstruktivnih pločastih elemenata. Time se postiže slična nosivost za manji utrošak materijala, kao i ušteda u ceni. Međutim, vitki elementi postaju osetljivi na izbočavanje, što uzrokuje upotrebu ploča sa ukrućenjima.

Ploče sa ukrućenjima imaju široku primenu u građevinarstvu i drugim inženjerskim disciplinama, posebno pri projektovanju, na primer, mostova većih raspona i manjih poprečnih preseka, te izradi oplata brodova, konstrukcija aviona. Tokom svog radnog veka, ove konstrukcije često su izložene dinamičkom opterećenju, te je

Emilija Damnjanović, student doktorskih studija, Univerzitet u Beogradu – Građevinski fakultet, Bulevar kralja Aleksandra 73, 11000 Beograd, Srbija,
e-mail: damnjanovicema@gmail.com, +381 11 3218 581
Miroslav Marjanović, docent, Univerzitet u Beogradu – Građevinski fakultet, Bulevar kralja Aleksandra 73, 11000 Beograd, Srbija, e-mail: mmarjanovic@grf.bg.ac.rs, +381 11 3218 551
Marija Nefovska-Danilović, docent, Univerzitet u Beogradu – Građevinski fakultet, Bulevar kralja Aleksandra 73, 11000 Beograd, Srbija, e-mail: marija@grf.bg.ac.rs, +381 11 3218 552
Miloš Jočković, asistent, Univerzitet u Beogradu – Građevinski fakultet, Bulevar kralja Aleksandra 73, 11000 Beograd, Srbija, e-mail: mjockovic@grf.bg.ac.rs, +381 11 3218 581
Nevenka Kolarević, docent, Univerzitet u Beogradu – Građevinski fakultet, Bulevar kralja Aleksandra 73, 11000 Beograd, Srbija,
e-mail: nevenka@grf.bg.ac.rs, +381 11 3218 551

1 INTRODUCTION

Application of building materials of high mechanical properties (i.e. steel), leads to the reduction of dimensions (thickness) of structural plate-like elements. This maintains the same structural capacity with reduced material cost, as well the price reduction. However, slender elements become vulnerable to buckling, leading to the use of stiffened plates.

Stiffened plates are widely used in civil engineering and other engineering fields, especially in design of long-span bridges with small cross-sections, construction of ship hulls, aircrafts, etc. During their working life, these structures are usually exposed to dynamic loading, thus the calculation of dynamic structural response is of high

Emilija Damnjanovic, PhD Student, University of Belgrade – Faculty of Civil Engineering, Bulevar kralja Aleksandra 73, 11000 Belgrade, Serbia,
e-mail: damnjanovicema@gmail.com, +381 11 3218 581
Miroslav Marjanovic, Assistant Professor, University of Belgrade - Faculty of Civil Engineering, Bulevar kralja Aleksandra 73, 11000 Belgrade, Serbia,
e-mail: mmarjanovic@grf.bg.ac.rs, +381 11 3218 551
Marija Nefovska-Danilovic, Assistant Professor, University of Belgrade - Faculty of Civil Engineering, Bulevar kralja Aleksandra 73, 11000 Belgrade, Serbia,
e-mail: marija@grf.bg.ac.rs, +381 11 3218 552
Milos Jockovic, Teaching Assistant, University of Belgrade - Faculty of Civil Engineering, Bulevar kralja Aleksandra 73, 11000 Belgrade, Serbia, e-mail: mjockovic@grf.bg.ac.rs, +381 11 3218 581
Nevenka Kolarevic, Assistant Professor, University of Belgrade - Faculty of Civil Engineering, Bulevar kralja Aleksandra 73, 11000 Belgrade, Serbia,
e-mail: nevenka@grf.bg.ac.rs, +381 11 3218 551

proračun njihovog dinamičkog odgovora veoma značajan u inženjerskoj praksi. U takvim slučajevima, neophodno je odrediti osnovne dinamičke karakteristike sistema, kao što su sopstvene frekvencije i oblici oscilovanja.

Dinamički odgovor tankih ploča može se odrediti primenom Kirchhoff-ove klasične teorije ploča (*classical plate theory* - CPT). U slučaju debelih ploča, ova teorija ne daje adekvatne rezultate zbog zanemarivanja deformacije smicanja, pa je potrebno primeniti Mindlin-ovu teoriju (*first-order shear deformation theory* - FSDT), koja uzima u obzir uticaj deformacije smicanja, pretpostavljajući da je klizanje konstantno po debljini ploče. Paralelno sa razvojem različitih teorija ploča, razvijale su se i odgovarajuće analitičke metode [1]. Međutim, one se zasnivaju na tačnom rešenju diferencijalnih jednačina kretanja ploča, sa specijalnim uslovima oslanjanja. Leissa [2] je dao sveobuhvatan pregled analitičkih rešenja slobodnih vibracija ploča različitih oblika, zasnovan na Kirchhoff-ovoj klasičnoj teoriji ploča. Liew i ostali [3] analizirali su slobodne vibracije debelih ploča sa proizvoljnim konturnim uslovima, primenom Raylegh-Ritz-ove metode. Primena pomenutih metoda ograničena je na analizu slobodnih vibracija pojedinačnih ploča i ne može se lako proširiti na analizu složenijih sistema ploča sa različitim geometrijskim i materijalnim karakteristikama, kakvi najčešće jesu u inženjerskoj praksi (npr. ploče sa ukrućenjima, sendvič-paneli, ploče promenljive debljine). U takvim slučajevima, u analizi se primenjuju numeričke metode, kao što je metoda konačnih elemenata (MKE) [4]. Poznata je činjenica da u dinamičkoj analizi primenom MKE veličina konačnog elementa zavisi od dužine talasa najviše frekvencije od interesa za analizu. Prema [5, 6], odnos između talasne dužine najviše frekvencije i veličine konačnog elementa trebalo bi da se kreće u granicama između 10 i 20, kako bi se dobili rezultati zadovoljavajuće tačnosti. Minimalan broj konačnih elemenata direktno je proporcionalan najvišoj razmatranoj frekvenciji, pa u slučaju složenih konstrukcija (gde je pri analizi potrebno imati u vidu i više tonove oscilovanja) potreban broj konačnih elemenata postaje veliki, čime se povećava ukupno trajanje proračuna.

U poslednje vreme, za analizu slobodnih vibracija ploča sve češće se koristi metoda dinamičke krutosti (MDK) [7-15]. MDK kombinuje karakteristike MKE - kao što su fizička diskretizacija i mogućnost povezivanja elemenata u jedinstveni globalni sistem - sa rešenjem polja pomeranja, koje predstavlja tačno rešenje diferencijalne jednačine slobodnih vibracija. Kako interpolacione funkcije kojima se opisuje polje pomeranja u MDK predstavljaju tačno rešenje diferencijalne jednačine kretanja u frekventnom domenu, greške usled aproksimacije su eliminisane. Podela ploče na manje dinamičke elemente neophodna je samo ukoliko unutar ploče postoji neki geometrijski i/ili fizički diskontinuitet. Time se smanjuju broj elemenata u analizi, broj stepeni slobode, kao i vreme potrebno za rad i mogućnost javljanja greške, u poređenju s MKE. Za razliku of MKE - gde je masa koncentrisana u čvorovima konačnih elemenata, u MDK masa je kontinualno raspodeljena. Takođe, materijalno prigušenje može se na jednostavan način uključiti u analizu putem kompleksnog modula elastičnosti $E_c = E\,(1+2i\zeta)$, gde je ζ koeficijent relativnog prigušenja.

importance in engineering practice. In these cases, it is necessary to derive fundamental dynamic properties of the system, such as natural frequencies and mode shapes.

Dynamic response of thin plates can be obtained using Kirchhoff classical plate theory (CPT). In the case of thick plates, this theory fails to provide adequate results because the transverse shear deformation is neglected. Therefore, it is necessary to use Mindlin plate theory (first-order shear deformation theory - FSDT), which accounts for the constant transverse shear deformation through the plate thickness. Along with the development of different plate theories, the adequate analytical methods have been derived, too [1]. However, these methods are based on the exact solution of differential equations of motion of plates having special boundary conditions. Leissa [2] provided the comprehensive review of analytical solutions of the free vibration problem for plates of different shape, based on the Kirchhoff classical plate theory. Liew et al. [3] studied the free vibration of thick plates with arbitrary boundary conditions using the Raylegh-Ritz method. The application of the above mentioned methods is restricted to the free vibration analysis of single plates and cannot be easily extended to the analysis of more complex plate assemblies with different geometry and material properties, which are mostly used in engineering practice (stiffened plates, sandwich panels, stepped plates, etc.). In such cases, numerical methods are applied, i.e. the finite element method (FEM) [4]. It is a well-known fact that in the dynamic finite element analysis, the size of the finite element depends on the wavelength of the highest frequency of interest for the analysis. According to [5, 6], the ratio between the wavelength of the highest frequency and the finite element size should be between 10 and 20, in order to obtain the results of satisfactory accuracy. Minimum number of finite elements is directly proportional to the highest considered frequency, thus for the complex structures (where higher modes of vibration must be taken into account), the number of finite elements becomes very high, increasing the overall computational time.

Lately, the dynamic stiffness method (DSM) [7-15] is increasingly used in the free vibration analysis of plates. DSM combines the properties of the FEM (such as physical discretization and the possibility of assembly of single elements into the unique global system) with the solution of the displacement field in the form of exact solution of differential equation of the free vibration problem. Having in mind that interpolation functions which describe the displacement field in the DSM represent the exact solution of the differential equation of motion in the frequency domain, the approximation errors are eliminated. The plate discretization is necessary only if some geometrical and/or physical discontinuity is present. This reduces both the numbers of elements in the analysis and degrees of freedom, as well as computational time and error possibility, in comparison with the FEM. In contrary to the FEM where the mass is lumped in nodes of finite elements, in the DSM the mass is continuously distributed. In addition, material damping can be easily included in the analysis using the complex elasticity modulus $E_c = E(1+2i\zeta)$, where ζ is the relative damping coefficient. Using this

Na taj način, omogućeno je da različiti elementi konstrukcije imaju različito prigušenje, što je još jedna od prednosti MDK u poređenju s MKE.

U okviru ovog rada, prikazan je numerički model za analizu slobodnih neprigušenih vibracija Mindlin-ovih ploča sa ukrućenjima sa proizvoljnim graničnim uslovima, primenom MDK. Na osnovu dinamičkih matrica krutosti za analizu slobodnih poprečnih vibracija i vibracija u ravni, izvedena je matrica rotacije za različite položaje ploča koje su pod pravim uglom u odnosu na referentnu ravan [16]. Primenjen je sličan postupak kao u MKE za formiranje globalne dinamičke matrice krutosti ploče sa ukrućenjima i razvijen je računarski program u MATLAB-u [17] za analizu slobodnih vibracija sistema ploča. Prikazani postupak verifikovan je upoređivanjem tih rezultata sa rezultatima dobijenim primenom programskog paketa Abaqus [18].

2 POSTUPAK FORMIRANJA DINAMIČKE MATRICE KRUTOSTI PRAVOUGAONE PLOČE

Postupak formiranja dinamičke matrice krutosti pravougaonog elementa ploče za poprečne i vibracije u ravni detaljno je prikazan u radovima [13, 15], dok će ovde biti prikazani osnovni koraci u postupku formiranja dinamičke matrice krutosti. Polaznu tačku predstavljaju jednačine kretanja elementa Mindlin-ove ploče u vremenskom domenu:

approach, it is possible that different structural members have different damping values, which is one of the advantages of the DSM in comparison with the FEM.

In the paper, the numerical model for free undamped vibration analysis of stiffened Mindlin plates with arbitrary boundary conditions, based on the DSM, has been presented. Starting from the dynamic stiffness matrices for the free vibration analysis of transverse and in-plane vibrations, rotation matrix for different plate positions (perpendicular to the reference plane), has been derived [16]. Similar procedure as in the FEM has been applied for the development of the global dynamic stiffness matrix of stiffened plate assembly. Computer program in MATLAB [17] has been developed for the free vibration analysis of plate assemblies. The validation of the presented procedure has been performed by comparison of the obtained results with those obtained by using the software package Abaqus [18].

2 PROCEDURE FOR DEVELOPMENT OF DYNAMIC STIFFNESS MATRIX OF RECTANGULAR PLATE

Development of the dynamic stiffness matrix for rectangular plate element undergoing transverse and in-plane vibrations has been given in detail in [13, 15]. In the paper, only the basic steps in the procedure will be presented. The procedure starts from with equations of motion of Mindlin plate element in the time domain:

$$\begin{aligned}
&\frac{\partial^2 u}{\partial x^2}+a_1\frac{\partial^2 u}{\partial y^2}+a_2\frac{\partial^2 v}{\partial x\partial y}=\frac{r\,h}{D_1}\frac{d^2u}{dt^2}\\
&\frac{\partial^2 v}{\partial y^2}+a_1\frac{\partial^2 v}{\partial x^2}+a_2\frac{\partial^2 u}{\partial x\partial y}=\frac{r\,h}{D_1}\frac{d^2v}{dt^2}
\end{aligned} \tag{1a}$$

$$\begin{aligned}
&kGh\left(\frac{\partial^2 w}{\partial x^2}+\frac{\partial^2 w}{\partial y^2}+\frac{\partial f_y}{\partial x}-\frac{\partial f_x}{\partial y}\right)=r\,h\frac{d^2w}{dt^2}\\
&D\left(\frac{\partial^2 f_x}{\partial y^2}-\frac{1+n}{2}\frac{\partial^2 f_y}{\partial x\partial y}+\frac{1-n}{2}\frac{\partial^2 f_x}{\partial x^2}\right)+kGh\left(\frac{\partial w}{\partial y}-f_x\right)=\frac{r\,h^3}{12}\frac{d^2f_x}{dt^2}\\
&D\left(\frac{\partial^2 f_y}{\partial x^2}-\frac{1+n}{2}\frac{\partial^2 f_x}{\partial x\partial y}+\frac{1-n}{2}\frac{\partial^2 f_y}{\partial y^2}\right)-kGh\left(\frac{\partial w}{\partial x}+f_y\right)=\frac{r\,h^3}{12}\frac{d^2f_y}{dt^2}
\end{aligned} \tag{1b}$$

gde u, v, w, f_x, f_y predstavljaju komponentalna pomeranja i rotacije, h je debljina ploče, ρ je gustina, E je modul elastičnosti, G je modul smicanja, n je Poisson-ov koeficijent, $D=Eh^3/12/(1-n^2)$ je krutost ploče na savijanje, $D_1=Eh/(1-n^2)$ je krutost ploče u ravni, $a_1=(1-n)/2$, $a_2=(1+n)/2$ i $k=5/6$ je faktor korekcije smicanja.

Pretpostavlja se da su pomeranja harmonijske funkcije frekvencije ω, odnosno:

where u, v, w, f_x, f_y are the displacement components, h is the plate thickness, ρ is the mass density, E is the modulus of elasticity, G is the shear modulus, n is the Poisson's coefficient, $D=Eh^3/12/(1-n^2)$ is the flexural plate stiffness, $D_1=Eh/(1-n^2)$ is the in-plane plate stiffness, $a_1=(1-n)/2$, $a_2=(1+n)/2$, while $k=5/6$ is the shear correction factor.

It is assumed that the displacements are the harmonic functions of frequency ω, i.e.:

$$\mathbf{u}(x,y,t)=\hat{\mathbf{u}}(x,y,w)e^{iwt} \tag{2}$$

gde $\hat{\mathbf{u}}(x,y,w)$ predstavlja amplitudu polja pomeranja (u, v, w, f_x ili f_y) u frekventnom domenu. Na osnovu ove pretpostavke, jednačine kretanja (1) iz vremenskog domena transformišu se u frekventni domen.

Na slici 1a prikazano je polje pomeranja pravougaone ploče po Mindlin-ovoj teoriji.

where $\hat{\mathbf{u}}(x,y,w)$ is the amplitude of the displacement field (u, v, w, f_x or f_y) in the frequency domain. Using the above assumption, equations of motion (1) are transformed from time to frequency domain.

Figure 1 shows the displacement field of the rectangular plate based on Mindlin plate theory

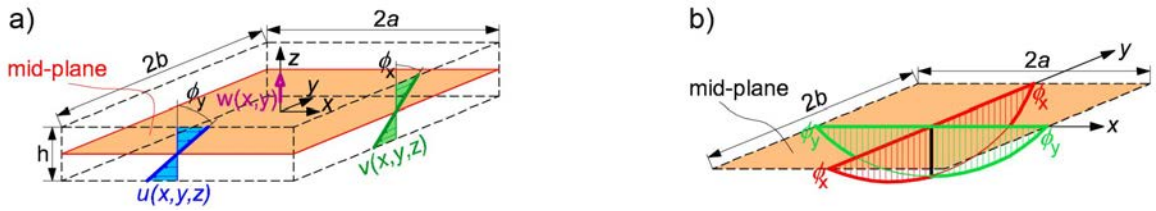

Slika 1. (a) Polje pomeranja u Mindlin-ovoj teoriji i (b) simetrična deformacija ploče (SS)
Figure 1. (a) Displacement field in Mindlin plate theory and (b) double-symmetric plate deformation (SS)

Proizvoljno polje pomeranja može se prikazati kao superpozicija rešenja za četiri slučaja simetrije u odnosu na *x* i *y* koordinatne ose: simetrija-simetrija (SS), simetrija-antimetrija (SA), antimetrija-simetrija (AS) i antimetrija-antimetrija (AA):

Arbitrary displacement field can be represented as a superposition of four symmetry contributions with respect to *x* and *y* coordinate axes: symmetric-symmetric (SS), symmetric-anti-symmetric (SA), anti-symmetric-symmetric (AS) and anti-symmetric-anti-symmetric (AA):

$$\hat{\mathbf{u}}\left(x,y,w\right)=\hat{\mathbf{u}}^{SS}\left(x,y,w\right)+\hat{\mathbf{u}}^{SA}\left(x,y,w\right)+\hat{\mathbf{u}}^{AS}\left(x,y,w\right)+\hat{\mathbf{u}}^{AA}\left(x,y,w\right) \tag{3}$$

Na slici 1b prikazana je simetrična deformacija ploče u odnosu na obe koordinatne ose (SS). Podelom polja pomeranja na četiri slučaja simetrije, moguće je analizirati samo jednu četvrtinu ploče, čime se znatno umanjuje red dinamičkih matrica krutosti i ubrzava proračun. Rešenje jednačina kretanja u frekventnom domenu pretpostavlja se u obliku beskonačnog Fourier-ovog reda u sledećem obliku:

Figure 1b illustrates the double-symmetric plate deformation with respect to both coordinate axes (SS). By dividing the displacement field into four symmetry contributions, it is possible to analyze only a quarter of a plate, which significantly reduces the order of the dynamic stiffness matrices and accelerates the calculation. The solution of the equations of motion in the frequency domain is assumed in the form of an infinite Fourier's series as:

$$\hat{\mathbf{u}}^{ij}\left(x,y,w\right)=\sum_{m=0,1}^{\infty}C_m^{ij}f_m^{ij}\left(x\right)g_m^{ij}\left(y\right) \tag{4}$$

gde su: $f_m^{ij}(x), g_m^{ij}(y)$ bazne trigonometrijske funkcije koje zavise od slučaja simetrije (*i,j*) i rešenja odgovarajućih jednačina kretanja, C_m^{ij} su integracione konstante, a *i*, *j* = *S*, *A*.

Na osnovu poznatih kinematičkih i konstitutivnih relacija ploče, kao i jednačine (4), vektor sila u preseku u proizvoljnoj tački ploče može se napisati u obliku:

where $f_m^{ij}(x), g_m^{ij}(y)$ are the basis trigonometric functions which depend both on symmetry case (*i,j*) and the solution of corresponding equations of motion, C_m^{ij} are the integration constants, while *i*, *j* = *S*, *A*.

Based on the well-known kinematic and constitutive relations of the plate, as well as the equation (4), the force vector in an arbitrary point of the plate can be written as:

$$\hat{\mathbf{f}}^{ij}\left(x,y,w\right)=\sum_{m=0,1}^{\infty}C_m^{ij}f_m^{f,ij}\left(x\right)g_m^{f,ij}\left(y\right) \tag{5}$$

gde su: $f_m^{f,ij}(x), g_m^{f,ij}(y)$ izvodi baznih funkcija u zavisnosti od usvojene teorije ploče.

U praktičnoj primeni, beskonačni red u jednačinama (4) i (5) potrebno je prekinuti u tački *M* (usvojeni broj članova reda), tako da tačnost rešenja praktično zavisi samo od *M*.

Sledeći korak predstavlja formiranje vektora pomeranja $\hat{\mathbf{q}}^{ij}$, na konturama ***x = a*** *i* ***y = b*** četvrtine ploče za svaki od četiri slučaja simetrije, koji se dobijaju zamenom koordinata kontura u jednačinu (4):

where $f_m^{f,ij}(x), g_m^{f,ij}(y)$ are derivations of the base functions depending on assumed plate theory.

For practical purposes, the infinite series in equations (4) and (5) is truncated to point *M* (the number of terms in the series expansion), thus the accuracy of the solution practically depends only on *M*.

The next step is the definition of the displacement vectors $\hat{\mathbf{q}}^{ij}$ along boundaries ***x = a*** *and* ***y = b*** of the quarter of the plate, for each symmetry contribution, which are derived by substituting the boundary coordinates in the equation (4):

$$\hat{\mathbf{q}}^{ij}=\begin{bmatrix}\hat{\mathbf{u}}^{ij}\left(a,y,w\right)\\ \hat{\mathbf{u}}^{ij}\left(x,b,w\right)\end{bmatrix} \tag{6}$$

Na sličan način, vektor sila $\hat{\mathbf{Q}}^{ij}$ na konturama ploče dobija se zamenom koordinata kontura u jednačinu (5):

In a similar manner, the force vector $\hat{\mathbf{Q}}^{ij}$ on the plate boundaries is obtained by replacing the coordinates of the boundaries in equation (5):

$$\hat{\mathbf{Q}}^{ij} = \begin{bmatrix} \hat{\mathbf{f}}^{ij}(a,y,w) \\ \hat{\mathbf{f}}^{ij}(x,b,w) \end{bmatrix} \tag{7}$$

S obzirom da su komponente vektora pomeranja i sila na konturama ploče funkcije prostornih koordinata *x* i *y*, nije moguće direktno uspostaviti vezu između tih vektora - sa jedne strane i vektora integracionih konstanti **C** - sa druge strane. Ovaj problem može se rešiti pomoću metode projekcije koja se bazira na predstavljanju funkcija pomeranja i sila na konturi ploče u vidu Fourier-ovog reda:

Since the components of the displacement and force vectors along plate boundaries are functions of spatial coordinates *x* and *y*, it is impossible to establish a direct relation between these vectors on one side, and the vector of integration constants **C** on the other side. This problem can be solved by using the projection method, which is based on the representation of the displacement and force functions along the plate boundary in the Fourier series form:

$$\begin{aligned} \mathbf{q}^{ij} &= \frac{2}{L}\int_s \mathbf{H}^{ij}\hat{\mathbf{q}}^{ij}ds = \mathbf{D}^{ij}\mathbf{C}^{ij} \\ \mathbf{Q}^{ij} &= \frac{2}{L}\int_s \mathbf{H}^{ij}\hat{\mathbf{Q}}^{ij}ds = \mathbf{F}^{ij}\mathbf{C}^{ij} \end{aligned} \tag{8}$$

gde je $\mathbf{H}^{ij}$ matrica baznih funkcija za odgovarajući slučaj simetrije, *L*=*a* za konturu paralelnu sa *x*-osom, dok je *L*=*b* za konturu paralelnu sa *y*-osom. Eliminacijom vektora integracionih konstanti iz jednačina (8) dobija se dinamička matrica krutosti četvrtine ploče $\mathbf{K}_D^{ij}$ za svaki od četiri slučaja simetrije:

where $\mathbf{H}^{ij}$ is the matrix of the base functions for the symmetry contribution, *L*=*a* for the boundary parallel with x-axis, while *L*=*b* for the boundary parallel with *y*-axis. By eliminating the vector of integration constants from equations (8), the dynamic stiffness matrix of the quarter of the plate $\mathbf{K}_D^{ij}$ is obtained for all four symmetry contributions:

$$\mathbf{Q}^{ij} = \mathbf{F}^{ij}\left(\mathbf{D}^{ij}\right)^{-1}\mathbf{q}^{ij} = \mathbf{K}_D^{ij}\mathbf{q}^{ij} \tag{9}$$

Dinamička matrica krutosti čitave ploče $\mathbf{K}_D$ može se dobiti primenom transfer matrice, kao što je pokazano u radovima [13, 15].

Dynamic stiffness matrix of the entire plate $\mathbf{K}_D$ can be derived using the transfer matrix, as given in Refs. [13, 15].

3 PLOČE SA UKRUĆENJIMA

Poprečne vibracije i vibracije u ravni za jednu izotropnu ploču predstavljaju dva nezavisna stanja. Stoga, dinamička matrica krutosti ploče može se napisati kao:

3 STIFFENED PLATES

Transverse and in-plane vibrations of a single plate represent two independent states. Therefore, the dynamic stiffness matrix of the single plate can be written as:

$$\mathbf{K}_D = \begin{bmatrix} \mathbf{K}_{Dt} & 0 \\ 0 & \mathbf{K}_{Di} \end{bmatrix} \tag{10}$$

gde je $\mathbf{K}_{Dt}$ dinamička matrica krutosti ploče izložene poprečnim vibracijama, dok je $\mathbf{K}_{Di}$ dinamička matrica krutosti ploče za vibracije u ravni.

Saglasno jednačini (10), vektor projekcija pomeranja i sila na konturi ploče može se prikazati u sledećem obliku:

where $\mathbf{K}_{Dt}$ is the dynamic stiffness matrix of plate element for transverse vibrations, while $\mathbf{K}_{Di}$ is the dynamic stiffness matrix of plate element for in-plane vibrations.

According to equation (10), displacement and force projection vectors on the plate boundary can be written in the following form:

$$\hat{\mathbf{q}} = \begin{bmatrix} \hat{\mathbf{q}}_t \\ \hat{\mathbf{q}}_i \end{bmatrix}, \quad \hat{\mathbf{Q}} = \begin{bmatrix} \hat{\mathbf{Q}}_t \\ \hat{\mathbf{Q}}_i \end{bmatrix} \tag{11}$$

U slučaju ploča sa ukrućenjima, gde su ploče međusobno spojene pod pravim uglom, poprečne vibracije jedne ploče izazivaju vibracije u ravni druge ploče i obrnuto. Zbog toga je potrebno uspostaviti vezu između vektora projekcija pomeranja i sila $\hat{\mathbf{q}}$ i $\hat{\mathbf{Q}}$ u lokalnom i vektora $\hat{\mathbf{q}}^*$ i $\hat{\mathbf{Q}}^*$ u globalnom koordinatnom sistemu (slike 2 i 3), pomoću matrice rotacije **T**:

For stiffened plates (where the plates are perpendicular to each other), transverse vibrations of a single plate cause the in-plane vibrations of a corresponding perpendicular plate, and vice versa. Consequently, it is necessary to establish the relation between the projection vectors of displacements $\hat{\mathbf{q}}$ and forces $\hat{\mathbf{Q}}$ in the local, and the corresponding projection vectors $\hat{\mathbf{q}}^*$ and $\hat{\mathbf{Q}}^*$ in the global c. s. (Figures 2 and 3). This is accomplished by using the rotation matrix **T**:

$$\hat{\mathbf{q}} = \mathbf{T}\hat{\mathbf{q}}^*, \quad \hat{\mathbf{Q}} = \mathbf{T}\hat{\mathbf{Q}}^* \tag{12}$$

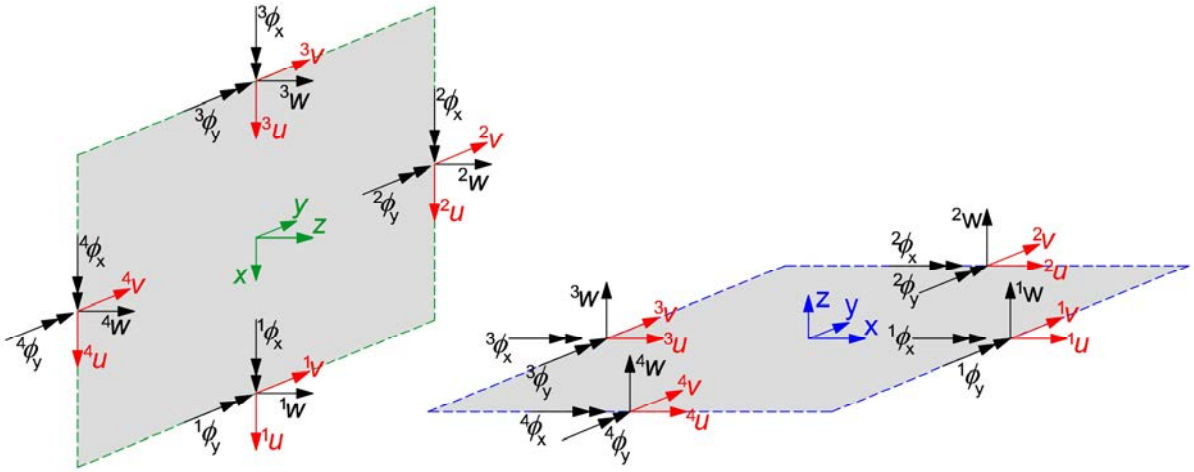

Slika 2. Komponente pomeranja na konturama ploča u lokalnom koordinatnom sistemu
Figure 2. Displacement components on the plate boundaries in the local coordinate system

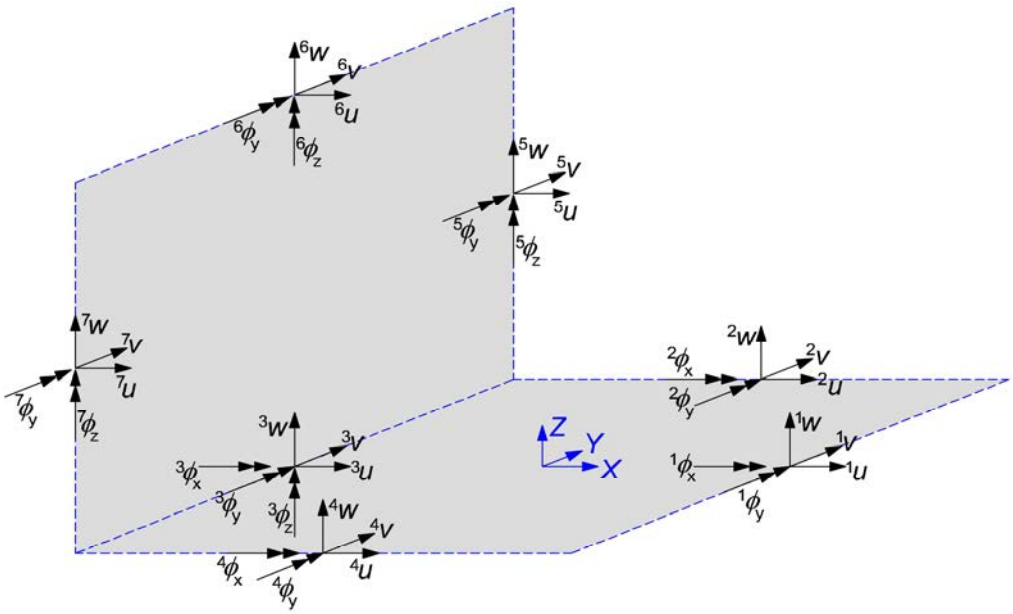

Slika 3. Komponente pomeranja na konturama ploča u globalnom koordinatnom sistemu
Figure 3. Displacement components on the plate boundaries in the global coordinate system

U skladu sa definisanim relacijama projekcija u lokalnom i globalnom koordinatnom sistemu, dinamička matrica krutosti ploče u globalnom koordinatnom sistemu dobija se kao:

According to the established relations between the projection vectors in the local and global coordinate systems, dynamic stiffness matrix of the plate in global coordinate system is derived as:

$$\mathbf{K}_D^* = \mathbf{T}^T \mathbf{K}_D \mathbf{T} \tag{13}$$

Dinamičke matrice krutosti pojedinačnih ploča sabiraju se u globalnu dinamičku matricu krutosti sistema ploča, slično kao u MKE, s tom razlikom što su ploče povezane duž kontura, umesto u čvorovima. U analizi je moguće primeniti proizvoljne granične uslove.

Dinamička matrica krutosti je kvadratna, frekventno zavisna matrica čiji red zavisi od broja članova reda *M* usvojenog rešenja. Sopstvene frekvencije određuju se iz sledeće jednačine:

Dynamic stiffness matrices of individual plates are assembled in the global dynamic stiffness matrix of the plate assembly, using similar assembly procedure as in the conventional FEM. Note that the plates are connected along the boundaries instead at nodes. In the analysis, arbitrary boundary conditions can be applied.

The dynamic stiffness matrix is the square, frequency-dependent matrix whose size depends on the number of terms *M* in the general solution. The natural frequencies can be determined from the following equation:

$$\det\left|\mathbf{K}_{DG,nn}^*(w)\right| = 0 \tag{14}$$

gde je $\mathbf{K}_{DG,nn}^*$ globalna dinamička matrica krutosti sistema uz nepoznata pomeranja.

Kako elementi dinamičke matrice krutosti $\mathbf{K}_{DG,nn}^*$ sadrže transcedentne funkcije, rešenja se mogu dobiti primenom neke od tehnika pretraživanja. Kako bi se izbegle numeričke poteškoće prilikom određivanja nule jednačine (14), sopstvene frekvencije mogu se odrediti kao maksimumi izraza:

where $\mathbf{K}_{DG,nn}^*$ is the global dynamic stiffness submatrix of the plate assembly related to the unknown generalized displacement projections.

Since the elements of the dynamic stiffness matrix $\mathbf{K}_{DG,nn}^*$ contain transcendental functions, the solutions can be obtained applying some of the search methods. To avoid numerical difficulties when calculating the zeroes of equation (14), the natural frequencies can be determined as maxima of the following expression:

$$g(w) = \log \frac{1}{\det\left|\mathbf{K}_{DG,nn}^*(w)\right|} \tag{15}$$

4 NUMERIČKI PRIMERI

Primena metode dinamičke krutosti u analizi slobodnih vibracija ploča sa ukrućenjima ilustrovana je u narednim primerima. Na osnovu izloženog postupka, napisan je program u MATLAB-u [17] za određivanje sopstvenih frekvencija i oblika oscilovanja ploča sa ukrućenjima za različite uslove oslanjanja. Dobijeni rezultati upoređeni su sa rezultatima dobijenim primenom komercijalnog programa Abaqus [18].

U prvom primeru, razmatran je armirano-betonski nosač sandučastog poprečnog preseka, (E = 31.5 *GPa*, n = 0.2 i r = 2500 *kg/m*^{3}), čija su geometrija i granični uslovi prikazani na slici 4a. Ploča je podeljena na devet elemenata, što predstavlja minimalni broj elemenata u ovom slučaju, sa obzirom na geometriju nosača. Ukupan broj kontura je 26. Konture paralelne sa *x*- i *z*-osom slobodno su oslonjene (S_x, S_z), dok su konture paralelne sa *y*-osom slobodne (F) ili uklještene (C). Granični uslovi na konturama zadati su na sledeći način:

- slobodno oslonjena ivica paralelna sa *x*-osom (S_x): $u=v=w=f_y=f_z=0$,
- slobodno oslonjena ivica paralelna sa *z*-osom (S_z): $u=v=w=f_x=f_y=0$,

4 NUMERICAL EXAMPLES

Application of the dynamic stiffness method in the free vibration analysis of stiffened plates is illustrated in the following examples. In order to validate the presented method based on the DSM, a computer code in MATLAB [17] was developed for the free vibration analysis of stiffened plates with arbitrary boundary conditions. The results were compared with the results obtained using Abaqus [18].

The first example is concerned with a reinforced concrete girder of a box cross-section, (E = 31.5*GPa*, n = 0.2 and r = 2500*kg/m*^{3}). The geometry and boundary conditions are presented in Figure 4a. In this case, the number of dynamic stiffness elements is equal to 9 (which is minimal number of elements), while the number of boundary lines is 26. Boundary lines parallel to *x*- and *z*-axis are simply supported (S_x, S_z), while the boundary lines parallel to *y*-axis are either free (F) or clamped (C). Boundary conditions are assigned in the following way:

- simply supported edge parallel to *x*-axis (S_x): $u=v=w=f_y=f_z=0$,
- simply supported edge parallel to *z*-axis (S_z): $u=v=w=f_x=f_y=0$,

• uklještena ivica paralelna sa *y*-osom (C): $u=v=w=f_x=f_y=f_z=0$,

• slobodna ivica paralelna sa *y*-osom (F): $f_z=0$.

Prvih deset sopstvenih frekvencija $f = w/2p$ sračunato je primenom različitog broja članova reda, kako bi se utvrdila konvergencija rešenja. Rezultati su prikazani u Tabeli 1 i upoređeni sa numeričkim rešenjem dobijenim primenom 46250 konačnih elemenata tipa S4R u Abaqus-u (dimenzija elemenata 0.1 *m*). Za rešenje s M=7 članova reda, sračunato je odstupanje D od rešenja u Abaqus-u.

• clamped edge parallel to *y*-axis (C): $u=v=w=f_x=f_y=f_z=0$,

• free edge parallel to *y*-axis (F): $f_z=0$.

In order to check the convergence of the proposed method, the first ten natural frequencies $f = w/2p$ have been calculated using different number of terms in the general solution. The results are presented in Table 1 and compared with the numerical solutions obtained using 46250 Abaqus S4R type plate elements (element size 0.1 *m*). For the solutions with M = 7 terms in the series expansion, the differences D from the solutions obtained in Abaqus are calculated.

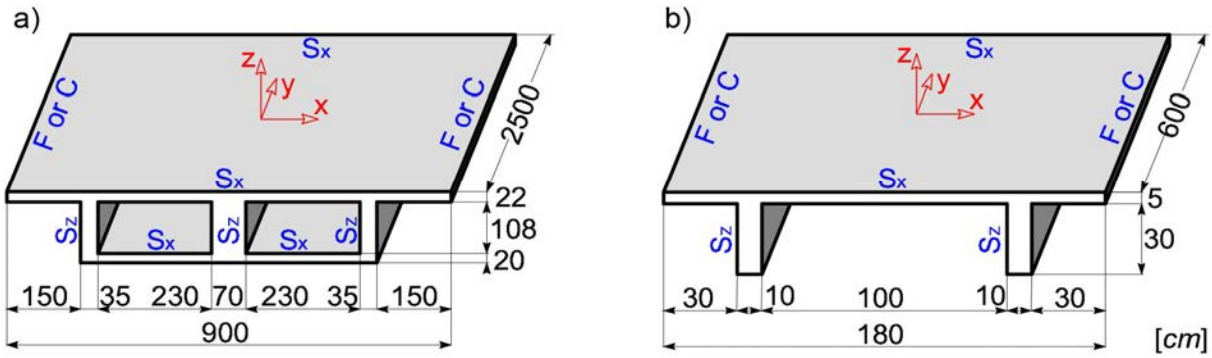

Slika 4. Geometrija i granični uslovi: (a) armirano-betonskog nosača sandučastog preseka i (b) armirano-betonske korube

Figure 4. Geometry and boundary conditions of: (a) reinforced concrete girder with box cross-section and (b) reinforced concrete ribbed slab

Prvih deset sopstvenih frekvencija odlično se poklapaju sa rešenjem dobijenim primenom MKE (prosečno odstupanje je 0.33% za slučaj S-F-S-F, odnosno 2.67% za slučaj S-C-S-C), što potvrđuje izuzetne mogućnosti primene izvedenih dinamičkih matrica krutosti u analizi vibracija armirano-betonskih ploča, čak i kada se uzme u obzir mali broj članova reda (M=7). Diskretizacija modela svedena je na minimum, čime se smanjuje ukupno trajanje proračuna u poređenju sa klasičnom metodom konačnih elemenata.

The first ten natural frequencies computed using the proposed method are in excellent agreement with the results obtained using the FEM (the average difference is 0.33% for S-F-S-F and 2.67% for S-C-S-C case), which confirms the exceptional possibilities of the application of the dynamic stiffness method in the free vibration analysis of reinforced concrete plates, even for a small number of terms in the general solution (M=7). Discretization of the model is reduced to a minimum, thus the computational time have been significantly decreased in comparison with the FEM.

Tabela 1. Sopstvene frekvencije [Hz] armirano-betonskog nosača sandučastog preseka
Table 1. Dimensionless natural frequencies [Hz] of reinforced concrete girder of a box cross-section

n	S – F – S – F						S – C – S – C					
	DSM				Abaqus	D [%]	DSM				Abaqus	D [%]
	M=1	*M*=3	*M*=5	*M*=7			*M*=1	*M*=3	*M*=5	*M*=7		
1	7.8	10.0	9.9	9.9	9.9	0.35	7.8	17.6	17.5	17.5	16.8	4.06
2	8.6	16.8	16.7	16.6	16.6	0.29	8.6	31.0	30.8	30.7	29.2	5.31
3	9.7	24.3	23.9	23.8	23.7	0.52	9.6	33.3	33.2	33.2	32.9	1.01
4	10.2	27.7	27.4	27.3	27.2	0.45	12.1	34.0	39.2	39.1	38.8	0.85
5	12.1	27.9	27.8	27.7	27.7	-0.05	13.3	36.3	42.6	42.5	41.5	2.35
6	13.3	31.0	29.1	29.0	28.9	0.40	14.0	39.2	47.7	47.5	45.5	4.32
7	13.6	33.8	37.9	37.8	37.6	0.59	16.0	43.0	50.8	50.7	50.5	0.35
8	14.0	34.0	38.1	38.0	37.9	0.24	17.9	43.2	52.6	52.4	51.2	2.33
9	16.0	36.3	39.0	38.9	38.7	0.41	18.3	45.4	57.0	56.9	55.4	2.79
10	17.6	38.4	43.7	43.7	43.7	0.04	20.2	48.3	64.5	64.0	61.9	3.32

U drugom primeru, razmatrane su slobodne vibracije armirano-betonske korube (E = 31.5 *GPa*, n = 0.2 i r = 2500 *kg/m*^{3}), čija su geometrija i granični uslovi prikazani na slici 4b. Ploča je diskretizovana sa pet elemenata (16 kontura). Prvih deset sopstvenih frekvencija $f = w/2p$ sračunate su primenom različitog broja članova reda. Rezultati su prikazani u Tabeli 2 i upoređeni sa MKE rešenjem dobijenim primenom 23520 konačnih elemenata tipa S4R u Abaqus-u (dimenzija elemenata 0.025 m). Za rešenje sa M=7 članova reda, sračunato je odstupanje D od rešenja u Abaqus-u. Kao i u prethodnom primeru, sračunate frekvencije primenom prikazanog modela se odlično poklapaju sa numeričkim rešenjem (prosečno Δ = 0.22% za slučaj S-F-S-F, odnosno 0.14% za slučaj S-C-S-C).

The second example is concerned with the reinforced concrete ribbed slab, (E = 31.5*GPa*, n = 0.2 and r = 2500*kg/m*^{3}), whose geometry and boundary conditions are presented in Figure 4b. In this case the number of dynamic stiffness elements is equal to 5, while the number of boundary lines is equal to 16. The first ten natural frequencies $f = w/2p$ have been calculated using different number of terms in the general solution. The results are presented in Table 2 and compared with the FEM numerical solutions obtained using 23520 Abaqus S4R type plate element (element size 0.025 *m*). For the solutions with M = 7 terms in the series expansion, the differences D from the solutions obtained using Abaqus are calculated. As in the previous example, the natural frequencies computed using the proposed method are in excellent agreement with the FEM (the average difference is 0.22% for S-F-S-F and 0.14% for S-C-S-C case).

Tabela 2. Sopstvene frekvencije [Hz] armirano-betonske korube
Table 2. Dimensionless natural frequencies [Hz] of reinforced concrete ribbed slab

n	S – F – S – F						S – C – S – C					
	DSM				Abaqus	D [%]	DSM				Abaqus	D [%]
	M=1	M=3	M=5	M=7			M=1	M=3	M=5	M=7		
1	33.9	33.0	32.9	32.9	32.8	0.34	34.0	57.7	57.5	57.5	57.5	0.03
2	36.4	35.5	35.4	35.3	35.3	0.14	40.7	85.7	84.9	84.7	84.5	0.20
3	40.7	55.4	58.0	57.9	57.9	-0.06	52.3	110.8	110.7	110.7	110.7	-0.02
4	52.2	77.8	76.9	76.7	76.5	0.32	52.7	116.6	115.7	115.4	115.1	0.22
5	52.6	87.2	86.2	85.9	85.5	0.43	58.4	129.8	141.6	141.2	141.0	0.13
6	60.0	91.7	90.5	90.1	89.8	0.29	59.7	134.9	145.7	145.4	145.1	0.21
7	67.1	96.9	96.3	96.1	95.8	0.27	67.3	137.3	155.1	164.6	164.5	0.03
8	78.4	109.7	108.6	108.3	108.3	0.05	78.8	144.4	189.0	188.9	189.0	-0.04
9	79.4	129.3	133.1	132.7	132.3	0.29	79.6	146.7	200.3	199.6	199.1	0.27
10	82.8	133.9	136.1	135.6	135.6	0.01	82.7	155.8	201.6	201.6	202.0	-0.22

Na slici 5 izvršeno je upoređivanje pojedinih oblika oscilovanja i odgovarajućih sopstvenih frekvencija (tonovi 2, 4, 7 i 8) armirano-betonske korube, za kombinaciju konturnih uslova S-C-S-C i M=7 članova reda. Oblici oscilovanja sračunati su primenom originalnog programa u MATLAB-u – zasnovanog na metodi dinamičke krutosti, kao i primenom komercijalnog programa Abaqus. Dobijeno je odlično poklapanje oblika oscilovanja.

Kako bi se ilustrovala prednost MDK u odnosu na MKE - u pogledu potrebnog vremena za proračun, uporediće se broj stepeni slobode u numeričkom modelu sandučastog nosača, formulisanog prema MDK i prema MKE. Treba imati u vidu i to da broj stepeni slobode u MDK zavisi od broja kontura i broja članova reda M, dok u MKE zavisi od broja čvorova i tipa elementa (u razmatranom primeru, konačni element ima 6 stepeni slobode u čvoru). Broj stepeni slobode u MDK (za M=7) i MKE je prema gorenavedenom:

Figure 5 illustrates the comparison of some mode shapes and the corresponding natural frequencies (modes 2, 4, 7 and 8) of the reinforced-concrete ribbed slab, for the combination of boundary conditions S-C-S-C and M=7 terms in the series expansion. Mode shapes have been calculated using the original MATLAB code based on the dynamic stiffness method, as well as by using the commercial software Abaqus. Excellent agreement has been obtained.

To illustrate the advantage of the DSM in comparison with the FEM by means of the necessary computational time, number of degrees of freedom in the numerical model of the girder with the box cross-section, formulated using the DSM or the FEM, will be compared. It is worth mentioning that the number of degrees of freedom in the DSM depends on the number of contours and number of terms in series expansion M, while in the FEM it depends on the number of nodes and the element type (in the considered example, the finite element has 6 nodal degrees of freedom). Number of degrees of freedom in the DSM (for M=7)and the FEM is therefore:

$$NDOF_{DSM} = N_{contours} \cdot (9M + 18) = 26 \cdot (9 \cdot 7 + 18) = 1924$$
$$NDOF_{FEM} = N_{nodes} \cdot 6 = 46250 \cdot 6 = 277500 \quad (16)$$

što pokazuje potencijal prikazane metode u smislu potrebnog vremena proračuna.

that confirms the potential of the presented method by means of the necessary computational time.

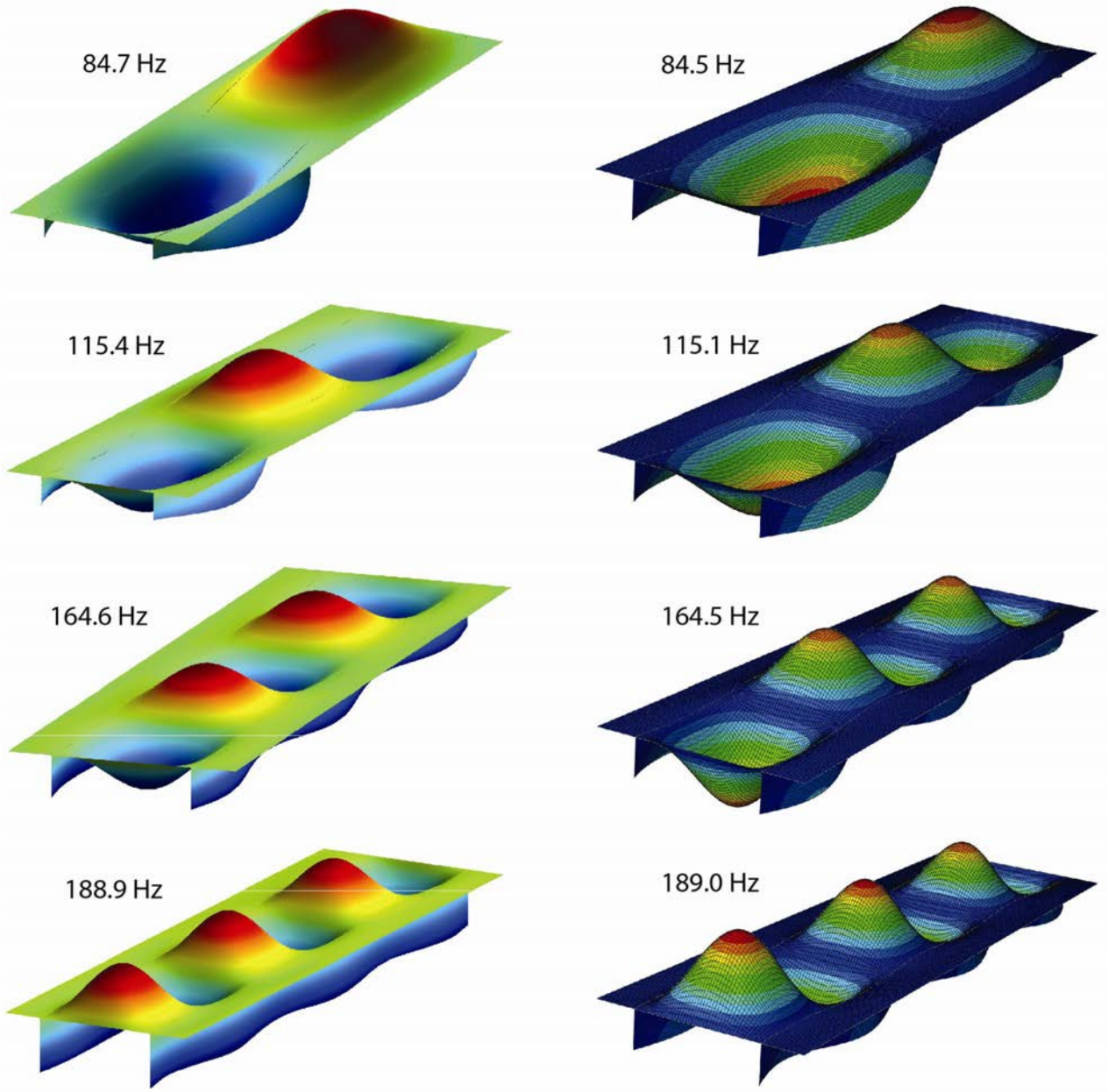

Slika 5. Oblici oscilovanja i odgovarajuće sopstvene frekvencije armirano-betonske korube (slučaj S-C-S-C, M=7): (a) metoda dinamičke krutosti i (b) Abaqus

Figure 5. Mode shapes and corresponding natural frequencies of reinforced-concrete ribbed slab (S-C-S-C case, M=7): (a) dynamic stiffness method and (b) Abaqus

5 ZAKLJUČAK

U ovom radu prikazana je primena metode dinamičke krutosti u analizi slobodnih vibracija ploča sa ukrućenjima. Takođe, prikazan je postupak dobijanja dinamičke matrice krutosti ploče, kao i matrica rotacije za različite položaje ploča koje su pod pravim uglom u odnosu na referentnu ravan. Primenjen je sličan postupak kao u MKE za formiranje globalne dinamičke matrice krutosti ploče sa ukrućenjima. Razvijen je računarski program u MATLAB-u za analizu slobodnih vibracija sistema ploča. Sopstvene frekvencije i oblici oscilovanja određeni su za različite kombinacije konturnih uslova.

5 CONCLUSION

This paper deals with the application of the dynamic stiffness method in the free vibration analysis of stiffened plates. The procedure for the development of dynamic stiffness matrix of rectangular plate, as well as rotation matrices for different plate orientations and perpendicularly oriented with respect to the reference plane, has been provided. The similar procedure as in the FEM for the development of the global dynamic stiffness matrix of the stiffened plate, has been applied. Computer program in MATLAB has been developed for the free vibration analysis of plate assemblies. The natural

Dobijeni rezultati verifikovani su upoređivanjem sa rezultatima dobijenim primenom programskog paketa Abaqus zasnovanog na MKE. Tačnost rezultata dobijenih primenom MDK zavisi isključivo od broja članova reda usvojenog rešenja. Uočena je brza konvergencija rezultata dobijenih po MDK. Već sa tri člana do pet članova reda, dobijaju se rezultati visoke tačnosti. Međutim, za više tonove oscilovanja - povećava se broj potrebnih članova reda.

Na osnovu dobijenih rezultata, može se zaključiti da MDK poseduje veliki potencijal u dinamičkoj analizi konstrukcija, koji se može proširiti na analizu ploča i ljuski zasnovane na teoriji višeg reda, ploče spojene pod proizvoljnim uglom, kao i konstruktivne elemente sačinjene od modernih kompozitnih materijala.

frequencies and mode shapes were calculated for various combinations of boundary conditions. Verification of the results was performed by comparing the results obtained using Abaqus software package based on the FEM. The accuracy of the results obtained by the DSM depends solely on the number of terms in the series expansion of the adopted solution. Rapid convergence of the results obtained by the DSM has been detected. By using only three to five terms, the results of high accuracy have been obtained. However, for the higher modes of vibration, the number of required members in the series expansion should be increased.

Based on these results, it can be concluded that the DSM has great potential in the dynamic analysis of structures that can be extended to the analysis of plates and shells using higher-order theory, the plates connected with arbitrary angles, as well as for the structural elements made of modern composite materials.

ZAHVALNICA

Autori zahvaljuju Ministarstvu prosvete, nauke i tehnološkog razvoja Republike Srbije na finansijskoj podršci u okviru projekata TR-36046 i TR-36048.

ACKNOWLEDGMENTS

The authors express the gratitude to the Ministry of Education, Science and Technological Development of the Republic of Serbia for the financial support under the projects TR-36046 and TR-36048.

6 LITERATURA REFERENCES

[1] Leissa AW. Vibration of plates. National Aeronautics and Space Administration, Washington; 1969.
[2] Leissa AW. The free vibration of rectangular plates. Journal of Sound and Vibration, Vol. 31, No. 3, 1973, pp.257-293.
[3] Liew KM, Xiang Y, Kitipornchai S. Transverse vibration of thick rectangular plates – I. Comprehensive sets of boundary conditions. Computers & Structures, Vol. 49, No. 1, 1993, pp.1-29.
[4] Bathe KJ, Wilson E. Numerical method in finite element analysis. Prentice-Hall; 1976.
[5] Alford RM, Kelly KR, Boore DM. Accuracy of finite difference modeling of the acoustic wave equation. Geophysics, 1974: 834-842.
[6] Lysmer J. Analytical Procedures in Soil Dynamics. Report No EERC-78/29, University of California, Berkeley, 1978.
[7] Doyle JF. Wave propagation in structures. Springer-Verlag, New York; 1997.
[8] Boscolo M, Banerjee JR. Dynamic stiffness elements and their application for plates using first order shear deformation theory. Computers & Structures, Vol. 89, 2011, pp.395-410.
[9] Boscolo M, Banerjee JR. Dynamic stiffness formulation for composite Mindlin plates for exact modal analysis of structures. Part I: Theory. Computers & Structures, Vol. 96-97, 2012, pp.61-73.
[10] Boscolo M, Banerjee JR. Dynamic stiffness formulation for composite Mindlin plates for exact modal analysis of structures. Part II: Results and application, Computers & Structures, Vol. 96-97, 2012, pp.74-83.
[11] Fazzolari F, Boscolo M, Banerjee JR. An exact dynamic stiffness elementa using a higher order shear deformation theory for free vibration analysis of composite plate assemblies. Composite Structures, Vol. 96, 2013, pp.262-278.
[12] Boscolo M, Banerjee JR. Layer-wise dynamic stiffness solution for free vibration analysis of laminated composite plates. Journal of Sound and Vibration, Vol. 333, 2014, pp.200-227.
[13] Kolarević N, Nefovska-Danilović M, Petronijević M. Dynamic stiffness elements for free vibration analysis of rectangular Mindlin plate assemblies. Journal of Sound and Vibration, Vol. 359, 2015, pp.84-106.
[14] Kolarević N, Marjanović M, Nefovska-Danilović M, Petronijević M. Free vibration analysis of plate assemblies using the dynamic stiffness method based on the higher order shear deformation theory. Journal of Sound and Vibration, Vol. 364, 2016, pp.110-132.
[15] Nefovska-Danilović M, Petronijević M. In-plane free vibration and response analysis of isotropic rectangular plates using dynamic stiffness method. Computers & Structures, Vol. 152, 2015, 82-95.
[16] Damnjanović E. Slobodne vibracije ploče sa ukrućenjima primenom Metode spektralnih elemenata. MSc Thesis, Faculty of Civil Engineering, University of Belgrade; 2015.
[17] MathWorks Inc. The Language of Technical Computing, MATLAB 2011b, 2011.
[18] Abaqus: User manual. Version 6.9, Providence, RI, USA: DS SIMULIA Corp, 2009.

REZIME

PRIMENA METODE DINAMIČKE KRUTOSTI U NUMERIČKOJ ANALIZI SLOBODNIH VIBRACIJA PLOČA SA UKRUĆENJIMA

Emilija DAMNJANOVIĆ
Miroslav MARJANOVIĆ
Marija NEFOVSKA DANILOVIĆ
Miloš JOČKOVIĆ
Nevenka KOLAREVIĆ

U okviru ovog rada, analizirane su slobodne vibracije ploča sa ukrućenjima, primenom metode dinamičke krutosti. Formulisan je pravougaoni element Mindlin-ove ploče, zasnovan na metodi dinamičke krutosti. Primenom matrica rotacije, formirane su dinamičke matrice krutosti pojedinačnih ploča u globalnom koordinatnom sistemu. Korišćenjem sličnog postupka kao u metodi konačnih elemenata, izvedena je globalna dinamička matrica krutosti sistema ploča. Određene su sopstvene frekvencije ploča sa ukrućenjima za različite konturne uslove i upoređene sa vrednostima dobijenim u komercijalnom programskom paketu Abaqus. Dobijeni su rezultati visoke tačnosti.

Ključne reči: slobodne vibracije, dinamička matrica krutosti, ploče sa ukrućenjima

SUMMARY

APPLICATION OF DYNAMIC STIFFNESS METHOD IN NUMERICAL FREE VIBRATION ANALYSIS OF STIFFENED PLATES

Emilija DAMNJANOVIC
Miroslav MARJANOVIC
Marija NEFOVSKA-DANILOVIC
Milos JOCKOVIC
Nevenka KOLAREVIC

The free vibration analysis of stiffened plate assemblies has been performed in this paper by using the dynamic stiffness method. Rectangular Mindlin plate dynamic stiffness element has been formulated. Using the rotation matrices, dynamic stiffness matrices of single plates have been derived in global coordinate system. The global dynamic stiffness matrix of plate assembly has been derived by using similar assembly procedure as in the finite element method. The natural frequencies of stiffened plate assemblies with different boundary conditions have been computed and validated against the results obtained by using the commercial software package Abaqus. High accuracy of the results has been demonstrated.

Key words: free vibrations, dynamic stiffness matrix, stiffened plates

METODE ISPITIVANJA I TEHNIČKI USLOVI ZA SISTEME ŠINSKIH PRIČVRŠĆENJA ZA BETONSKE PRAGOVE

TEST METHODS AND REQUIREMENTS FOR FASTENING SYSTEMS FOR CONCRETE SLEEPERS

Milica VILOTIJEVIĆ
Zdenka POPOVIĆ
Luka LAZAREVIĆ

STRUČNI RAD
PROFESSIONAL PAPER
UDK: 625.142.4
doi:10.5937/grmk1702033V

1 UVOD

Harmonizacija tehničke regulative u oblasti železničke infrastrukture još uvek je u toku u Republici Srbiji. Evropski komitet za standardizaciju (*European Committee for Standardization - CEN*) izradio je seriju standarda EN 13481 – *Primene na železnici – Kolosek – Tehnički uslovi za sisteme pričvršćenja*, koja se sastoji iz sledećih osam delova:

– Deo 1: Definicije [1];
– Deo 2: Sistemi šinskih pričvršćenja za betonske pragove [2];
– Deo 3: Sistemi šinskih pričvršćenja za drvene pragove [3];
– Deo 4: Sistemi šinskih pričvršćenja za čelične pragove [4];
– Deo 5: Sistemi šinskih pričvršćenja za konstrukciju koloseka bez zastora, sa šinom položenom na gornju površinu ili u kanalu ploče [5];
– Deo 6 (nacrt evropskog standarda): Specijalni sistemi šinskih pričvršćenja za prigušenje vibracija [6];
– Deo 7: Specijalni sistemi šinskih pričvršćenja za skretnice, ukrštaje i šine vođice [7];

Asistent Milica VILOTIJEVIĆ, msr.inž.građ.
Univerzitet u Beogradu, Građevinski fakultet,
Bulevar kralja Aleksandra 73, Beograd, Srbija,
mvilotijevic@grf.bg.ac.rs
Prof. dr Zdenka POPOVIĆ, dipl.građ.inž.
Univerzitet u Beogradu, Građevinski fakultet,
Bulevar kralja Aleksandra 73, Beograd, Srbija
zdenka@grf.bg.ac.rs
Doc. dr Luka LAZAREVIĆ, msr.inž.građ.
Univerzitet u Beogradu, Građevinski fakultet,
Bulevar kralja Aleksandra 73, Beograd, Srbija
llazarevic@grf.bg.ac.rs

1 INTRODUCTION

Harmonization of technical regulation in the area of railway infrastructure is still in progress in the Republic of Serbia. European Committee for Standardization (CEN) has created a group of standards EN 13481 - *Railway applications - Track - Performance requirements for fastening systems*, which consists of eight parts as listed below:

– Part 1: Definitions [1],
– Part 2: Fastening systems for concrete sleepers [2],
– Part 3: Fastening systems for wood sleepers [3],
– Part 4: Fastening systems for steel sleepers [4],
– Part 5: Fastening systems for slab track with rail on the surface or rail embedded in a channel [5],
– Part 6 (European Prestandard): Special fastening systems for attenuation of vibration [6],
– Part 7: Special fastening systems for switches and crossings and check rails [7],
– Part 8: Fastening systems for track with heavy axle loads [8].

Teaching assistant Milica VILOTIJEVIĆ, MSc Civil Eng.,
University of Belgrade, Faculty of Civil Engineering,
Bulevar kralja Aleksandra 73, Belgrade, Serbia,
mvilotijevic@grf.bg.ac.rs
Professor Zdenka POPOVIĆ, PhD Civil Eng.,
University of Belgrade, Faculty of Civil Engineering,
Bulevar kralja Aleksandra 73, Belgrade, Serbia,
zdenka@grf.bg.ac.rs
Assistant professor Luka LAZAREVIĆ, PhD Civil Eng.,
University of Belgrade, Faculty of Civil Engineering,
Bulevar kralja Aleksandra 73, Belgrade, Serbia
llazarevic@grf.bg.ac.rs

– Deo 8: Sistemi šinskih pričvršćenja za velika osovinska opterećenja [8].

Gorepomenute delove – od 1 do 8 – usvojio je Institut za standardizaciju Srbije (ISS) [9], kao što je prikazano u tabeli 1. Srpska serija standarda SRPS EN 13481 identična je sa evropskom serijom standarda EN 13481.

Pored toga, serija standarda EN 13146 – *Primene na železnici – Kolosek – Postupci ispitivanja sistema šinskih pričvršćenja* podržava zahteve iz serije EN 13481 i sastoji se iz sledećih delova:

– Deo 1: Određivanje otpora podužnom pomeranju šine [10];
– Deo 2: Određivanje otpora zaokretanju šine [11];
– Deo 3: Određivanje prigušenja udarnog opterećenja [12];
– Deo 4: Ispitivanje uticaja ponavljanja opterećenja [13];
– Deo 5: Određivanje električnog otpora [14];
– Deo 6: Uticaj agresivne sredine [15];
– Deo 7: Određivanje sile pritezanja [16];
– Deo 8: Ispitivanje pod saobraćajem [17];
– Deo 9: Određivanje krutosti [18].

Delovi od 1 do 9 serije standarda EN 13146 usvojio je ISS [19], kao što je prikazano u tabeli 2. Srpska serija standarda SRPS EN 13146 identična je sa evropskom serijom standarda EN 13146.

The above mentioned parts 1 - 8 are adopted by the Institute for standardization of Serbia (ISS) [9], as shown in Table 1. SRPS EN 13481 Serbian standard series is identical with EN 13481 European Standard series.

In addition, EN 13146 - *Railway applications - Track - Test methods for fastening systems* supports the requirements defined in EN 13481 series and consists of the following parts:

– Part 1: Determination of longitudinal rail restraint [10],
– Part 2: Determination of torsional resistance [11],
– Part 3: Determination of attenuation of impact loads [12],
– Part 4: Effect of repeated loading [13],
– Part 5: Determination of electrical resistance [14],
– Part 6: Effect of severe environmental conditions [15],
– Part 7: Determination of clamping force [16],
– Part 8: In service testing [17],
– Part 9: Determination of stiffness [18].

The parts 1 - 9 of EN 13146 standard series are adopted by the ISS [19], as shown in Table 2. SRPS EN 13146 Serbian standard series is identical with the EN 13146 European Standard series.

Tabela 1. Trenutno stanje srpske serije standarda SRPS EN 13481 prema [9]
Table 1. The latest stage of SRPS EN 13481 Serbian standard series according to [9]

Srpska oznaka standarda, naslov (*Serbian standard designation, title*)	Status u Srbiji (*Status in Serbia*)	Identičan kao evropski standard (*Identical with European standard*)
SRPS EN 13481-1:2013, Primene na železnici - Kolosek - Tehnički uslovi za sisteme šinskih pričvršćenja - Deo 1: Definicije	Objavljen (*Published*) 24.06.2013	EN 13481-1:2012, Railway applications - Track - Performance requirements for fastening systems - Part 1: Definitions [1]
SRPS EN 13481-2:2013, Primene na železnici - Kolosek - Tehnički uslovi za sisteme šinskih pričvršćenja - Deo 2: Sistemi šinskih pričvršćenja za betonske pragove		EN 13481-2:2012, Railway applications - Track - Performance requirements for fastening systems - Part 2: Fastening systems for concrete sleepers [2]
SRPS EN 13481-3:2013, Primene na železnici - Kolosek - Tehnički uslovi za sisteme šinskih pričvršćenja - Deo 3: Sistemi šinskih pričvršćenja za drvene pragove		EN 13481-3:2012, Railway applications - Track - Performance requirements for fastening systems - Part 3: Fastening systems for wood sleepers [3]
SRPS EN 13481-4:2013, Primene na železnici - Kolosek - Tehnički uslovi za sisteme šinskih pričvršćenja - Deo 4: Sistemi šinskih pričvršćenja za čelične pragove		EN 13481-4:2012, Railway applications - Track - Performance requirements for fastening systems - Part 4: Fastening systems for steel sleepers [4]
SRPS EN 13481-5:2013, Primene na železnici - Kolosek - Tehnički uslovi za sisteme šinskih pričvršćenja - Deo 5: Sistemi šinskih pričvršćenja za konstrukciju koloseka bez zastora sa šinom položenom na gornju površinu ili u kanalu ploče		EN 13481-5:2012, Railway applications - Track - Performance requirements for fastening systems - Part 5: Fastening systems for slab track with rail on the surface or rail embedded in a channel [5]
SRPS ENV 13481-6:2012, Primene na železnici - Kolosek - Tehnički uslovi za sisteme šinskih pričvršćenja - Deo 6: Specijalni sistemi šinskih pričvršćenja za prigušenje vibracija	Povučen (*Withdrawn*) 31.01.2014	ENV 13481-6:2002, Railway applications - Track - Performance requirements for fastening systems - Part 6: Special fastening systems for attenuation of vibration [6]
SRPS EN 13481-7:2013, Primene na železnici - Kolosek - Tehnički uslovi za sisteme šinskih pričvršćenja - Deo 7: Specijalni sistemi šinskih pričvršćenja za skretnice, ukrštaje i šine vođice	Objavljen (*Published)* 24.06.2013	EN 13481-7:2012, Railway applications - Track - Performance requirements for fastening systems - Part 7: Special fastening systems for switches and crossings and check rails [7]
SRPS EN 13481-8:2011, Primene na železnici - Kolosek - Tehnički uslovi za sisteme šinskih pričvršćenja - Deo 8: Sistemi šinskih pričvršćenja za velika osovinska opterećenja	Povučen (*Withdrawn*) 31.01.2014	EN 13481-8:2006, Railway applications - Track - Performance requirements for fastening systems - Part 8: Fastening systems for track with heavy axle loads [8]

Usvojene serije standarda SRPS EN 13481 i SRPS EN 13146 nisu prevedene na srpski jezik, izuzev naslova i oblasti važenja. Značajna prepreka za efikasnu primenu usvojenih standarda SRPS EN u inženjerskoj praksi jeste nepostojanje njihovog zvaničnog prevoda na srpski jezik.

S obzirom na veliko interesovanje inženjerske stručne javnosti za ovu temu, ovaj rad jeste opširnija verzija rada koji su autori uspešno predstavili na međunarodnoj konferenciji RAILCON 2016 u Nišu, 13. oktobra 2016. godine [20].

U ovom radu razmatraju se tehnički zahtevi za sisteme šinskih pričvršćenja na prugama s projektovanim osovinskim opterećenjem do 350 kN, u skladu sa serijama standarda SRPS EN 13481 i SRPS EN 13146.

The adopted SRPS EN 13481 and SRPS EN 13146 standard series are not translated into Serbian language, except the titles and scopes. Significant obstacle to the effective implementation of the adopted SRPS EN standards in engineering practice is the lack of official translation in Serbian language.

Since there was a great interest by the engineering public for the subject, this paper is the wider version of the paper presented at the International conference RAILCON 2016 held in Niš, Serbia on 13th of October, 2016 [20].

In this paper, performance requirements for rail fastening systems on rail lines axle load up to 350 kN were considered according to the adopted SRPS EN 13481 and SRPS EN 13146 standard series.

Tabela 2. Trenutno stanje srpske serije standarda SRPS EN 13146 prema [19]
Table 2. The latest stage of SRPS EN 13146 Serbian standard series according to [19]

Srpska oznaka standarda, naslov (*Serbian standard designation, title*)	Status u Srbiji (*Status in Serbia*)	Identičan kao evropski standard (*Identical with European standard*)
SRPS EN 13146-1:2015, Primene na železnici - Kolosek - Postupci ispitivanja sistema šinskih pričvršćenja - Deo 1: Određivanje otpora podužnom pomeranju šine	Objavljen (*Published*) 28.07.2015	EN 13146-1:2012+A1:2014, Railway applications - Track - Test methods for fastening systems - Part 1: Determination of longitudinal rail restraint [10]
SRPS EN 13146-2:2013, Primene na železnici - Kolosek - Postupci ispitivanja sistema šinskih pričvršćenja -Deo 2: Određivanje otpora zaokretanju šine	Objavljen (*Published*) 24.06.2013	EN 13146-2:2012, Railway applications - Track - Test methods for fastening systems - Part 2: Determination of torsional resistance [11]
SRPS EN 13146-3:2013, Primene na železnici - Kolosek - Postupci ispitivanja sistema šinskih pričvršćenja - Deo 3: Određivanje prigušenja udarnog opterećenja		EN 13146-3:2012, Railway applications - Track - Test methods for fastening systems - Part 3: Determination of attenuation of impact loads [12]
SRPS EN 13146-4:2015, Primene na železnici - Kolosek - Postupci ispitivanja sistema šinskih pričvršćenja - Deo 4: Ispitivanje uticaja ponavljanja opterećenja	Objavljen (*Published*) 28.07.2015	EN 13146-4:2012+A1:2014, Railway applications - Track - Test methods for fastening systems - Part 4: Effect of repeated loading [13]
SRPS EN 13146-5:2013, Primene na železnici -Kolosek - Postupci ispitivanja sistema šinskih pričvršćenja - Deo 5: Određivanje električnog otpora	Objavljen (*Published*) 24.06.2013	EN 13146-5:2012, Railway applications - Track - Test methods for fastening systems - Part 5: Determination of electrical resistance [14]
SRPS EN 13146-6:2013, Primene na železnici - Kolosek - Postupci ispitivanja sistema šinskih pričvršćenja - Deo 6: Uticaj agresivne sredine		EN 13146-6:2012, Railway applications - Track - Test methods for fastening systems - Part 6: Effect of severe environmental conditions [15]
SRPS EN 13146-7:2013, Primene na železnici - Kolosek - Postupci ispitivanja sistema šinskih pričvršćenja - Deo 7: Određivanje sile pritezanja		EN 13146-7:2012, Railway applications - Track - Test methods for fastening systems - Part 7: Determination of clamping force [16]
SRPS EN 13146-8:2013, Primene na železnici - Kolosek - Postupci ispitivanja sistema šinskih pričvršćenja - Deo 8: Ispitivanje pod saobraćajem		EN 13146-8:2012, Railway applications - Track - Test methods for fastening systems - Part 8: In service testing [17]
SRPS EN 13146-9:2011, Primene na železnici - Kolosek - Postupci ispitivanja sistema šinskih pričvršćenja - Deo 9: Određivanje krutosti	Objavljen (*Published*) 30.09.2011	EN 13146-9:2009+A1:2011, Railway applications - Track - Test methods for fastening systems - Part 9: Determination of stiffness [18]

2 METODE ISPITIVANJA SISTEMA ŠINSKIH PRIČVRŠĆENJA

S obzirom na to što su sistemi pričvršćenja značajni za bezbednost, potrebno je da postoje standardne procedure za ocenu njihovih tehničkih karakteristika u uslovima normalnog korišćenja. Očigledno je da se realni uslovi u koloseku ne mogu uvek u potpunosti simulirati u laboratorijskim ispitivanjima u EN 13146 Delovi 1–7 [10–16] i Deo 9 [18]. Stoga, tehničke karakteristike sistema šinskih pričvršćenja na evropskoj železničkoj mreži određuju se metodama laboratorijskih ispitivanja i ispitivanjem pod saobraćajem (Deo 8 [17]), u skladu sa serijom standarda EN 13146. Ove procedure ispitivanja primenjuju se na kompletan sklop pričvršćenja. Definicije termina koji se koriste u seriji EN 13146 navedene su u evropskom standardu EN 13481-1 [1].

Nakon sprovođenja merenja prema [10–18], neophodno je sastaviti izveštaje o ispitivanjima koji sadrže informacije, u skladu sa zahtevima relevantnog dela serije standarda.

2.1 Određivanje otpora podužnom pomeranju šine

Evropski standard EN 13146-1 [10] određuje procedure laboratorijskih ispitivanja za određivanje maksimalne aksijalne sile koja deluje na šinu pričvršćenu pomoću sklopa šinskog pričvršćenja za prag, dugački prag skretničke građe ili element čvrste kolosečne podloge, bez pojave neelastičnih pomeranja šine (slika 1). Navedene procedure ispitivanja primenjuju se na kompletan sklop pričvršćenja, imajući u vidu sledeće:

2 TEST METHODS FOR RAIL FASTENING SYSTEMS

Since fastening systems are safety critical, there is a need to have a standardised procedure to evaluate their performance in normal use. It is obvious that the real conditions in track cannot always be simulated in laboratory tests from EN 13146 Parts 1 to 7 [10 - 16] and Part 9 [18]. Consequently, performance of rail fastening systems on European railway network is determined by laboratory test methods and in service testing (Part 8 [17]) in accordance with the EN 13146 standard series. These test procedures are applied to a complete fastening assembly. The definitions of the terms used in the EN 13146 series were specified in the EN 13481-1 European Standard [1].

After performing the measurements according to [10 - 18], it is necessary to draw up a test reports, which includes information in accordance with the requirements of the relevant part of standard series.

2.1 Determination of longitudinal rail restraint

The European Standard EN 13146-1 [10] specifies a laboratory test procedure for determination of maximum axial load that can be applied to a rail, secured to a sleeper, bearer or element of slab track by a rail fastening assembly, without non-elastic displacement of the rail (Figure 1). The specified test procedure applies to a complete fastening assembly taking into account the following:

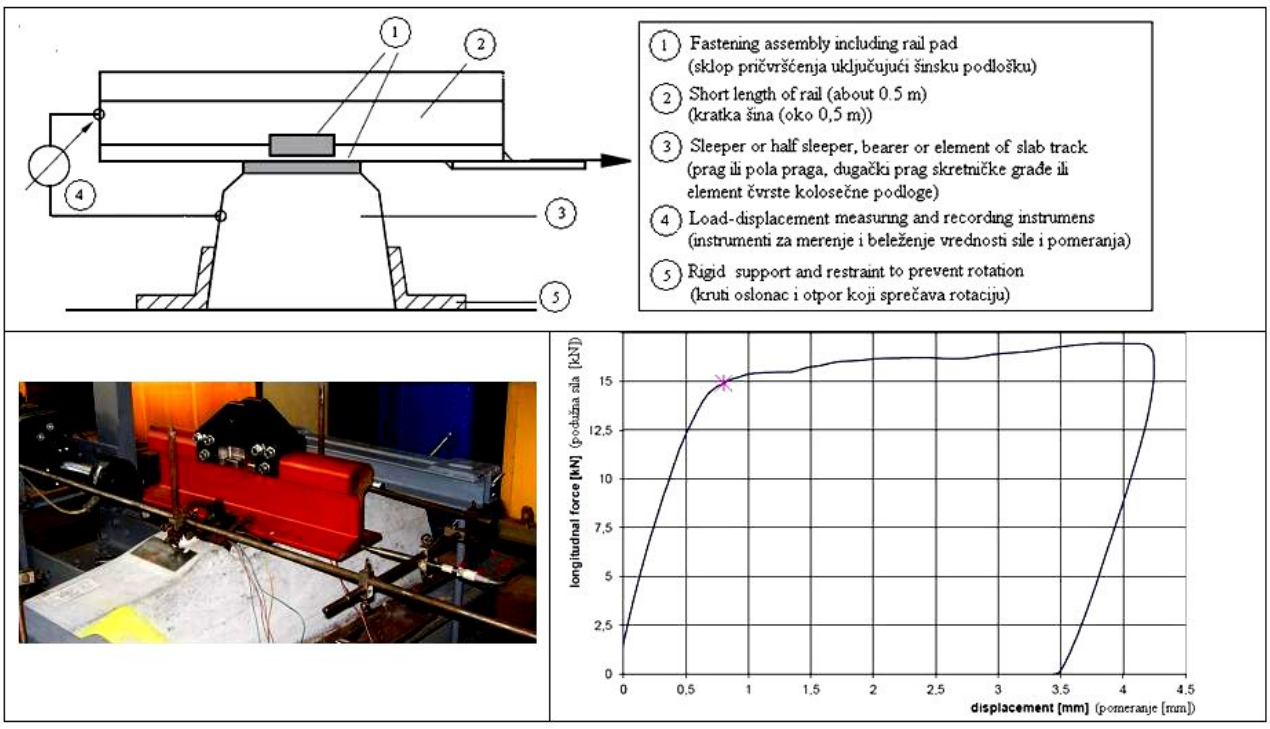

Slika 1. Postavka ispitivanja za određivanje otpora podužnom pomeranju šine i primer dijagrama sila-pomeranje (sa izmerenim otporom podužnom pomeranju šine 15 kN) [21]

Figure 1. Test arrangement for determination the longitudinal rail restraint and an example of force-displacement diagram (with measured longitudinal rail restraint 15 kN) [21]

– procedura ispitivanja meri podužni otpor šine za diskretne sisteme pričvršćenja sa šinom fiksiranom za oslonac (prag, dugački prag skretničke građe ili element čvrste kolosečne podloge) u diskretnim intervalima;

– procedura ispitivanja meri podužnu krutost za athezivne sisteme pričvršćenja sa „utopljenom" šinom (embedded rail).

– the test procedure measures the longitudinal rail restraint for discrete fastening systems, with rail fixed to a supporting base (sleeper, bearer or element of slab track) at discrete intervals, and

– the test procedure measures the longitudinal stiffness for an adhesive fastening system with an embedded rail.

2.2 Određivanje otpora zaokretanju šine

Evropski standard EN 13146-2 [11] određuje proceduru laboratorijskog ispitivanja za određivanje torzionog otpora za kompletan sklop pričvršćenja, koji se meri kao momenat potreban da se šina zaokrene za 1° u ravni koja je paralelna oslonačkoj podlozi (slika 2). Dobijene vrednosti torzionog otpora koriste se u proračunima stabilnosti koloseka.

2.2 Determination of torsional resistance

EN 13146-2 European Standard [11] specifies a laboratory test procedure to determine torsional resistance of complete fastening assembly, which is measured as the moment necessary to rotate a rail through 1° in a plane parallel to the base of the support (Figure 2). The obtained value of torsional resistance is used in track stability calculations.

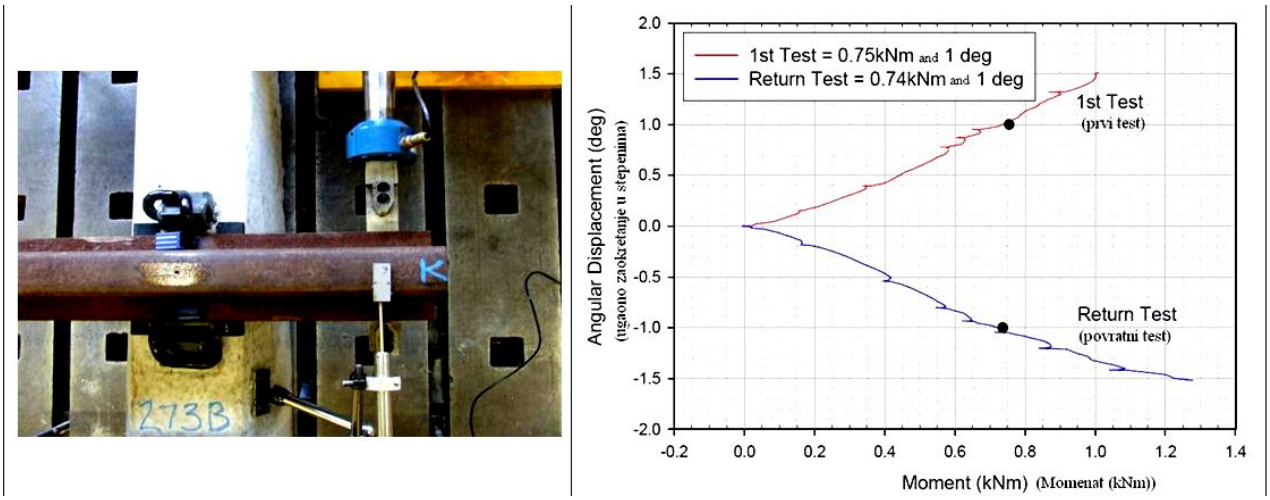

Slika 2. Postavka ispitivanja za određivanje otpora zaokretanju šine i primer dijagrama otpora zaokretanju šine
Figure 2. Test arrangement for determination of torsional resistance and an example of torsional resistance diagram

2.3 Određivanje prigušenja udarnog opterećenja

Evropski standard EN 13146-3 [12] određuje procedure laboratorijskog ispitivanja za poređenje naprezanja izazvanih korišćenjem referentne šinske podloške s malim prigušenjem i podloške koja se ispituje u sistemu pričvršćenja. Udarno opterećenje nanosi se tegom koji pada na glavu šine (slika 3). Šina je pričvršćena za betonski prag ili dugački betonski prag skretničke građe.

2.3 Determination of attenuation of impact loads

EN 13146-3 European Standard [12] specifies laboratory test procedures for comparing the strains induced with a low attenuation reference rail pad and with the test pad in the fastening system. An impact load is applied by dropping a mass onto the rail head (Figure 3). Rail is fastened to a concrete sleeper or bearer.

2.4 Ispitivanje uticaja ponavljanja opterećenja

Evropski standard EN 13146-4 [13] određuje proceduru za laboratorijsko ispitivanje delovanja pokretnog opterećenja koje se ponavlja u ciklusima i koje simulira opterećenje koloseka od saobraćaja (slika 4). Rezultati ispitivanja koriste se za ocenu dugoročnog ponašanja sistema direktnih šinskih pričvršćenja, u kojima je šina pričvršćena za oslonačku podlogu s podložnom pločom ili bez nje (*direktni sistemi pričvršćenja* prema [1]). Uz ostale neophodne informacije, izveštaj o ispitivanju sadrži rezultate vizuelne inspekcije nakon ispitivanja (slika 5),

2.4 Determination of effect of repeated loading

EN 13146-4 European Standard [13] specifies a laboratory test procedure for applying repeated loading which simulates the load caused by traffic on railway track (Figure 4). This test is used for assessing the long term performance of fastening system in which a rail is directly secured to the supporting structure with or without a beseplate ("direct fastening systems" as in [1]). In addition to other necessary information, test report contains result of visual inspection after the test (Figure 5), mean vertical static stiffness before and after cyclic

Slika 3. Postavka ispitivanja za određivanje prigušenja udarnog opterećenja

Figure 3. Test arrangement for determination of attenuation of impact loads

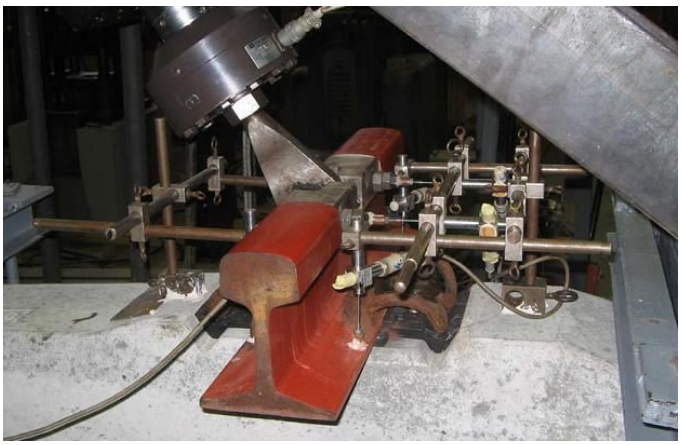

Slika 4. Laboratorijsko ispitivanje sa ponavljanjem opterećenja [21]

Figure 4. Laboratory test with repeated loading [21]

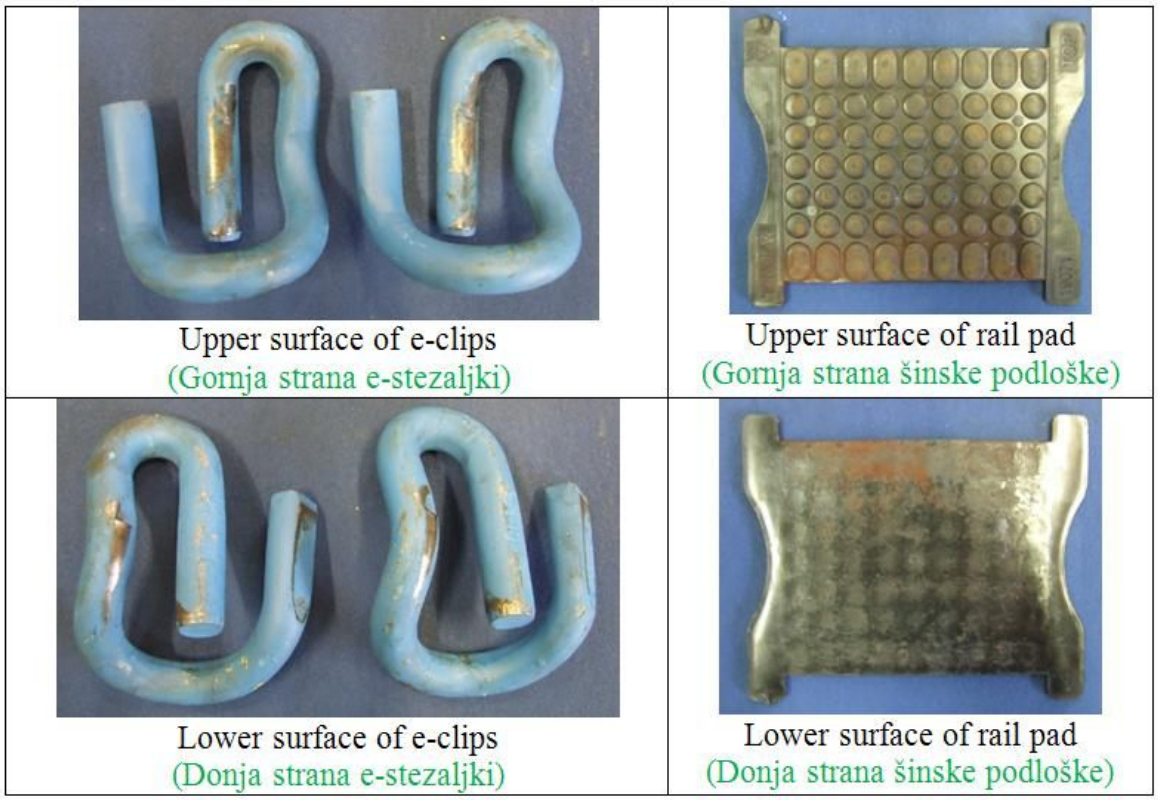

Slika 5. Elementi pričvršćenja nakon ispitivanja sa ponavljanjem opterećenja
Figure 5. Fastening elements after repeated load test

srednju vertikalnu statičku krutost pre i posle ciklusa opterećenja, podužni otpor šine pre i posle ciklusa opterećenja, silu pritezanja pre i posle ciklusa opterećenja, srednje dinamičko pomeranje šine na početku i na kraju ispitivanja pomoću ponavljanja opterećenja, srednje zaostalo pomeranje pri maksimalnom opterećenju na početku i na kraju ispitivanja pomoću ponavljanja opterećenja.

loading, longitudinal rail restraint before and after cyclic loading, clamping force before and after cyclic loading, mean dynamic rail displacement at the beginning and the end of the repeated load test, mean residual displacement at maximum load at the end of the repeated load test.

2.5 Određivanje električnog otpora

Evropski standard EN 13146-5 [14] određuje proceduru za laboratorijsko ispitivanje za određivanje električnog otpora u vlažnim uslovima. Električni otpor meri se između dve kratke šine koje su pričvršćene za oslonac (čelični ili betonski prag, dugački prag skretničke građe ili element čvrste kolosečne podloge), dok se ceo oslonac i pričvršćenja prskaju vodom kontrolisanom brzinom (slika 6).

2.5 Determination of electrical resistance

EN 13146-5 European Standard [14] specifies a laboratory test procedure for determining electrical resistance in wet conditions. The electrical resistance between two short lengths of rail fastened to the support (steel or concrete sleeper, bearer or element of slab track) is measured whilst the whole support and fastenings are sprayed with water at a controlled rate (Figure 6).

Slika 6. Određivanje električnog otpora u vlažnim uslovima u laboratoriji
Figure 6. Determining the electrical resistance in wet conditions in laboratory

2.6 Uticaj agresivne sredine

Evropski standard EN 13146-6 [15] određuje proceduru laboratorijskog ispitivanja za određivanje uticaja agresivne sredine na sistem pričvršćenja (slika 7). Tokom ispitivanja, ceo sklop pričvršćenja izložen je dejstvu slanog spreja (tzv. so-sprej) i beleži se efekat lakog rasklapanja i ponovnog sklapanja, kao i stanje pojedinačnih komponenata. Izveštaj o ispitivanju sadrži promene u izgledu svake komponente tokom ispitivanja i svaku nemogućnost rasklapanja i ponovnog sklapanja sistema pričvršćenja. Buduće izmene ovog standarda treba da uključe procedure za ispitivanja koja obuhvataju i ostale uticaje sredine.

2.6 Effect of severe environmental conditions

EN 13146-6 European Standard [15] specifies a laboratory test procedure for determining the effects of severe environmental conditions on the fastening system (Figure 7). During the test, the complete fastening assembly is exposed to a salt spray and the effect on ease of dismantling, and reassembly, and condition of individual components is recorded. Test report includes change in appearance of each component during the test and any failure to dismantle or reassemble the fastening system. The future revisions of this standard should include test procedures for covering other environmental conditions.

Slika 7. Oprema za ispitivanje pomoću slanog spreja
Figure 7. The equipment for the salt spray test

2.7 Određivanje sile pritezanja

Evropski standard EN 13146-7 [16] određuje procedure za laboratorijsko ispitivanje za određivanje sile pritezanja (*sila koja se nanosi na gornju površ nožice šine delovanjem stezaljki sklopa pričvršćenja* [1]) koja deluje na nožicu šine. Sila pritezanja za kompletan sklop pričvršćenja određuje se merenjem sile potrebne za odvajanje šine od površi na koju je oslonjena (slika 8). Procedura ispitivanja može se primeniti za sisteme pričvršćenja s podložnom pločom i bez nje na pragovima, dugačkim pragovima skretničke građe i elementima čvrste kolosečne podloge.

2.7 Determination of clamping force

EN 13146-7 European Standard [16] specifies laboratory test procedures for measuring clamping force ("force applied to the upper surface of one rail foot by the fastening assembly clips" as in [1]) acting on the foot of a rail. The clamping force for a complete rail fastening assembly is determined by measuring the force necessary to separate the rail from the surface on which it is supported (Figure 8). The test procedure is applicable to fastening systems with and without baseplates on sleepers, bearers and elements of slab track.

Slika 8. Postavka ispitivanja za merenje vertikalne sile neophodne za odvajanje šina od oslonačke konstrukcije u laboratoriji

Figure 8. Test arrangement for measuring the vertical force necessary to separate the rail from support structure in laboratory

2.8 Ispitivanje pod saobraćajem

Evropski standard EN 13146-8 [17] određuje procedure koje se mogu primeniti za poređenje tehničkih karakteristika u koloseku novog ili modifikovanog sistema pričvršćenja sa sistemom čije su tehničke karakteristike poznate. Sistem pričvršćenja koji se ispituje ugrađuje se u kolosek u isto vreme i pod istim uslovima (isti kvalitet šinskog čelika i profil šine, pragovi, dugački pragovi skretničke građe ili čvrsta kolosečna podloga od istog materijala i prema istom projektu, kao i položaj u koloseku sa sličnim uslovima geometrije koloseka i uslovima saobraćaja) kao i referentni sistem pričvršćenja. Dužina test-deonice ne treba da bude kraća od 500 pragova sa ugrađenim sistemom pričvršćenja koje se ispituje i 500 pragova sa ugrađenim referentnim sistemom pričvršćenja (po 200 pragova za metro sistem) ili njihovim ekvivalentom (kolosek na čvrstoj podlozi). Ispitivanje treba da traje toliko koliko je potrebno da određeni saobraćaj prođe preko koloseka koji se ispituje (npr. 20×10^6 bruto tona u koloseku s maksimalnim osovinskim opterećenjem > 100 kN), a ne sme biti kraće od godinu dana. Za vreme ispitivanja, svaki sistem pričvršćenja treba da se održava u skladu sa instrukcijama proizvođača. Inspekcija sistema pričvršćenja koji se ispituje i referentnog sistema pričvršćenja uključuje:

2.8 In service testing

EN 13146-8 European Standard [17] provides a procedure which can be used to compare the performance of new or modified fastening systems in track with systems whose performance is known. The fastening system under test is installed in track at the same time and at the same conditions (the same grade and section of rail, sleepers, bearers or slab track of the same material and design, as well as location in track with similar geometry and service conditions) as a reference fastening system. Length of the test section should not be less than 500 sleepers with installed test fastening system and 500 sleepers with installed reference fastening system (200 sleepers each on metro systems), or their equivalent (slab track). Duration of the test corresponds to the traffic dynamics required to pass over the test track (e.g. 20 × 106 gross t in track with maximum axle loads > 100 kN) and shall not be less than one year. During the test each fastening system shall be maintained in accordance with the manufacturer's instructions. Inspection of the test and reference fastening systems includes:

– merenje širine koloseka;
– podužno pomeranje šine, relativno u odnosu na prag ili čvrstu kolosečnu podlogu i maksimalni raspon dnevne temperature;
– uticaj na performanse signalnih sistema;
– silu pritezanja (na ne manje od deset sklopova) korišćenjem metode ispitivanja u koloseku, koju preporučuje proizvođač;
– sigurnost veze s pragovima;
– stanje na glavi šine;
– stanje pragova uključujući zonu oslanjanja šine na prag;
– stanje pojedinačnih komponenata pričvršćenja;
– jednostavno ugrađivanje i demontiranje korišćenjem alata po preporuci proizvođača.

– track gauge measurement,
– longitudinal movement of rail, relative to the sleeper or slab support, and maximum daily temperature range,
– effect on performance of signalling systems,
– clamping force (on not less than 10 assemblies) using the manufacturer's recommended test method for use in track,
– security of attachment to the sleepers,
– condition of the rail head,
– condition of sleepers including rail seat area,
– condition of individual fastening components,
– ease of assembly and removal using the tools recommended by the manufacturer.

2.9 Određivanje krutosti

Evropski standard EN 13146-9 [18] daje zajedno metode ispitivanja za merenje krutosti podloški i sklopa pričvršćenja pod statičkim, niskofrekventnim i visokofrekventnim dinamičkim opterećenjem. Postavka ispitivanja za podloške prikazana je na slici 9.

Procedure ispitivanja za kompletan sklop šinskog pričvršćenja sadrže procedure statičkog ispitivanja, dinamičkog niskofrekventnog i dinamičkog visokofrekventnog ispitivanja (slika 10).

2.9 Determination of stiffness

EN 13146-9 European Standard [18] provides together test methods for measuring the stiffness of pads and fastening assemblies under static, low frequency and high frequency dynamic loading. Test arrangement for pads is shown in Figure 9.

Test procedures for complete rail fastening assemblies include static test procedure, dynamic low frequency test and dynamic high frequency test (Figure 10).

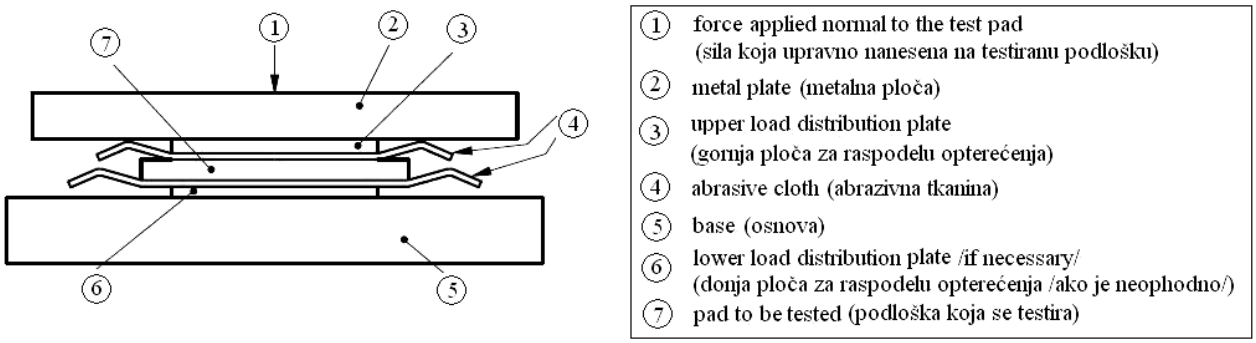

Slika 9. Postavka ispitivanja za merenje krutosti podloške
Figure 9. Test arrangement for measuring the stiffness of pad

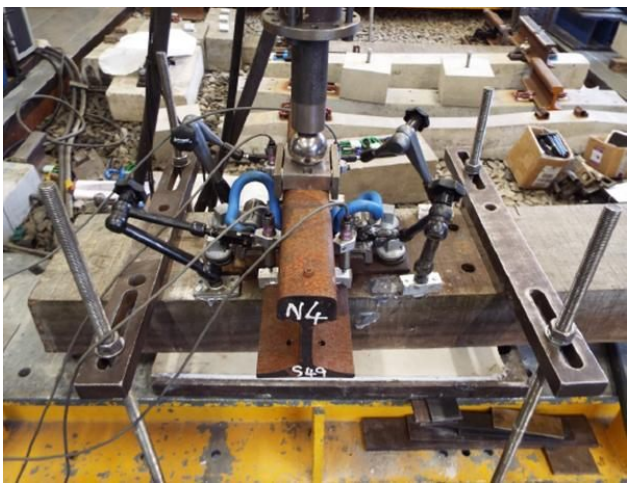

Slika 10. Postavka ispitivanja za dinamičku krutost kompletnog sklopa pričvršćenja
Figure 10. Dynamic stiffness test arrangement for complete rail fastening assemblies

Dobijena vrednost krutosti koristi se u proračunu stabilnosti koloseka.

3 TEHNIČKI USLOVI ZA SISTEME ŠINSKIH PRIČVRŠĆENJA ZA BETONSKE PRAGOVE

Definicije termina korišćene u seriji EN 13481 navode se u evropskom standardu EN 13481-1 [1]. U skladu sa [1], *sistem pričvršćenja jeste sklop komponenata koji pričvršćuje šinu za podlogu i zadržava je u zahtevanoj poziciji uz omogućavanje potrebnog vertikalnog, bočnog i podužnog pomeranja.*

Ova serija standarda razmatra specifične zahteve za sisteme pričvršćenja u zavisnosti od tipa oslonačke konstrukcije (betonski pragovi [2], drveni pragovi [3], čelični pragovi [4], čvrsta kolosečna podloga [5]), kao i zahteve za specijalne sisteme pričvršćenja (za prigušenje vibracija [6], skretnice i ukrštaje, te šine vođice [7] i za kolosek za teška osovinska opterećenja [8]).

S obzirom na to što su u primeni najčešće sistemi pričvršćenja za betonske pragove u zastoru od tucanika, u radu se prikazuju tehnički uslovi za sisteme pričvršćenja u skladu sa [2]. Ovi zahtevi primenjuju se na glavnim prugama, kao i za lake šinske sisteme u skladu s tabelom 3.

The obtained value of stiffness is used in track stability calculations.

3 PERFORMANCE REQUIREMENTS FOR FASTENING SYSTEMS ON CONCRETE SLEEPERS

The definitions of the terms used in EN 13481 European Standard series were specified in EN 13481-1 [1]. In accordance with [1], *"fastening system is assembly of components which secures a rail to the supporting structure and retains it in the required position whilst permitting any necessary vertical, lateral and longitudinal movement".*

This standard series considers specific requirements for fastening systems depending on the type of supporting structure (concrete sleepers [2], wood sleepers [3], steel sleepers [4], slab track [5]), as well as requirements for special fastening systems (for attenuation of vibration [6], switches and crossings and check rails [7] and for track with heavy axle loads [8]).

Since the fastening systems on concrete sleepers in ballasted track are usually in use, the paper presents performance requirements for fastening systems in accordance with [2]. These requirements apply to main lines, as well as to light rail systems according to Table 3.

Tabela 3. Kategorije pričvršćenja u skladu sa [1, 2]
Table 3. Fastening categories in accordance with [1, 2]

Kategorije sistema pričvršćenja (*Categories of fastening system*)		A	B	C	D	E
Tipična maksimalna brzina [km/h] (*Typical maximum speed [km/h]*)		100	140	250	≥250	200
Osovinsko opterećenje [kN] (*Axle load [kN]*)	Tipično [1] (*Typical [1]*)	100	160	225	180	300
	Maksimum [2] (*Maximum [2]*)	130	180	260	260	350
Radijus krivine [m] (*Curve radius [m])*	Tipično [1] (*Typical [1]*)	80	100	400	800	150
	Minimum [2] (*Minimum [2]*)	40	80	150	400	150
Tipičan profil šine (*Typical rail section*)		40E1	54E1	60E1	60E1	60E1
Tipičan razmak pragova [m] (*Typical sleeper spacing [m]*)		0.8	0.6	0.6	0.6	0.6
Napomena: Maksimalno osovinsko opterećenje za kategorije A i B se ne primenjuje za vozila za održavanje (*Note: The maximum axle load for A and B categories does not apply to maintenance vehicles*)						

Ovi tehnički uslovi primenjuju se za direktne i indirektne sisteme pričvršćenja koji deluju na nožicu i/ili vrat šine (slika 11). Nadalje, oni se primenjuju za profile šine u skladu sa [22] (izuzev 49E4) i u skladu sa [23]. Treba naglasiti i to da se ovaj standard ne primenjuje za krute sisteme pričvršćenja (npr. K kruti sistem pričvršćenja koji je često zastupljen na prugama u Srbiji).

These requirements apply to direct and indirect fastening systems which act on the foot and/or web of the rail (Figure 11). Further, they apply for the rail sections in accordance with [22] (excluding 49E4) and according to [23]. It should be noted that this standard is inapplicable to rigid fastening systems (e.g. K fastening system which is still mostly in use on railway lines in Serbia).

Slika 11. Sistem pričvršćenja koji pridržava vrat šine
(Vanguard – Pandrol sistem pričvršćenja, snimljeno u stanici Beograd Centar, 2016)

Figure 11. Fastening system supporting the rail web
(Vanguard – Pandrol fastening system, foto taken in Beograd Centar station, 2016)

Tehnički uslovi za sisteme pričvršćenja za korišćenje na betonskim pragovima koloseka u zastoru od tucanika obuhvataju podužni otpor šine, otpor zaokretanju šine (torzioni otpor), prigušenje udarnog opterećenja, uticaj ponavljanja opterećenja, električni otpor sistema pričvršćenja i praga, uticaj izloženosti agresivnim uslovima sredine, ukupne dimenzije, uticaj tolerancija sistema pričvršćenja na širinu koloseka, silu pritezanja i ispitivanje pod saobraćajem.

Zahtevani podužni otpor šine zavisi od ograničenja za brzinu i specijalnih zahteva konstrukcije donjeg stroja. U tom smislu, podužni otpor šine ne treba da bude manji od 7 kN (kontrolisano na osnovu procesa merenja u skladu sa EN 13146-1) na konvencionalnim prugama i ne treba da bude manji od 9 kN na prugama za velike brzine (≥ 250 km/h).

U skladu s projektom konstrukcije kolosečne podloge, minimalni uslovi za podužni otpor mogu da se redukuju na osnovu ugovora kupca i proizvođača. Na primer, korišćenje dilatacionih sprava za sprečavanje prekomernih podužnih pomeranja i sila na dugačkim železničkim mostovima je skupo i loše rešenje u pogledu bezbednosti saobraćaja i udobnosti, kao i troškova održavanja. Zbog toga se mogu primeniti alternativna rešenja sistema pričvršćenja s redukovanim otporom podužnom pomeranju šine. Slike 12 i 13 prikazuju PANDROL® ZLR (Zero Longitudinal Restraint – nulti podužni otpor) sistem koji je projektovan tako da se ne prenesu sile s koloseka na most, da se zadrži šina u vertikalnoj poziciji, da se obezbedi bočni otpor i da se spreči prevrtanje šine.

Performance requirements for fastening systems for use on concrete sleepers in ballasted track include longitudinal rail restraint, torsional resistance, attenuation of impact loads, effect of repeated loading, electrical resistance of fastening system and sleeper, effect of exposure to severe environmental conditions, overall dimensions, effect of fastening system tolerances on track gauge, clamping force, and in-service testing.

Required longitudinal rail resistance depends on the speed limit and the special requirements of substructure. In that sense, the longitudinal rail resistance shall be not less than 7 kN (controlled over the measurement process according to EN 13146-1) on the conventional rail lines and not less than 9 kN on high-speed lines (≥ 250 km/h).

In accordance with the design of the track supporting structure, the minimum requirement for longitudinal restraint may be reduced by agreement between the purchaser and manufacturer. For example, the utilization of expansion devices to prevent excessive longitudinal displacements and forces on the long railway bridges is expensive and bad solution in regard to traffic safety and comfort, as well as maintenance costs. Therefore, it can be applied an alternative solution of fastening system with reduced rail longitudinal restraint. Figures 12 and 13 show the PANDROL® ZLR (Zero Longitudinal Restraint) system designed to keep track forces from being transmitted to bridge, to hold the rail vertically in place, to provide lateral restraint and to prevent rail rollover.

The torsional resistance is measured in accordance with [2] and the result reported.

Otpor zaokretanju šine (torzioni otpor) meri se u skladu sa [2], a rezultat se unosi u izveštaj.

Za sisteme pričvršćenja koji imaju srednje ili veliko prigušenje dinamičkog opterećenja, ispitivanje treba da bude sprovedeno u skladu sa [3], a rezultat se unosi u izveštaj. Rezultati za srednje prigušenje treba da budu u rangu od 15% do 30%, a za veliko prigušenje > 30%.

Statička krutost sklopa i niskofrekventna dinamička krutost sklopa treba da se mere u skladu sa [19]. Na zahtev naručioca, statička krutost šinske podloške, niskofrekventna dinamička krutost šinske podloške i sklopovi sa visokofrekventnom dinamičkom krutošću treba da se mere u skladu sa [19] i [2] (opterećenja za merenje krutosti su definisana u [2]).

For fastening systems described as having medium or high attenuation of dynamic loads, test shall be conducted in accordance with [3] and the result reported. Test results for medium attenuation shall be in the range from 15 % to 30 %, and for high attenuation over 30 %.

The assembly static stiffness and assembly low frequency dynamic stiffness shall be measured in accordance with [19]. At the request of the customer, the rail pad static stiffness, low frequency dynamic stiffness of the rail pad and the assembly high frequency dynamic stiffness should be measured in accordance with [19] and [2] (loads for measurement of stiffness were defined in [2]).

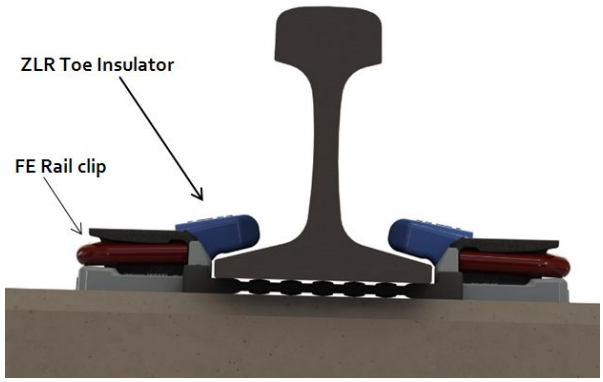

Slika 12. Sistem pričvršćenja Pandrol ZLR sa zazorom između izolatora stezaljke i nožice šine
Figure 12. Pandrol ZLR fastening system with the gap betwen toe insulator and foot of rail

Slika 13. Ugrađeni sistem pričvršćenja sa stezaljkom ZLR (sistem Pandrol VIPA) na mostu
Figure 13. Installed fastening system with ZLR clips (Pandrol VIPA system) on a bridge

Uticaj ponovljenog opterećenja treba da se odredi u skladu s procedurom definisanom u [13], korišćenjem opterećenja za ispitivanje i pozicije koje su definisane u [2].

U skladu sa [13], treba obaviti sledeća merenja pre i posle ponovljenog opterećenja:

– otpor podužnom pomeranju (dozvoljena promena ≤ 20 %);

– promena vertikalne statičke krutosti (dozvoljena promena ≤ 25 %);

– sila pritezanja (dozvoljena promena za sisteme šinskih pričvršćenja koji deluju na nožicu šine ≤ 20 %).

The effect of repeated loading shall be determined by the procedure defined in [13] using the test loads and positions defined in [2].

In accordance with [13], the following measurements shall be performed before and after repeated loading:

– longitudinal rail restraint (permitted change ≤20%),

– vertical static stiffness change (permitted change ≤25%), and

– clamping force (permitted change for fastening systems which act on the foot of the rail ≤20%).

Električna izolovanost ne treba da bude manja od 5 kΩ kada se meri u skladu sa [14]. Korisnik može da definiše veće vrednosti u slučaju kada se kolosek koristi kao povratni vod (smernice za struju za vuču vozila date su u [24] i SRPS EN 50122-2).

Uticaj izloženosti agresivnim uslovima sredine određuje se u skladu sa [15] na osnovu ispitivanja pomoću slanog spreja. Nakon ispitivanja, šinsko pričvršćenje treba da bude sposobno da se rasklopi bez oštećenja bilo koje komponente i da se ponovo sklopi ručnim alatom koji je namenjen za tu svrhu.

Slika 14 prikazuje anvelopu za sisteme šinskog pričvršćenja (koji deluju na nožicu šine) za betonske pragove u zastoru od tucanika i profil šine u skladu sa [22] (izuzev 49E4) i u skladu sa [23]. Ova anvelopa neophodna je da bi se sprečila kolizija s točkom uključujući vozila za održavanje.

Treba napomenuti i to da za sisteme pričvršćenja koji deluju na vrat šine minimum prostora za prolaz venca točka treba da bude u skladu s nacionalnim propisima, a anvelopu sistema pričvršćenja treba da obezbedi isporučilac.

The electrical insulation shall be not less than 5 kΩ when measured in accordance with [14]. The user may specify a higher value for use with certain track circuits (guidance on traction currents is given in [24] and SRPS EN 50122-2).

Effect of exposure to severe environmental conditions is determined in accordance with [15] based on the salt spray test. After the test, the fastening assembly shall be capable of being dismantled, without failure of any component and reassembled using manual tools provided for this purpose.

Figure 14 shows the envelope for rail fastening systems (which act on the foot of the rail) for concrete sleepers in ballasted track and rail section in accordance with [22] (excluding 49E4) and [23]. This envelope is necessary to avoid interference with vehicles including track maintenance vehicles.

It should be noted that for web support fastening systems, the minimum flangeway shall comply with national regulations and the envelope of the fastening systems shall be provided by the supplier.

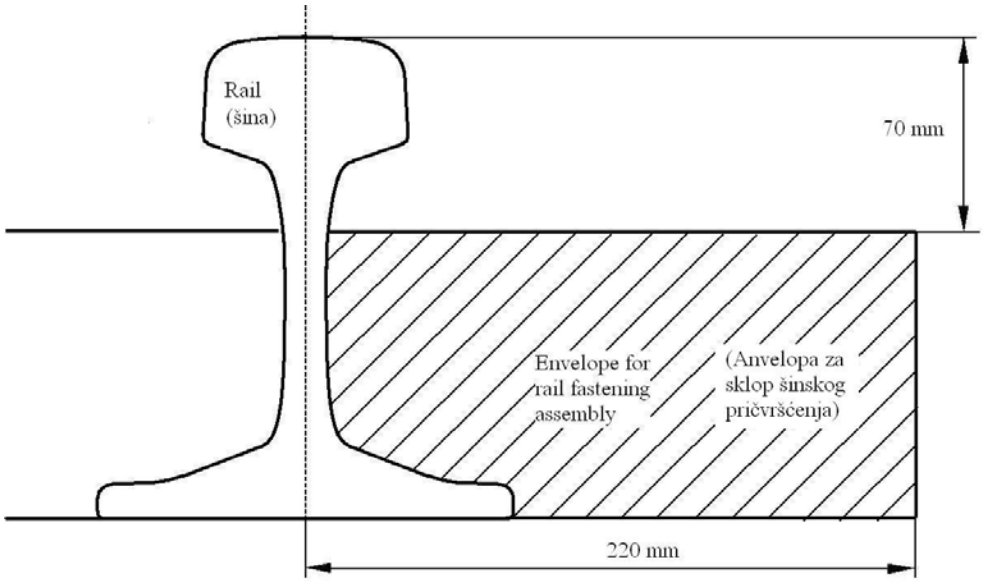

Slika 14. Anvelopa za sistem šinskog pričvršćenja (koji deluje na nožicu šine) za betonski prag u koloseku sa zastorom od tucanika

Figure 14. Envelope for rail fastening systems (which act on the rail foot) for concrete sleepers in ballasted track

Proizvođač treba da obezbedi tehničke crteže veze sistema pričvršćenja i praga. Promene statičke širine koloseka, koje se mogu pojaviti usled sistema pričvršćenja - ne treba da pređu ± 1 mm.

Sila pritezanja za sisteme pričvršćenja (koji deluju na nožicu šine) treba da se odredi po proceduri propisanoj u [16], a rezultati treba da se prikažu u izveštaju. Zahtevi za silu pritezanja ne mogu da se primene na sisteme pričvršćenja koji deluju na vrat šine.

Ispitivanje pod saobraćajem treba da se sprovede u skladu sa [17] - na zahtev kupca.

Druge posebne zahteve za sisteme šinskih pričvršćenja moraju da definišu korisnici.

The manufacturer shall provide a drawing of the interface between the fastening system and the sleeper. The variation in the static track gauge which can arise from the fastening system shall not exceed ± 1 mm.

Clamping force for fastening systems (acting on the rail foot) shall be determined by the procedure prescribed in [16] and the results shall be reported. The requirement for clamping force is inapplicable to web support fastening systems.

In-service testing shall be carried out in accordance with [17] at the request of the customer.

Other specific requirements for fastening system must be defined by the customer.

4 ZAKLJUČAK

U ovom radu razmatrani su tehnički zahtevi za sisteme šinskih pričvršćenja na prugama s projektovanim osovinskim opretećenjem do 350 kN, u skladu sa evropskom serijom standarda EN 13481. Ukazuje se na obavezne tehničke zahteve u skladu sa evropskim standardima i specifične zahteve, u skladu sa uslovima projekta.

Rad prikazuje tehničke uslove za sisteme pričvršćenja za betonske pragove u koloseku sa zastorom od tucanika zato što su ovi sistemi pričvršćenja najčešće u upotrebi u Srbiji.

Metode ispitivanja sistema pričvršćenja posebno su razmatrane u skladu sa evropskom serijom standarda EN 13146.

Obe pomenute serije standarda usvojio je Institut za standardizaciju Srbije kao srpske standarde SRPS EN 13481 (Delovi 1–8) i SRPS EN 13146 (Delovi 1–9). Trenutno stanje procesa harmonizacije za obe serije standarda prikazano je u tabelama 1 i 2. Primena strandarda SRPS EN otežana je zbog toga što su objavljeni samo na engleskom jeziku, nisu prevedeni na srpski jezik.

Cilj rada jeste da se inženjerska javnost u Srbiji upozna s pomenutim serijama standarda i da se olakša njihova praktična primena.

4 CONCLUSION

In this paper, technical requirements for rail fastening systems on rail lines with design axle load up to 350 kN were considered in accordance with EN 13481 European Standard series. It points to the mandatory requirements and according to the European standards and specific requirements according to the conditions of the project.

The paper presents the performance requirements for fastening systems on concrete sleepers in ballasted track since these fastening systems are commonly used in Serbia.

Test methods for fastening systems were particularly discussed in accordance with EN 13146 European Standard series.

Both of the above mentioned standard series were adopted by the Institute for Standardization of Serbia as Serbian standards SRPS EN 13481 (Parts 1 - 8) and SRPS EN 13146 (Parts 1 - 9). State of the art in the harmonization process of both standard series is shown in Tables 1 and 2. Implementation of SRPS EN standards is difficult because they were published only in English.

The aim of the paper is to introduce engineering public in Serbia with mentioned two standard series and to facilitate their practical implementation.

ZAHVALNICA

Ovaj rad je podržalo Ministarstvo prosvete, nauke i tehnološkog razvoja Republike Srbije broj 36012: „Istraživanje tehničko-tehnološke, kadrovske i organizacione osposobljenosti Železnica Srbije sa aspekta sadašnjih i budućih zahteva Evropske unije”.

ACKNOWLEDGEMENT

This work was supported by the Ministry of Education and Science of the Republic of Serbia through the research project No. 36012: “Research of technical-technological, staff and organizational capacity of Serbian Railways, from the viewpoint of current and future European Union requirements”.

5 LITERATURA
REFERENCES

[1] CEN/TC 256: EN 13481-1:2012, Railway applications - Track - Performance requirements for fastening systems - Part 1: Definitions, 2012.

[2] CEN/TC 256: EN 13481-2:2012, Railway applications - Track - Performance requirements for fastening systems - Part 2: Fastening systems for concrete sleepers, 2012.

[3] CEN/TC 256: EN 13481-3:2012, Railway applications - Track - Performance requirements for fastening systems - Part 3: Fastening systems for wood sleepers, 2012.

[4] CEN/TC 256: EN 13481-4:2012, Railway applications - Track - Performance requirements for fastening systems - Part 4: Fastening systems for steel sleepers, 2012.

[5] CEN/TC 256: EN 13481-5:2012, Railway applications - Track - Performance requirements for fastening systems - Part 5: Fastening systems for slab track with rail on the surface or rail embedded in a channel, 2012.

[6] CEN/TC 256: ENV 13481-6:2002, Railway applications - Track - Performance requirements for fastening systems - Part 6: Special fastening systems for attenuation of vibration, 2002.

[7] CEN/TC 256: EN 13481-7:2012, Railway applications - Track - Performance requirements for fastening systems - Part 7: Special fastening systems for switches and crossings and check rails, 2012.

[8] CEN/TC 256: EN 13481-8:2006, Railway applications - Track - Performance requirements for fastening systems - Part 8: Fastening systems for track with heavy axle loads, 2006.

[9] http://www.iss.rs/en/standard/?keywords=13481&Submit= (accessed on January 2017.)

[10] CEN/TC 256: EN 13146-1:2012+A1:2014, Railway applications - Track - Test methods for fastening systems - Part 1: Determination of longitudinal rail restraint, 2014.

[11] CEN/TC 256: EN 13146-2:2012, Railway applications - Track - Test methods for fastening systems - Part 2: Determination of torsional resistance, 2012.
[12] CEN/TC 256: EN 13146-3:2012, Railway applications - Track - Test methods for fastening systems - Part 3: Determination of attenuation of impact loads, 2012.
[13] CEN/TC 256: EN 13146-4:2012+A1:2014, Railway applications - Track - Test methods for fastening systems - Part 4: Effect of repeated loading, 2014.
[14] CEN/TC 256: EN 13146-5:2012, Railway applications - Track - Test methods for fastening systems - Part 5: Determination of electrical resistance, 2012.
[15] CEN/TC 256: EN 13146-6:2012, Railway applications - Track - Test methods for fastening systems - Part 6: Effect of severe environmental conditions, 2012.
[16] CEN/TC 256: EN 13146-7:2012, Railway applications - Track - Test methods for fastening systems - Part 7: Determination of clamping force, 2012.
[17] CEN/TC 256: EN 13146-8:2012, Railway applications - Track - Test methods for fastening systems - Part 8: In service testing, 2012.
[18] CEN/TC 256: EN 13146-9:2009+A1:2011, Railway applications - Track - Test methods for fastening systems - Part 9: Determination of stiffness, 2011.
[19] http://www.iss.rs/en/standard/?keywords=13146&Submit= (accessed on January 2017.)
[20] Vilotijević, M., Popović, Z., Lazarević, L.: Performance Requirements for Rail Fastening Systems on European Railway Network, International XVII Scientific-Expert Conference on Railways RAILCON '16, October 13-14, Niš, Serbia, 2016, pp. 137-140.
[21] Vojnotehnički institut: Izveštaj o ispitivanjima kolosečnog pričvrsnog pribora Vossloh W14, Beograd, 2007.
[22] CEN/TC 256: EN 13674-1:2011, Railway applications - Track - Rail - Part 1: Vignole railway rails 46 kg/m and above, 2011.
[23] CEN/TC 256: EN 13674-4:2006+A1:2009, Railway applications - Track - Rail - Part 4: Vignole railway rails from 27 kg/m to, but excluding 46 kg/m, 2009.
[24] CLC/SC 9XC: EN 50122-2:2010, Railway applications - Fixed installations - Electrical safety, earthing and the return circuit - Part 2: Provisions against the effects of stray currents caused by d.c. traction systems, 2010.

REZIME

METODE ISPITIVANJA I TEHNIČKI USLOVI ZA SISTEME ŠINSKIH PRIČVRŠĆENJA ZA BETONSKE PRAGOVE

Milica VILOTIJEVIĆ
Zdenka POPOVIĆ
Luka LAZAREVIĆ

Program rekonstrukcije i modernizacije železničke mreže Republike Srbije treba uskladiti s tehničkim uslovima evropske železničke mreže, kako bi se realizovali zahtevi interoperabilnosti železničkog sistema. Na osnovu usvojene serije standarda SRPS EN 13481 i SRPS EN 13146, analiziraju se tehnički uslovi za primenu sistema šinskih pričvršćenja za betonske pragove. Cilj rada jeste da se inženjerska javnost u Srbiji upozna s pomenutim serijama standarda i da se olakša njihova praktična primena.

Ključne reči: železnica, sistemi šinskih pričvršćenja, metode laboratorijskih ispitivanja, ispitivanje pod saobraćajem, tehnički uslovi, harmonizacija

SUMMARY

TEST METHODS AND REQUIREMENTS FOR FASTENING SYSTEMS FOR CONCRETE SLEEPERS

Milica VILOTIJEVIC
Zdenka POPOVIC
Luka LAZAREVIC

In order to realize interoperability of railway system, the reconstruction and modernization plan of railway network in the Republic of Serbia should be harmonized with technical requirements of European railway network. Performance requirements for fastening systems for concrete sleepers were analysed according to the adopted standard series SRPS EN 13481 and SRPS EN 13146. The aim of the paper is to introduce engineering public in Serbia with mentioned two standard series and to facilitate their practical implementation.

Key words: railway, fastening systems, laboratory test methods, in service testing, performance requirements, harmonization

ODREĐIVANJE IN-SITU KOEFICIJENTA TRENJA I IMPERFEKCIJE KABLOVA ZA PREDNAPREZANJE

DETERMINATION OF THE IN SITU COEFFICIENT OF FRICTION AND IMPERFECTION OF PRESTRESSING CABLES

Dragan BOJOVIĆ
Bojan ARANĐELOVIĆ
Ksenija JANKOVIĆ
Aleksandar SENIĆ
Marko STOJANOVIĆ

STRUČNI RAD
PROFESSIONAL PAPER
UDK: 624.042.7
doi:10.5937/grmk1702049B

1 UVOD

Savremena armiranobetonska konstrukcija značajnih raspona ne može se zamisliti bez njenog prednaprezanja. Projektovanje ustanovljeno na samim počecima ovakvih sistema, s malim izmenama nedavno uvedenim, u upotrebi je i danas širom sveta. Jedna od osnovnih premisa jeste to da sila u kablu na aktivnom kraju za vreme zatezanja ne sme preći vrednost datu obrascem (1):

$$P_{max} = A_p \cdot s_{p,max} \quad (1)$$

gde A_p predstavlja površinu poprečnog preseka kabla i $s_{p,max}$ maksimalni napon u kablu. Vrednost $s_{p,max}$ određena je manjom vrednošću od $k_1 \cdot f_{pk}$ i $k_2 \cdot f_{p0,1k}$. Vrednosti k_1 i k_2 definisane su nacionalnim standardima. Najčešće se koriste vrednosti k_1=0,8 i k_2=0.9 [1,2]. Prekoračenje najveće sile zatezanja dopušta se u posebnim slučajevima kada se koristi veoma precizna oprema za prednaprezanje. Tada se najveća sila prednaprezanja određuje pomoću obrasca $k_3 \cdot f_{p0,1k} \cdot A_p$, gde se za koeficijent k_3 usvaja vrednost 0,95.

Mr Dragan Bojović, istraživač saradnik, IMS Institut, Bul. vojvode Mišića 43, Beograd, dragan.bojovic@institutims.rs
Bojan Aranđelović, IMS Institut, Bul. vojovde Mišića 43, Beograd, bojan.arandjelovic@institutims.rs
Dr Ksenija Janković, viši naučni saradnik, IMS Institut, Bul. vojvode Mišića 43, Beograd, ksenija.jankovic@institutims.rs
Aleksandar Senić, asistent, Građevinski fakultet Beograd, Bul. kralja Aleksandra 73, Beograd
Marko Stojanović, MSc, istraživač saradnik, IMS Institut, Bul. vojovde Mišića 43, Beograd, marko.stojanovic@institutims.rs

1 INTRODUCTION

Modern reinforced concrete structure of significant spans cannot be imagined without its prestressing. Nowadays, the design established at the very beginning of such systems, with small changes introduced in the recent past, is in use worldwide. One of the basic premises is that the force in the cable at the active end during tensioning must not exceed the value given in the following formula (1):

where A_p represents the cross-sectional area of the cable and $s_{p,max}$, the maximum stress in the cable. Value $s_{p,max}$ is determined by the lower value of $k_1 \cdot f_{pk}$ and $k_2 \cdot f_{p0,1k}$. The values of k_1 and k_2 are defined by national standards. The most commonly used values are k_1=0.8 and k_2=0.9 [1,2]. Exceeding the highest tension force is allowed in special cases when highly accurate equipment for prestressing is used. Then the maximum tensioning force is determined by using the formula $k_3 \cdot f_{p0,1k} \cdot A_p$ where the coefficient k_3 adopts the value of 0.95.

Dragan Bojović, MSc, research assistant, IMS Institute, Bul. vojvode Mišića 43, Belgrade, dragan.bojovic@institutims.rs
Bojan Aranđelović, PhD student, IMS Institute, Bul. vojvode Mišića 43, Belgrade, bojan.arandjelovic@institutims.rs
Ksenija Janković, PhD, senior research fellow, IMS Institute, Bul. vojvode Mišića 43, Belgrade, ksenija.jankovic@institutims.rs
Aleksandar Senić, assistant, Faculty of Civil Engineering, Bul. kralja Aleksandra 73, Belgrade
Marko Stojanović, MSc, research assistant, IMS Institute, Bul. vojvode Mišića 43, Belgrade, marko.stojanovic@institutims.rs

Za dobro projektovanje prednapregnutih konstrukcija u proračun se uvode i koeficijenti trenja i nepravilnosti, odnosno ugaonog odstupanja.

U proizvodnji čelika i plastičnih materijala, svakodnevno se uvode novine koje omogućavaju izradu bezbednijih konstrukcija. Tako, primenom savremenih čelika za prednaprezanje, relaksacija kablova svedena je na minimum. U građevinskoj praksi veoma često, u slučaju prednapregnutih konstrukcija, za trasiranje kablova upotrebljavaju se plastične orebljene cevi od novih vrsta plastike. Uticaj primene novih vrsta materijala na vrednosti koeficijenta trenja često se ostavlja na procenu projektantu. Najčešće se na nivou projekta uzimaju vrednosti koeficijenata iz važećih pravilnika i propisa koji možda i nisu uzeli u obzir primenu novih materijala u prednaprezanju. Dosadašnja iskustva na polju određivanja koeficijenata trenja i nepravilnosti izvođenja u slučaju prednaprezanja uglavnom su u vezi s teorijskim i laboratorijskim ispitivanjima. Kao što je već napomenuto, koeficijent trenja umnogome zavisi od primenjenih materijala, dok koeficijent nepravilnosti zavisi ponajviše od stepena obučenosti i savesnosti izvođača da izvede radove na prednaprezanju [3,4]. Parametri se usvajaju iskustveno, u granicama koje propisuju nacionalni standardi i propisi zemlje u kojoj se konstrukcija izvodi. Stvarno određivanje navedenih parametara jeste veoma komplikovano i zahteva dodatna sredstva od izvođača, kao i angažovanje specifične opreme. Samim tim, projektovani parametri najčešće se ne proveravaju.

Pri naknadnom utezanju kablova, sila prethodnog naprezanja i odgovarajuće izduženje kabla moraju da se provere merenjima, a moraju da se kontrolišu i stvarni gubici usled trenja. Pored ovih parametara, za projektante i izvođače na konstrukciji veoma bi korisno bilo da se analiziraju parametri u vezi s koeficijentom trenja i koeficijentom nepravilnosti izvođenja radova na prethodnom naprezanju [5].

2 TEORIJSKE POSTAVKE

Srednja vrednost sile prethodnog naprezanja $P_{m,t}(x)$ u datom trenutku vremena t, na rastojanju x od aktivnog kraja kabla, jednaka je najvećoj sili P_{max} kojom se kabl zateže na aktivnom kraju, umanjenoj za trenutne gubitke i gubitke koji zavise od vremena. Svi gubici razmatraju se u apsolutnim vrednostima.

Vrednost početne sile prednaprezanja $P_{m0}(x)$ za $t=t_0$, kojoj je beton izložen neposredno posle utezanja i ankerovanja kablova, ili posle prenošenja prethodnog naprezanja na beton, dobija se kada se sila prednaprezanja P_{max} umanji za trenutne gubitke ΔP_i (x), i ne treba da prekorači vrednost dobijenu obrascem (2):

For good design of prestressed structures, the coefficients of friction and imperfection, or angular deviation are introduced in the calculation.

In the production of steel and plastic materials new things which enable the production of safer structures are introduced every day. Thus, with the application of modern steel for prestressing the relaxation of cables is reduced to a minimum. In construction practice in the case of prestressed structures for tracing cables plastic corugated pipes made of new types of plastics are used very often. The effect of the application of new types of materials on the values of the coefficient of friction is often left for the designer to estimate. Most often at the design level coefficient values are taken from applicable policies and regulations that may not take into account the application of new materials in prestressing. Previous experience in the field of determining the coefficients of friction and imperfection of the execution of prestressing are mainly related to the theoretical and laboratory testing. As it is already mentioned, the coefficient of friction depends largely on the applied materials, while the coefficient of imperfection depends largely on the level of training and conscientiousness of the contractor to perform work on the prestressing [3.4]. The parameters are adopted empirically within the limits prescribed by national standards and regulations of the country where the structure is performed. Actual determination of the aforementioned parameters is a very complicated process which requires additional resources from the contractor, as well as the involvement of specific equipment. Therefore the designed parameters are usually not checked.

In post-tensioning of the cables the prestressing force and the corresponding elongation of the cable must be checked by measurements, and actual losses since the friction have to be controlled. In addition to these parameters, it would be of great use for designers and contractors of the structure to analyze the parameters related to the coefficient of friction and the coefficient of imperfection of execution of work on prestressing [5].

2 THEORETICAL PREMISES

Mean value of prestressing force $P_{m,t}(x)$ at a given time t, at a distance x from the active end of the cable is equal to the maximum force P_{max} which tension the cable on the active end, reduced for current losses and losses that depend on the time. All losses are considered in absolute values.

The value of the initial prestressing force $P_{m0}(x)$ for $t=t_0$, where the concrete is exposed immediately after the tensioning and anchoring of the cables, or after the transmission of the prestressing to concrete, is obtained when the prestressing force P_{max} is reduced by the current loss ΔP_i (x), and should not exceed the value obtained by the equation (2):

$$P_{m0}(x) = A_p \, s_{pm0}(x) \tag{2}$$

gde je $s_{pm0}(x)$ napon u kablu neposredno posle utezanja ili prenošenja sile kao manja vrednost od $k_7 \cdot f_{pk}$ i $k_8 \cdot f_{p0,1}$. Preporučene vrednosti za koeficijente jesu k_7=0,75 i k_8=0.85.

where $s_{pm0}(x)$ is the stress in the cable immediately after the tensioning or transmitting the force as a smaller value of $k_7 \cdot f_{pk}$ and $k_8 \cdot f_{p0.1}$. The recommended values for the coefficients are k_7=0.75 and k_8=0.85.

Sila prednaprezanja najčešće nije konstantna duž kabla usled trenja kabla o zidove kanala kroz koji prolazi i trenja usled promene pravca kabla. Pored toga, sila prednaprezanja se tokom vremena i smanjuje usled relaksacije čelika, skupljanja i tečenja betona.

Prema tome, u jednom preseku kabla imamo početnu silu P_{m0} u trenutku prednaprezanja, silu $P_{m,t}$ u nekom vremenu „t" i trajnu silu za $t \longrightarrow \infty$, $P_{m\infty}$. Za trajnu silu uzima se u obzir i promena sile usled dejstva stalnog i pokretnog opterećenja nakon prednaprezanja. Gubici koji se proračunavaju dati su u standardu SRPS EN:1992-1-1:2004 [6].

Kada se određuju trenutni $t=t_0$ gubici $\Delta P_i(x)$, razmatraju se sledeći trenutni uticaji usled kojih nastaju gubici pri utezanju, u zavisnosti koji od tih uticaja je relevantan:

– gubici pri ankerovanju - usled uvlačenja klina - ΔPsl;

– gubici usled elastičnih deformacija betona - ΔPel;

– gubici usled kratkotrajnog dejstva relaksacije - ΔPr;

– gubici usled trenja - ΔPμ(x).

Srednja vrednost sile prethodnog naprezanja $P_{m,t}(x)$ u vremenu $t > t_0$ određuje se u zavisnosti od metode utezanja. Pored navedenih trenutnih gubitaka, treba da se imaju u vidu i gubici prednaprezanja, koji zavise od vremena $\Delta P_{c+s+r}(x)$, a rezultat su tečenja i skupljanja betona i dugotrajne relaksacije čelika za prethodno naprezanje, tako da je

$$P_{m,t}(x) = P_{m0}(x) - \Delta P_{c+s+r}(x).$$

Početna sila u kablu (P_{po}) manja je od početne sile na presi (P_p), usled uvlačenja klinova u toku prenošenja sile s prese na kotvu. Prilikom uvlačenja klinova istovremeno, u približno istoj veličini, uvlače se i užad, što dovodi do pada sile u kablu usled izgubljenog izduženja. Uvlačenje klinova javlja se na strani aktivne i pasivne kotve. Uvlačenje klinova kod pasivne kotve ne mora uticati na smanjenje početne sile ukoliko se ukupno izduženje kod prese poveća za ovu vrednost. Uvlačenje klinova na strani prese, aktivne kotve, dovodi do smanjenja početne sile u kablu za veličinu izgubljenog izduženja, što može dati znatnu vrednost kod kratkih kablova. Uvlačenje klinova kod aktivne i pasivne kotve približno je isto i uzima se na nivou od 3 mm do 5 mm. Postoje načini da se ovaj gubitak delimično ili potpuno eliminiše, uz primenu posebnih procedura.

Elastično skraćenje konstrukcije dovodi do gubitka ukupne početne sile konstrukcije ukoliko se uteže više od jednog kabla. Gubitak je znatan u slučaju jako napregnutih elemenata malog preseka (npr. vešaljke, stubovi). Tada treba voditi računa o gubitku sile u kablu usled deformacije betona, kao i o zavisnosti od redosleda zatezanja kablova (prema SRPS EN:1992-1-1:2004).

Gubitak sile prednaprezanja javlja se u slučaju naknadno prednapregnutih elemenata usled trenja između kablova i zaštitnih cevi u betonu. Veličina ovog gubitka jeste funkcija oblika trase kabla - efekat zakrivljenosti i odstupanja prilikom montaže trase kablova - ugaono odstupanje. Vrednosti koeficijenata koji definišu gubitke sile često se preciziraju dok se

The prestressing force is usually not constant along the cable due to the friction of the cable on the walls of the channels through which it passes and friction due to the changes in the direction of the cable. In addition, the tensioning force is reduced over time due to relaxation of steel, shrinkage and creeping of concrete.

Accordingly, in a cross-section of the cable there is the initial force P_{m0} in the moment of prestressing, force $P_{m,t}$ in some time „t" and permanent force for $t \longrightarrow \infty$, $P_{m\infty}$. For the permanent force the changes of the force due to the effect of permanent and moving load after prestressing should also be taken into account. Losses that are computed are presented in standard SRPS EN:1992-1-1:2004 [6].

When determining the current $t=t_0$ losses $\Delta P_i(x)$ the following current impacts which lead to losses in tensioning are considered, depending on which of these impacts is relevant:

– losses at anchorage - due to insertion of the wedge - ΔP_{sl},

– losses due to elastic deformation of concrete - ΔP_{el},

– losses due to the short-term effects of relaxation - ΔP_r ,

– losses due to friction - $\Delta P_\mu(x)$.

Mean value of prestressing force $P_{m,t}(x)$ at time $t > t_0$ is determined depending on the method of tensioning. In addition to these current losses, the losses of prestressing which depend on the time $\Delta P_{c+s+r}(x)$, which are the result of creeping and shrinkage of concrete and long-lasting relaxation of steel for prestressing should be taken into account, so that:

$$P_{m,t}(x) = P_{m0}(x) - \Delta P_{c+s+r}(x).$$

Initial force in cable (P_{po}) is less than the initial force on the press (P_p) due to the insertion of wedges during the transmission of force to the anchor. During the insertion of wedges simultaneously at approximately the same size, cables are also drawn, leading to a drop in force in the cable due to the lost elongation. Insertion of wedges occurs on the side of the active and passive anchor. Insertion of wedges in the passive anchor need not to affect the reduction of the initial force if total elongation at press is increased by this amount. Insertion of wedges on the side of the press, active anchor, leads to a reduction in the initial force in the cable for the size of the lost elongation, which can have significant value for short cables. Insertion of wedges of active and passive anchor is approximately the same and is taken at the level of 3-5mm. There are ways to partially or completely eliminate this loss with the use of special procedures.

Elastic deformation of structures, leads to a total loss of the initial force of the structure if more than one cable is being tensioned. The loss is significant with highly prestressed elements with small cross-section: hangers, piles and the like. Then the loss of force in the cable due to deformation of concrete, as well as dependence from the order of tensioning cables (according to EN: 1992-1-1: 2004) have to be taken into account.

Loss of tensioning force occurs in post-prestressed elements due to friction between the cables and protective pipes in concrete. The value of this loss is a function of the form of the route of the cable-effect of

obavlja priprema projekta izborom različitih tipova i oblika trase kablova. Pošto je efekat zakrivljenosti unapred određen, ugaono odstupanje jeste rezultat slučajnog ili neizbežnog odstupanja, pošto ne postoji mogućnost da se trasa zaštitnih cevi idealno montira [7].

Treba imati u vidu da će maksimalna vrednost gubitka sile usled trenja biti na drugom kraju elementa, ako se zateže s jednog kraja. Stoga, gubitak usled trenja se menja linearno duž raspona elementa i može se interpolirati za posebne položaje ako je potrebna veća tačnost.

Gubici usled trenja $\Delta P_\mu(x)$, pri utezanju kablova, mogu da se procene prema obrascu (3):

curvature and deviation during the installation of cable route-angular deviation. The values of coefficients that define the losses of force is often specified while the preparation of the project by selecting different types and shapes of cable route is being done. As the effect of the curvature is predetermined, angular deviation is the result of accidental or unavoidable deviation, as there is no possibility for the trace of protective pipes to be ideally instaled [7].

It should be kept into account that the maximum value of the loss of force due to friction will be on the other end of the element, if it is tension from one end. Therefore, loss due to friction varies linearly along the element span and can be interpolated for specific positions if there is a need for greater accuracy.

Losses due to friction $\Delta P_\mu(x)$ when tensioning cables can be assessed according to the formula (3):

$$\Delta P_\mu(x)=P_{\max}(1-e^{-m\,(q\,+\,kx)}) \tag{3}$$

U prethodnom obrascu q predstavlja zbir skretnih uglova na rastojanju x izražen u rad; m je koeficijent trenja između kabla i cevi u koju je postavljen izražen u rad^{-1}; k određuje nenamerno ugaono skretanje unutrašnjih kablova izraženo u rad/m; i x predstavlja rastojanje izraženo u metrima duž kabla od tačke u kojoj je sila u kablu jednaka P_{max} to jest sila na aktivnom kraju kabla za vreme utezanja.

Za koeficijent trenja μ treba naglasiti da veoma zavisi od površinskih karakteristika kablova i cevi, a naročito od stepena korozije dodirnih površina. Veličina trenja zavisi i od vrste cevi koja se koristi i od tipa kabla. Postoje dva mehanizma koja proizvode trenje; prvi je zakrivljenost kabla, a drugi - slučajna razlika između težišta kablova i cevi.

In previous formula q represents the sum of the diverting angles at a distance x expressed in rad; m is the coefficient of friction between the cable and pipes in which it is placed, expressed in rad^{-1}; k determines accidental diverting angle of internal cables expressed in rad/m; and x is the distance expressed in m` along the cable from the point where the force in the cable is equal to P_{max} i.e. the force on the active end of the cable during tension time.

For the friction coefficient μ it should be emphasized that it is highly dependent on surface characteristics of cables and pipes, in particular on the degree of corrosion of contact surfaces. Amout of friction also depends on the type of pipes used and the type of cable used. There are two mechanisms that produce friction. The first is the curvature of the cable, and the other is a random difference between the center of gravity of the cables and the pipe.

3 IN-SITU EKSPERIMENTALNI RAD

Kompletan eksperiment urađen je na gradilištu, prilikom izgradnje mosta Borča-Zemun. Izvođač radova bio je CRBC (*China Road and Bridge Corporation*). Konstrukcija mosta van vode imala je dva sistema. Jedan od sistema uključivao je izradu prednapregnutih nosača statičke dužine 26 i 36 metara. U eksperimentu je korišćen nosač dužine 26 metara. Projektom je bilo predviđeno utezanje nosača sa četiri kabla od po sedam užadi prečnika 15,2 mm, dok je za trasu kablova korišćena plastična rebrasta cev. Karakteristični poprečni preseci i podužni presek nosača s trasama dva ispitivana kabla prikazani su na slici 1.

3 EXPERIMENTAL WORK IN SITU

The complete experiment was performed on construction site during the construction of the bridge Zemun-Borca. The contractor was the CRBC (China Road and Bridge Corporation). The construction of the bridge outside the water had two systems. One of the system included the making of prestressed girders with static length 26 and 36m. The experiment used the girder with the length of 26 meters. In the design tensioning of the girder with 4 cables of 7 ropes each with the diameter of 15,2mm was planned, while for the trace of cables corrugated plastic pipe was used. A typical cross-sections and longitudinal-section of the girder with traces of two tested cables are shown in Figure 1.

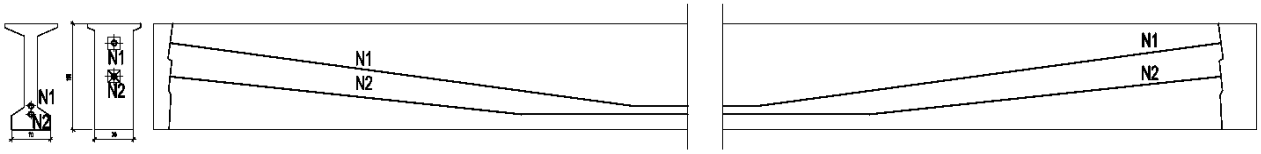

Slika 1. Karakteristični poprečni i podužni presek AB nosača
Figure 1. Typical cross section and longitudinal section of RC girders

Slika 2. Aktivni kraj
Figure 2. Active end

Slika 3. Pasivni kraj
Figure 3. Passive end

Eksperiment je obuhvatio određivanje koeficijenta trenja i koeficijenta imperfekcije, s tim što nisu uzimani u obzir efekti zaklinjavanja i elastične deformacije betona. Efekti zaklinjavanja nisu se imali u vidu, jer su procedurama i modifikacijama IMS sistema prednapre-zanja uticaji svedeni na minimum. Presa za utezanje modifikovana je tako da se zaklinjavanje vrši pre otpuštanja kablova. Poštujući proceduru upravljanja presom, efekat zaklinjavanja se može zanemariti. Projektom je predviđeno utezanje kompletnog nosača sa četiri kabla, a u eksperimentu je planirano utezanje s jednim kablom do ~90% projektovane sile. Efekat elastične deformacije betona na ovom nosaču i pri usvojenoj dispoziciji ispitivanja može se zanemariti, jer se vrši utezanje samo s jednim kablom koji se otpušta pre utezanja sledećeg kabla.

Planirano je da se prvo uteže kabl N1 do 95% projektovane sile u kablovima. Potom, vršeno je zaklinjavanje i praćenje sile naredna 24 sata. Pri utezanju kabla, merenja su sprovođena na svakih 20% maksimalno projektovane sile. Praktično, sila se merila na 20%, 40%, 60% i 80% maksimalne projektovane sile u kablovima. Merenja su natavljena i nakon 24 sata. Potom, izvršeno je rasklinjavanje utegnutog kabla N1 i pristupilo se utezanju kabla N2. Merilo se sve, kao i u slučaju kabla N1. Nakon postizanja predviđene sile, vršeno je zaklinjavanje i praćenje sile naredna 24 sata. Naposletku, izvršeno je rasklinjavanje kabla N2. Rezultati merenja sile utezanja na aktivnom i pasivnom kraju dati su u tabeli 1.

The experiment included the determination of the coefficient of friction and the coefficient of imperfection, except that the effects of wedging and elastic deforma-tion of concrete were not taken into account. The effects of wedging were not taken into account because the procedures and modifications of the IMS system of presstresing minimized the impact. Press for tensioning has been modified so that wedge done before releasing the cables. By respecting procedures of using press wedging effect can be ignored. Design is anticipated tensioning of the complete girder with 4 cables, while the experiment tensioning with one cable up to ~90% designed force is planned. Effect of elastic deformation of concrete at such girders in adopted disposition tests can be ignored becouse it performs tensioning with only one cable which is released before tensioning second cable.

It was planned for cable N1 to be tensioned first and up to ~90% of the designed force in the cables. Then wedging was carried out and the force was monitored for the next 24 hours. While tensioning the cable measure-ments were conducted for every 20% of the maximum designed force. Practically force measurements were conducted at 20, 40, 60 and 85-95% of the maximum designed force in the cables. Measurements were also carried out after 24 hours. Then the released of tensioned cable N1 was performed and tensioning of cable N2 was started. All measurements were performed the same as for cable N1. After reaching the planned force wedging was performed and the force was followed for the next 24 hours. At the end released of cable N2 was performed. The results of the tensioning force measurements on the active and passive end are given in table 1.

Tabela 1. Rezultati merenja sile utezanja u kablovima N1 i N2
Table 1. The results of tensioning force measurements in cables N1 and N2

Sila / *Force*	Kabal N1 / *Cable N1*			Kabal N2 / *Cable N2*		
	Aktivni kraj *Active end*	Pasivni kraj / *Passive end*		Aktivni kraj *Active end*	Pasivni kraj / *Passive end*	
	t→0	t→0	t→24h	t→0	t→0	t→24h
20%	347kN	314kN	-	348kN	312kN	-
40%	694kN	649kN	-	694kN	675kN	-
60%	1041kN	982kN	-	1041kN	1026kN	-
~90%	1379kN	1304kN	1302kN	1276kN	1180kN	1179kN

4 DISKUSIJA I ZAKLJUČCI

Rezultati ispitivanja obrađeni su na dva načina. Izračunati su koeficijenti trenja i koeficijenti imperfekcije na osnovu sila utezanja na dva kabla, kao i procena poređenja koeficijenta trenja za različite nivoe utezanja kablova. kabal

Proračun koeficijenta trenja i koeficijenta imperfekcije svodi se na rešavanje sistema jednačina s dve nepoznate. Jednačine su prikazane obrascima (4) i (5).

$$\ln(P_{1,x} / P_{1,max}) = -\mu*(\theta_1 + kx) \quad (4)$$

$$\ln(P_{2,x} / P_{2,max}) = -\mu*(\theta_2 + kx) \quad (5)$$

Ukupni skretni ugao θ_1 u kablu N1 iznosio je 15.346°, a θ_2 u kablu N2 iznosio - 12.136°. Dužina na kojoj je merena vrednost smanjenja sile jeste kraj kabla x=26,097 m. Na osnovu ulaznih podataka i rešavanja sistema jednačina s dve nepoznate, dobijene su vrednosti za koeficijent trenja kablova μ=0,22 i koeficijent imperfekcije k=0,004.

Nakon rešavanja sistema jednačina, izvršen je i proračun koeficijenta trenja pojedinačno za kablove za različite nivoe utezanja kablova. Proračun je vršen posebno za svaki kabl i raspon koeficijenta imperfekcije od 0,001 do 0,01 s korakom 0,001. Dobijeni rezultati prikazani su na slikama 4 i 5.

4 DISCUSION AND CONCLUSIONS

Test results processing was done in two ways. Coefficients of friction and coefficients of imperfection on the basis of tension forces in two cables as well as an evaluation of the comparison of the coefficient of friction for different levels of tension cables.

Calculation of the coefficient of friction and the coefficient of imperfection is reduced to solving a system of equations ((4) and (5)) with two unknowns.

Total deviation angle θ_1 in the cable N1 was 15.346°, and θ_2 in the cable N2 amounted to 12.136°. Length at which the measured value of the reduction in force is the end of the cable x=26.097m. Based on the input data and solving the system of equations with two unknowns, the values for the coefficient of friction of cables μ=0.22 and imperfection coefficient k=0.004 were obtained.

After solving the system of equations a calculation of the coefficient of friction of cables was made separately for different levels of cables tensioning. The calculation was done separately for each cable and imperfection coefficient ranging from 0.001 to 0.01 with step 0.001. The obtained results are shown in Figures 4 and 5.

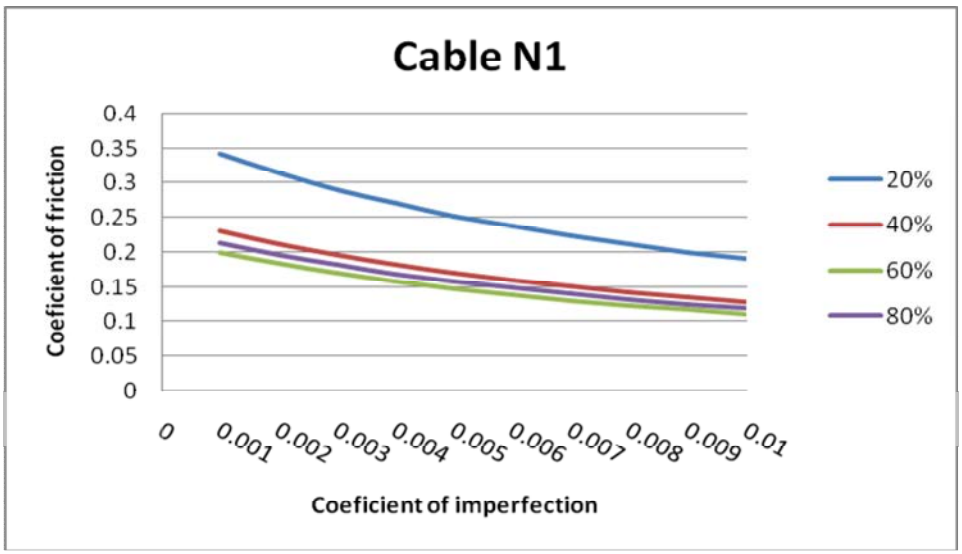

Slika 4. Koeficijent trenja kabla N1 u zavisnosti od koeficijenta imperfekcije
Figure 4. The coefficient of friction of the cable N1 depending on the coefficient of imperfection

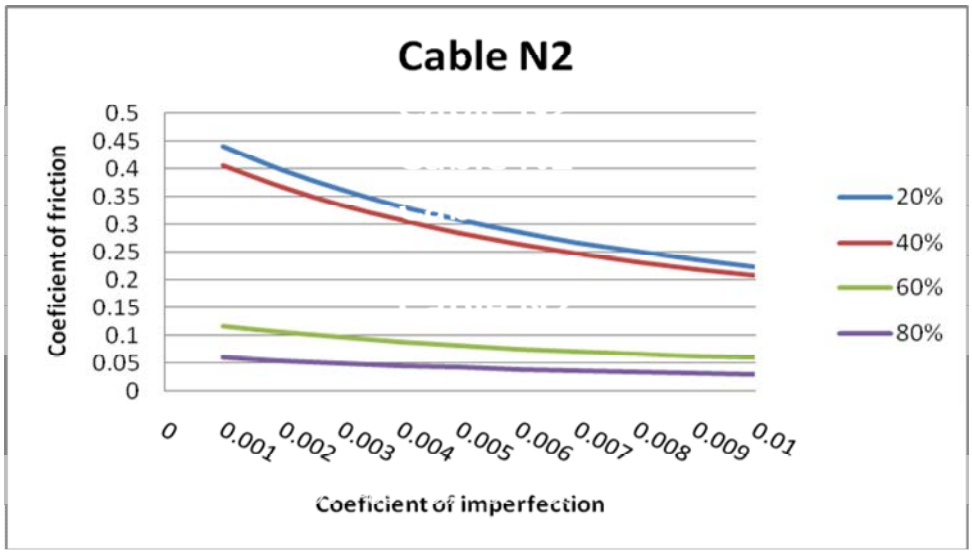

Slika 5. Koeficijent trenja kabla N2 u zavisnosti od koeficijenta imperfekcije
Figure 5. The coefficient of friction of the cable N2 depending on the coefficient of imperfection

Zajedničkom obradom rezultata ispitivanja dva kabla, dobijeni su rezultati koji se mogu uporediti sa standardom i preporukama definisanim vrednostima iz tabele 2. Kao što se može videti, dobijena vrednost za plastične rebraste cevi, koeficijenta trenja μ=0,22 nešto je veća, dok je koeficijent imperfekcije k=0,004 u predloženim granicama. Koeficijent imperfekcije zavisi umnogome od izvođača radova i od njegove sposobnosti da što bolje postavi kabl. Time se imperfekcije znatno smanjuju i uticaj se može svesti na minimum. Koeficijent trenja jeste nešto na šta se ne može uticati i njegova vrednost će zavisiti najviše od materijala koji se koriste za vođenje kabla.

By joint processing of the test results for two cables the obtained results are comparable with the standard and recommendations defined by the values from Table 2. As it can be seen, the value obtained for plastic corrugated pipes, the friction coefficient μ=0.22 is slightly higher, while the coefficient of imperfection k=0.004 is in the suggested limits. The coefficient of imperfections depends greatly on the contractor and its ability to instal the cord as good as possible. This significantly reduces the imperfections and the impact can be brought down to a minimum. The coefficient of friction cannot be influenced and its value depends the most on the materials used for tracing the cable.

Tabela 2. Preporučene vrednosti proizvođača za koeficijente trenja i imperfekcije
Table 2. Manufacturers recommended values for the coefficients of friction and imperfection

Tip cevi *Type of pipe*	μ (rad^{-1})		k (rad/m)	
	Opseg vrednosti *Value range*	Preporuka za proračun *Recommendation for design*	Opseg vrednosti *Value range*	Preporuka za proračun *Recommendation for design*
Rebrasta metalna *Corugated metal*	0.18 ÷ 0.26	0.22	$(1\text{-}10)\cdot10^{-3}$	$3\cdot10^{-3}$
Rebrasta plastična *Corugated plastic*	0.10 ÷ 0.14	0.12	$(1\text{-}10)\cdot10^{-3}$	$4\cdot10^{-3}$
Plastična sa mašću *Plastic with grease*	0.05 ÷ 0.08	0.06	$(2\text{-}6)\cdot10^{-3}$	$4\cdot10^{-3}$
Beton / *Concrete*	0.34 ÷ 0.62	0.48	$(1\text{-}10)\cdot10^{-3}$	$5\cdot10^{-3}$

Razmatrajući rezultate po nivoima unošenja sile u kablove, jasno je da je na manjim silama utezanja koeficijent trenja daleko veći. Prilikom postavljanja kabla i manjih sila u kablovima, prvo dolazi do nameštanja kablova i gubici od aktivnog do pasivnog kraja su znatni. Kasnije, kada se kabl namesti u konačnu poziciju, trenje se smanjuje i dolazi na vrednosti koje se mogu pretpostaviti, u zavisnosti od materijala cevi za vođenje kablova.

Considering the results according to the levels of force application in the cables, it is clear that for lower tension forces coefficient of friction is far greater. When setting up the cable and lower forces in the cables, the cables are first being installed and losses from the active to the passive end are considerable. Later, when the cable is installed in the final position the friction decreased and the values that can be assumed depending on the material of the pipes for cables are obtained.

5 LITERATURA
REFERENCES

[1] ETAG 013 (Guideline for European Technical Approval of post-tensioning kits for prestressing of structures), EOTA, 2002.
[2] Sistem za prednaprezanje SPB SUPER, Institut IMS, Beograd, 2009.
[3] Nigel R. Hewson Prestressed concrete bridges: design and construction, Thomas Telford LTD, III Edition, 2003.
[4] Edward G. Nawy, Prestressed concrete: a fundamental approach, Prentice Hall, V edition, 2009.
[5] M.K. Hurst, Prestressed concrete design, CRC Press, II Edition, 2003.
[6] SRPS EN:1992-1-1, European Standard, 2004.
[7] Robert Benaim, The design of prestressed concrete bridges; concepts and principles, Taylor and francis Group, London and New York, 2008.
[8] Jordan Milev, Problems and Their Solutions in Practical Application of Eurocode in Seismic design of RC Structures, Building Materials and Constructiion, ISSN 2217-8139, 2016.
[9] Miloš Čokić, Petronijević P., Todorović M., Pecić N., Analiza Rezerve Energije i Emisije CO_2 za izvođenje mostovske konstrukcije sa stanovišta održivosti, Building Materials and Construction, ISSN 2217-8139, 2015.

REZIME

ODREĐIVANJE IN-SITU KOEFICIJENTA TRENJA I IMPERFEKCIJE KABLOVA ZA PREDNAPREZANJE

Dragan BOJOVIĆ
Bojan ARANĐELOVIĆ
Ksenija JANKOVIĆ
Aleksandar SENIĆ
Marko STOJANOVIĆ

Prednaprezanjem konstruktivnih elemenata omogućava se povećavanje raspona armiranobetonskih konstrukcija. Pri projektovanju i dimenzionisanju prednapregnutih armiranobetonskih konstrukcija, neophodno je poznavanje, odnosno usvajanje većeg broja parametara koji su empirijski određeni. Za prednapregnute konstrukcije od osnovnog je značaja da se odredi nivo sile naprezanja kablova. Nivo sile prednaprezanja, pored drugih parametara, umnogome zavisi od koeficijenta trenja kablova i koeficijenta imperfekcije izvođenja. Ovi koeficijenti definisani su standardima za projektovanje ili su ih definisali proizvođači sistema prednaprezanja. Koeficijenti su definisani u širokim opsezima, dok je za projektovanje neophodno poznavanje što tačnijih vrednosti, kako bi se dobio dobar projekat i jeftinija konstrukcija. Putem eksperimentalnog rada in-situ, određen je opseg vrednosti koeficijenta trenja kablova i upoređen je sa standardom definisanim opsezima.

Ključne reči: prednaprezanje, koeficijent trenja, koeficijent imperfekcije

SUMMARY

DETERMINATION OF THE IN SITU COEFFICIENT OF FRICTION AND IMPERFECTION OF PRESTRESSING CABLES

Dragan BOJOVIC
Bojan ARANDJELOVIC
Ksenija JANKOVIC
Aleksandar SENIC
Marko STOJANOVIC

Prestressing structural elements allows an increase in the spans of reinforced concrete structures. In the design and dimensioning of prestressed reinforced concrete structures it is necessary to know, that is to adopt a number of parameters which are empirically determined. Determining the level of the tension force of the cables is of primary importance for prestressed structures. The level of tensioning force, in addition to other parameters, greatly depends on the friction coefficient of cables and the imperfection coefficient of execution. These coefficients are defined by standards for the design or by the manufacturer of the prestressing system. The coefficients are defined in wide ranges, while for the design, the knowledge of the most accurate values is necessary in order to obtain a good design and cheaper structures. Through experimental work in-situ the range of the values of the coefficient of friction of cables is determined and compared with ranges defined by the standard.

Key words: prestressing, coefficient of friction, coefficient of imperfection

IMPLEMENTACIJA VLAKNASTOG "STUB-GREDA" ELEMENTA U AKADEMSKI *CAD* SOFTVER - *MATRIX 3D*

FIBER BEAM-COLUMN ELEMENT IMPLEMENTATION IN ACADEMIC *CAD* SOFTWARE *MATRIX 3D*

Đorđe JOVANOVIĆ
Drago ŽARKOVIĆ
Zoran BRUJIĆ
Đorđe LAĐINOVIĆ

PRETHODNO SAOPŠTENJE
PRELIMINARY REPORT
UDK: 624.072.2/.3:004.4
doi:10.5937/grmk1702057J

1 UVOD

Razvoj nelinearnih analiza konstrukcija, kao i napreci u aseizmičkom projektovanju, doveli su do potrebe za sofisticiranijim konačnim elementima (KE). Iako su 2D i 3D KE nesumnjivo tačniji kada je reč o preciznim nelinearnim analizama, postoje mnoge poteškoće s njihovom upotrebom. Neke od najvažnijih su komplikovana interpretacija rezultata, glomazne numeričke procedure koje zahtevaju dosta vremena, te komplikovana izrada geometrije i mreže samog modela. Kod okvirnih konstrukcija, sve ove prepreke mogu se otkloniti upotrebom vlaknastih linijskih KE. Vlaknasti KE mogu biti podeljeni u one koncipirane na metodi sila (FB) i na metodi deformacija. Iako je velika većina kompjuterskih programa za analizu konstrukcija bazirana na metodi deformacija, razvijeni su i efikasni algoritmi za implemen-

1 INTRODUCTION

Developments in earthquake engineering and nonlinear analysis have led to need for more sophisticated finite-elements (FE). Even though 2D or 3D FEs are certainly more accurate for precise nonlinear analysis, there are many drawbacks in its use. Some of the most relevant are complicated interpretation of results, cumbersome numerical analysis, and substantial time for modelling. All of these obstacles are surpassed with the use of fibre line elements, obviously provided frame-type structure is analysed. Fibre FE can be divided into force-based (FB) and displacement-based elements. Although great majority of software is displacement based, efficient algorithm for implementation of FB elements is developed in [22, 24]. Basic formulation of FB element used in this paper is designed by a group of scientists

Đorđe Jovanović, mast. inž. građ. - asistent
Fakultet tehničkih nauka Univerziteta u Novom Sadu,
Trg Dositeja Obradovića 6, 21000 Novi Sad,
e-mail: djordje.jovanovic@uns.ac.rs
Drago Žarković, mast. inž. građ. - asistent
Fakultet tehničkih nauka Univerziteta u Novom Sadu,
Trg Dositeja Obradovića 6, 21000 Novi Sad,
e-mail: dragozarkovic@uns.ac.rs
Docent dr Zoran Brujić, dipl. inž. građ.
Fakultet tehničkih nauka Univerziteta u Novom Sadu,
Trg Dositeja Obradovića 6, 21000 Novi Sad,
e-mail: zbrujic@gmail.com
Profesor dr Đorđe Lađinović, dipl. inž. građ.
Fakultet tehničkih nauka Univerziteta u Novom Sadu,
Trg Dositeja Obradovića 6, 21000 Novi Sad,
e-mail: ladjin@uns.ac.rs

Đorđe Jovanović, MSc, teaching assistant
Faculty of technical sciences, Universityof Novi Sad,
Trg Dositeja Obradovića 6, 21000 Novi Sad,
e-mail: djordje.jovanovic@uns.ac.rs
Drago Žarković, MSc, teaching assistant
Faculty of technical sciences, Universityof Novi Sad,
Trg Dositeja Obradovića 6, 21000 Novi Sad,
e-mail: dragozarkovic@uns.ac.rs
Zoran Brujić, docent, PhD
Faculty of technical sciences, Universityof Novi Sad,
Trg Dositeja Obradovića 6, 21000 Novi Sad,
e-mail: zbrujic@gmail.com
Đorđe Lađinović, professor, PhD
Faculty of technical sciences, Universityof Novi Sad,
Trg Dositeja Obradovića 6, 21000 Novi Sad,
e-mail: ladjin@uns.ac.rs

taciju FB konačnih elemenata u ove softvere [22, 24]. Osnovnu formulaciju FB elemenata korišćenih u ovom radu razvila je grupa naučnika predvođenih Fillipou-om [18,22-24] koja je kasnije istu formulaciju unapredila uključivši u nju neke aspekte kao što su smičuće deformacije [8,11], efekti deterioracije veze između armature i betona [6] i spregnuti preseci [3]. Ovi radovi predstavljaju teorijsku osnovu softvera *OpenSees*, razvijenog na Univerzitetu Kalifornije, Berkliju, koji je jedan od najpopularnijih softvera za nelinearne seizmičke analize u polju naučnih istraživanja. Prvobitno je formulacija razvijena za linearnu geometriju/nelinearan material [8,18], da bi ubrzo potom Neuenhofer i Filippou [19] prezentovali proceduru za nelinearnu geometriju/linearan material. Nedavno, De Souza je prezentovao u [9] unapređivanje njihovog rada uvodeći korotacionu formulaciju, omogućivši tako analizu s velikim deformacijama i velikim rotacijama. Njegov rad se može posmatrati kao uopštenje procedure određivanja stanja elementa razvijene u [8] i [19]. Različiti pristupi vodili su ka drugim unapređivanjima uključujući smičuće deformacije [16,17], čime se uspela obuhvatiti interakcija između aksijalnih, fleksionih i smičućih odgovora s velikom tačnošću. Svi navedeni vlaknasti KE prvenstveno su korišćeni za dinamičku analizu betonskih konstrukcija. Odlična sposobnost ovih KE u proceni ponašanja spregnutih konstrukcija potvrđena je u [13,20]. Thai i Kim [25,26] uveli su funkcije stabilnosti i nelinearne opruge u pomenutu formulaciju, i koristili FB elemente za analizu čeličnih konstrukcija.

U ovom radu, formulacija veoma slična onoj korišćenoj u [26] biće prezentovana, razmatrana i verifikovana, takođe na primeru čeličnih konstrukcija. Ova formulacija je implementirana u akademski softver za analizu konstrukcija – Matrix 3D [28,29], razvijen na Fakultetu tehničkih nauka u Novom Sadu, koji je prevashodno koncipiran za nelinearne analize. Softver je baziran na metodi konačnih elemenata i obuhvata analizu konstrukcija modeliranih linijskim, površinskim i prostornim konačnim elementima. U ovom radu su korišćeni samo linijski konačni elementi – Bernoulli-Euler-ova greda, tačkasta oslanjanja u smislu elastičnih opruga i tačkasto opterećenje. Matrica krutosti sistema $\boldsymbol{K_{sys}}$ i vektor ekvivalentnog čvornog opterećenja $\boldsymbol{P}$ sastavljeni su metodom kodnih brojeva, transformacijom u globalni koordinatni sitem. Rešenje nepoznatih pomeranja za datu matricu krutosti sistema i vektor čvornih opterećenja izvršeno je postupkom Gausove eliminacije. Matrix 3D ima razvijen kompletan grafički korisnički interfejs, što će biti prikazano u poglavlju 3.1.

2 FORMULACIJA VLAKNASTOG STUB-GREDA ELEMENTA

Postoje dve mogućnosti za numeričko opisivanje materijalno-nelinearnog ponašanja u gredama i stubovima: koncentrisana i raspodeljena plastičnost. Ukratko, koncentrisana plastičnost, najčešće modelirana nelinearnim zglobovima (*hindges*), podrazumeva dva velika ograničenja. Prvo, precizna pozicija očekivanih plastičnih zglobova mora biti poznata a priori, i drugo, nelinearna relacija je definisana kao zavisnost između presečnih sila i deformacija. Ovakvi tipovi zavisnosti su poznati iz eksperimenata, zatim uprosečeni i uprošćeni i potom specificirani u različitim tehničkim propisima kao

led by Fillipou [18,22-24] and is afterwards improved by same group to include some other aspects such as shear deformations [8,11], effects of bond deterioration [6], and composite sections [3]. This work established theoretical foundation of *OpenSees*, software developed on University of California, Berkley, and one of the most popular for academic research in the field of nonlinear seismic analyses. Firstly, formulation is developed for linear geometry/nonlinear materials [8,18], and shortly after Neuenhofer and Filippou [19] presented procedure for linear material/nonlinear geometry. Recently, De Souza presented in [9] extension of their work introducing corotational formulation, thus enabling analysis with large displacements and large rotations. His work can be viewed as a generalisation of the state determination procedures established in [8] and [19]. Different approaches led to other improvements on including shear deformations [16,17], thus enabling to capture interaction between axial, flexural and shear responses with great accuracy. All of the mentioned fibre elements are used primarily for dynamic analysis of concrete structures. Excellent ability of these elements to predict behaviour of composite structures is validated in [13,20]. Thai and Kim [25,26] included stability functions and nonlinear springs, and used FB elements for analysis of steel structure.

In this paper, formulation very similar to one used in [26] will be presented, discussed and tested, also on steel structure examples. This formulation is implemented in academic software for structural analysis - Matrix 3D [28,29], developed on the Faculty of technical sciences in Novi Sad, which is primarily developed for nonlinear analyses. Software is based on finite element method and includes analysis of structures modelled by line, surface and special elements. In this paper only line elements are used – Bernoulli-Euler beam, point supports as elastic springs and point loads. System stiffness matrix $\boldsymbol{K_{sys}}$ and equivalent node load vector $\boldsymbol{P}$ are assembled by code number method, with transformation to global coordinate system. Solution of unknown displacements for system stiffness matrix and node load vector is found using Gaussian elimination. Matrix 3D has graphical user interface developed, which will be shown in chapter 3.1.

2 FIBRE BEAM-COLUMN ELEMENT FORMULATION

There are two options for describing nonlinear material behaviour in beams and columns: lumped and distributed plasticity. Briefly, lumped plasticity, most often modelled with hinges, has two major shortcomings. Firstly, precise position of expected plastic hinge must be known a priori, and secondly nonlinear relation is specified as relation between force and deformation. These types of relations are known from experiments, further simplified and specified in various codes such as [21], textbooks etc. More realistic way of performing materially-nonlinear-only analysis (MNO) is through the

što je npr. [21], priručnicima i tako dalje. Realističniji način sprovođenja samo-materijalno-nelinearne analize (MNO) jeste kroz konstituisanje zakona materijalne nelinearnosti na nivou napon/deformacija, gde vlaknasti elementi imaju prednost.

Prvi vlaknasti KE korišćeni su na sličan način kao nelinearni zglobovi, pozicionirani na mestima na kojima se očekuju plastični zglobovi u konstrukciji, samo da bi se integracijom napona realističnije predstavila zavisnost sila/pomeranje. Vremenom je mogućnost korišćenja jednog konačnog elementa po štapu postala moguća. Stoga je priprema numeričkog modela postala manje vremenski zahtevna, i ako je cilj koristiti jedan KE po štapu, FB elementi su prikladniji izbor. Ipak, FB elementi se retko mogu pronaći u komercijalnim CAD softverima. Osnovna prepreka za široku upotrebu ovog tipa elemenata je teškoća integrisanja jedne faze proračuna (određivanja nelinearnog stanja u elementu) u program baziran na metodi deformacija [24]. Ova prepreka je prevaziđena procedurom određivanja stanja, predloženom u [22], u kojoj se iterativno određuju unutrašnje sile i matrica krutosti striktno zadovoljavajući uslove ravnoteže i kompatibilnosti u svakoj iteraciji. Ovim analiza postaje inkrementalno-iterativna, što je razmatrano u 2.4. Budući da analizu sistema s više stepeni slobode potpuno zasnovanu na metodi sila nije jednostavno automatizovati [18], većina CAD softvera je bazirana na metodi deformacija. Ovo znači da su linearni KE zasnovani na interpolacijskim funkcijama za opisivanje pomeranja štapa. Konvencionalni linijski KE u svojoj formulaciji uključuju Hermit-ove polinome za polje poprečnih pomeranja i Lagranž-ove funkcije oblika za polje aksijalnih pomeranja. Nasuprot ovome, formulacija FB elemenata se bazira na interpolacionim funkcijama za predstavljanje presečnih sila. Osnovna razlika je što se u klasičnom grednom KE sa dva čvora, zasnovanom na konceptu krutosti, krivina menja linearno duž elementa (dok u stvarnom nosaču krivina postaje veoma nelinearna kako dolazi do tečenja materijala). Kod FB elementa koji nema opterećenja duž štapa, pretpostavljena je linearna promena momenta savijanja, što je tačno i u slučaju plastifikacije. Kao posledica ovoga, dovoljno je koristiti jedan KE za modeliranje jednog štapa, a preciznost će zavisiti od usvojene tolerancije numeričke greške. S druge strane, kod elementa formulisanog prema metodi deformacija, pored numeričke greške javlja se i greška usled aproksimativne prirode interpolacijske funkcije. Ovo je osnovna prednost FB elemenata, dok su ostale pregledno prikazane u radovima [15,18].

U softver Matrix 3D implementiran je, i u ovom radu testiran, FB fiber element. Osnovna formulacija ovog elementa zasnovana je na mešovitoj metodi, kao što je to detaljno prikazano u [24], koja se za specifičan izbor konstitutivnih odnosa preseka svodi na klasičnu metodu fleksibilnosti. Osnovne pretpostavke formulacije elementa su male deformacije i Bernoulli-jeva pretpostavka o ravnim presecima tokom cele istorije opterećenja. Predloženom formulacijom elementa ravnoteža svih sila je zadovoljena u svakom trenutku, a kompatibilnost je zadovoljena ne samo na krajevima elementa, već i duž njega [24]. Samo izvođenje formulacije konačnog elementa stub-greda u ovom radu će biti izostavljeno, a može se pronaći u [24], dok će detaljno biti prikazana procedura proračuna implementirana u softver Matrix 3D.

constitution of material nonlinear law, where fibre elements come superior.

First fibre elements were used in the similar way as hinges, positioned in the area of expected plastic hinge, only to represent more realistic force/deformation dependence through integration of stresses. Later the possibility of using only one FE per element became possible. Hence, pre-processing became less time-consuming and, if the goal is to use one element per member, FB elements are more suitable. Still, FB elements may be scarcely found in commercial CAD software. Main obstacle in the widespread use of this type of elements is the difficulty of integrating nonlinear element state determination in an analysis program based on direct stiffness method [24]. This obstacle is overcome by a state determination procedure, proposed by [22] that iteratively determines the element resisting forces and stiffness matrix, while strictly satisfying element equilibrium and compatibility in each iteration. With this, analysis becomes incremental-iterative, which is discussed in 2.4. Since a pure flexibility formulation is not easily feasible in multi-degree freedom structure model [18], most of the CAD software is displacement-based. This means that linear elements are based on appropriate interpolation functions for member displacements. Conventional frame elements are based on Hermitian polynomials for transverse displacement fields, and Lagrange shape functions for axial displacements. On the contrary, formulation of FB elements is based on interpolation functions for the internal forces. The main difference is that in classical stiffness-based 2-node element, curvature distribution is assumed linear (and in real member it becomes highly nonlinear as material softening occurs), while in FB element in the absence of distributed element loads, moment distribution is assumed linear, which is true. As result, only one element per member can be used, with accuracy depending on adopted tolerance of numerical error. On the other hand, displacement-based elements, in addition to numerical error, suffer from error due to the approximate nature of interpolation functions. This is the basic advantage of the FB elements, while others are presented in [15,18].

In software Matrix 3D FB fibre element is implemented, and it is tested in this paper. Basic formulation of this element is based on the mixed method, as it is presented in detail in [24], which for a specific choice of section constitutive relation simplifies to the classical flexibility method. Fundamental assumptions of the element formulation are that deformations are small and plane sections remain plane during the loading history (Bernoulli assumption). With the proposed formulation, equilibrium along the element is always strictly satisfied, and compatibility is satisfied not only at the element ends, but also along the element [24]. Pure derivation of the beam-column element formulation will be omitted in this paper, and can be found in [24], while procedure of calculation implemented in Matrix 3D will be presented.

Process of calculation for a single load increment is achieved on three different levels: structure, element and section level. After calculating structure displacements using global stiffness matrix (1), another set of element degrees of freedom is adopted, and deformations are recalculated using transformation matrix $\boldsymbol{L}$ given in [23].

Proces proračuna za jedan inkrement opterećenja sprovodi se na tri različita nivoa: na nivou konstrukcije, štapa i nivou preseka. Nakon izračunavanja generalizovanih pomeranja konstrukcije koristeći globalnu matricu krutosti (1), usvaja se novi set stepeni slobode za svaki KE i deformacije se ponovo izračunavaju uz pomoć matrice transformacije ***L*** date u [23].

$$d\Delta \boldsymbol{p} = \boldsymbol{K}_{sys} \setminus \Delta \boldsymbol{P} \tag{1}$$

gde je $d\Delta \boldsymbol{p}$ vektor generalisanih pomeranja konstrukcije, $\boldsymbol{K}_{sys}$ je globalna matrica krutosti i $\Delta \boldsymbol{P}$ predstavlja inkrement opterećenja.

Poslednja jednačina važi samo za prvu *Newton-Raphson*-ovu (NR) iteraciju, dok se za naredne menja u:

where $d\Delta \boldsymbol{p}$ are displacements of structure, $\boldsymbol{K}_{sys}$ is a global stiffness matrix and $\Delta \boldsymbol{P}$ is increment of load.

Last equation is valid only for the first Newton-Raphson (NR) iteration, and for other iterations, it changes to:

$$d\Delta \boldsymbol{p} = \boldsymbol{K}_{sys} \setminus \boldsymbol{P}_U \tag{2}$$

gde je $\boldsymbol{P}_U$ vektor neuravnoteženih sila, i dat je u (14). Na početku svakog inkrementa vektor $\Delta \boldsymbol{p}$ je nula vektor, i kroz iteracije u njemu se akumuliraju vektori $d\Delta \boldsymbol{p}$ iz svake pojedinačne iteracije.

where $\boldsymbol{P}_U$ is unbalanced force vector, and is given by (14). At the beginning of each increment, the vector $\Delta \boldsymbol{p}$ is zero vector and it accumulates vectors $d\Delta \boldsymbol{p}$ of each individual iteration.

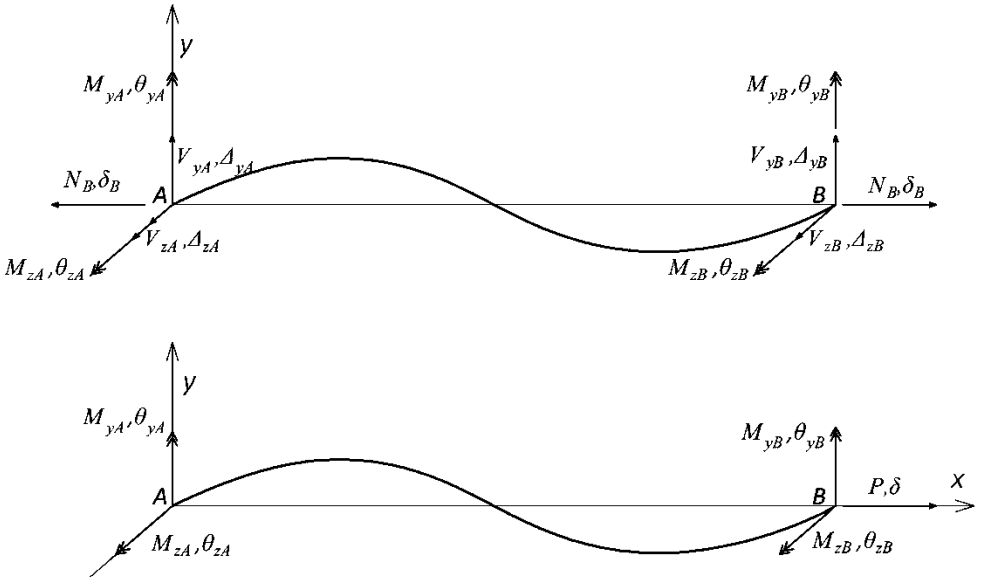

Slika 1. Stepeni slobode krajeva štapa(gore) i stepeni slobode dobijeni eliminisanjem pomeranja štapa kao krutog tela (dole)

Figure 1. The degrees of freedom of the element ends (top) and degrees of freedom obtained by eliminating rigid body displacement (bottom)

U formulaciji zasnovanoj na fleksibilnosti referentni sistem mora biti oslobođen pomeranja štapa kao krutog tela. Stoga, na nivou elementa postoji samo pet stepeni slobode, dobijenih eliminisanjem pomeranja krutog tela i prikazanih na slici 1. Pomeranja po ovim stepenima slobode označena su vektorom ***q***, a njima odgovarajuće presečne sile vektorom ***Q*** (3). Generisana pomeranja data jednačinom (4) predstavljaju aksijalno izduženje i po dva para rotacija u odnosu na tetivu štapa. Rotacije krajeva štapa i odgovarajući momenti sadržani u vektoru ***Q***, odgovaraju proizvoljnim ortogonalnim osama *y* i *z*.

In a flexibility-based formulation the reference system has to be free of rigid body modes. Therefore, on the element level, there is only 5 degrees of freedom, derived by eliminating rigid body modes, and presented in Figure 1. These element deformations are denoted by ***q***, and corresponding internal forces by ***Q*** (3). Generalised displacements given in equation (4) are axial extension and two rotations relative to the chord at each end node. The end rotations and corresponding moments, contained in ***Q***, refer to two arbitrary, orthogonal axes *y* and *z*.

$$\boldsymbol{Q} = \left\{ P\, M_{yA}\, M_{yB}\, M_{zA}\, M_{zB} \right\}^T \tag{3}$$

$$\boldsymbol{q} = \left\{ d\, q_{yA}\, q_{yB}\, q_{zA}\, q_{zB} \right\}^T \tag{4}$$

Priraštaj pomeranja po osnovnim deformacijski nezavisnim veličinama dobija se iz:

Generalised displacement increments are obtained by:

$$d\Delta\boldsymbol{q} = \boldsymbol{L}_{ele} \cdot d\Delta\boldsymbol{p}^T \tag{5}$$

Matrica $\boldsymbol{L_{ele}}$ je matrica transformacije za element i predstavlja kombinaciju dve transformacije: prva je transformacija iz globalnog referentnog sistema u lokalni sistem štapa, a druga predstavlja transformisanje tako dobijenih pomeranja u deformacije elementa po stepenima slobode dobijenim eliminisanjem pomeranja štapa kao krutog tela.

Formulacija korišćena u radu ne uključuje torziju ni deplanaciju preseka, ali se oni mogu jednostavno uključiti. Prirast sile na krajevima štapa $d\Delta\boldsymbol{Q}$ dobija se množenjem vektora prirasta deformacija $d\Delta\boldsymbol{q}$ i matrice krutosti elementa $\boldsymbol{K_{ele}}$, koja je u ovom slučaju kvadratna matrica 5x5 (6).

$\boldsymbol{L_{ele}}$ matrix is a transformation matrix for the element and it is combination of two transformations: the first is the transformation from the global coordinate system to the local system of element and the other represents the transformation of the obtained displacements to the deformation of element in degrees of freedom obtained by eliminating rigid body displacement.

Formulation presented herein does not include torsion or warping, but extension needed in order to include them is completely straightforward. Increment of element end forces $dD\boldsymbol{Q}$ is obtained are obtained by multiplying increment of element deformations with element stiffness matrix $\boldsymbol{K_{ele}}$, which is in this case 5x5 square matrix, as in (6).

$$d\Delta\boldsymbol{Q}^{j=1} = \boldsymbol{K}_{\boldsymbol{ele}} \cdot d\Delta\boldsymbol{q} \tag{6}$$

Ova jednačina se primenjuje samo u prvoj iteraciji petlje određivanja stanja elementa (*j=1*), dok za svako drugo *j* umesto nje treba koristiti jednačinu (7):

This relation holds only for the first iteration of element state determination loop (*j=1*), and for any other *j* equation (7) should be used instead.

$$d\Delta\boldsymbol{Q}^{j>1} = \boldsymbol{K}_{\boldsymbol{ele}} \cdot \boldsymbol{s} \tag{7}$$

gde je $\boldsymbol{s}$ dato u (18). Vektor sila na krajevima štapa je kumulativan:

where $\boldsymbol{s}$ is given in (18). Element forces vector is cumulative:

$$\boldsymbol{Q} = \boldsymbol{Q} + d\Delta\boldsymbol{Q} \tag{8}$$

$\boldsymbol{K_{ele}}$ se računa invertovanjem matrice fleksibilnosti $\boldsymbol{F}$ i modifikovanjem funkcijama stabilnosti, što je objašnjeno kasnije u radu. Za sada, ignorišući efekte normalne sile, matrica krutosti je krajnji rezultat dobijen proračunom na nivou elementa, nakon čega se pristupa formiranju globalne matrice krutosti konstrukcije uobičajenom procedurom. Radi konstruisanja $\boldsymbol{F}$ prema (9) potrebno je prethodno odrediti matrice fleksibilnosti preseka $\boldsymbol{f(x)}$, što znači da je neophodno započeti analizu na nivou preseka. Nije potrebno čuvati $\boldsymbol{F}$ u memoriji između inkremenata opterećenja, ali je potrebno snimati $\boldsymbol{K_{ele}}$.

$\boldsymbol{K_{ele}}$ is found by inverting element flexibility matrix $\boldsymbol{F}$ and afterwards it is further altered by stability functions, which will be explained in the next section. Ignoring effects of axial forces for now, element stiffness matrix is final result obtained from the element level of calculation, and then it is assembled in global stiffness matrix of structure by usual procedure. In order to calculate $\boldsymbol{F}$ by (9), flexibility matrix of each section $\boldsymbol{f(x)}$ is needed, which means that the section level of analyses is initiated. It is not needed to store F in memory between increments of load, but it is so for $\boldsymbol{K_{ele}}$.

$$\boldsymbol{F} = \int_0^L \boldsymbol{b}^T(x)\, \boldsymbol{f}(x)\, \boldsymbol{b}(x)\, dx \approx \frac{L}{2} \sum_{sec=1}^{nsec} w_{\mathrm{sec}}\, \mathbf{g}(\boldsymbol{b}^T(sec)\, \boldsymbol{f}(sec)\, \boldsymbol{b}(sec)) \tag{9}$$

Matrica fleksibilnosti preseka $\boldsymbol{f}(\mathrm{x})$ određuje se inverzijom matrice krutosti preseka $\boldsymbol{k_{sec}}$, date u (11):

Section flexibility matrix $\boldsymbol{f}(\mathrm{x})$ is determined by inversion of section stiffness matrix $\boldsymbol{k_{sec}}$, given by (11):

$$\boldsymbol{f}(\mathrm{x}) = \boldsymbol{k_{sec}}(x)^{-1} \tag{10}$$

$$\boldsymbol{k_{sec}}(x) = \sum_{i=1}^{nfib} \begin{bmatrix} E_i A_i & E_i A_i z_i & -E_i A_i y_i \\ E_i A_i z_i & E_i A_i z_i^2 & -E_i A_i z_i y_i \\ -E_i A_i y_i & -E_i A_i z_i y_i & E_i A_i y_i^2 \end{bmatrix} \tag{11}$$

U prvoj iteraciji prvog inkrementa, E_i uzima vrednost nominalnog Young-ovog modula materijala, dok se u svakom drugom slučaju računa na nivou vlakna i zavisi od naponskog stanja u posmatranom vlaknu. U (11), *nfib* je broj vlakana kojima je izdeljen presek, *z* i *y* su koordinate svakog vlakna od težišta preseka i *A* je površina vlakna, kao što je prikazano na slici 2.

In the first iteration of the first increment, E_i is taken as nominal Young's modulus of material, and in every other case, it is calculated in the fibre level and dependant on the stress state of the considered fibre. In (11), *nfib* is the number of fibres the section is divided in, *z* and *y* are coordinates of fibre from the centroid of section, and *A* is the area, as represented in Figure 2.

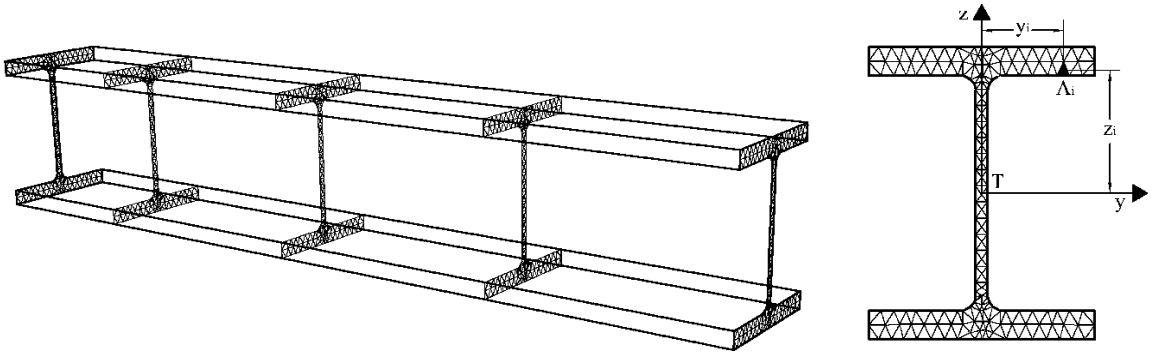

Slika 2. Stub-greda sa analiziranim presecima za 5 Gauss-Lobatto-vih tačaka integracije (levo) i podela preseka na vlakna (desno)

Figure 2. Beam-column with analysed sections for 5 Gauss-Lobatto points of integration (left) and division of section into fibres (right)

Pretpostavka o promeni presečnih sila duž elementa je sadržana u matrici ***b***. Za slučaj kada nema opterećenja duž štapa, ***b*** je prikazano u (12). Očigledno je da su sa (12) pretpostavljene linearna promena momenata duž elementa i konstantna normalna sila, ali mogu se napraviti i drugačije pretpostavke.

Assumptions of internal force's distribution in element are represented in matrix ***b***. For absence of element loads ***b*** is presented in (12). It is obvious that linear distribution of moment throughout the element and a constant axial force are assumed with (12), but other assumptions are possible too.

$$\boldsymbol{b}(x)=\begin{bmatrix}1 & 0 & 0 & 0 & 0\\ 0 & x-1 & x & 0 & 0\\ 0 & 0 & 0 & x-1 & x\end{bmatrix},\ x=x/L \tag{12}$$

Na nivou preseka, vektori sila u preseku i deformacija preseka su određeni primenom principa virtualnog rada u preseku, respektivno:

On the section level, section force and section deformation vectors, by the principle of virtual work, are respectively:

$$\boldsymbol{D}(x)=\begin{bmatrix}N(x)\\ M_y(x)\\ M_z(x)\end{bmatrix},\ \boldsymbol{d}(x)=\begin{bmatrix}e(x)\\ c_y(x)\\ c_z(x)\end{bmatrix} \tag{13}$$

Vektor sila u preseku je kumulativan i računa se prema (14):

Section force vector is cumulative and is calculated through (14):

$$\boldsymbol{D}(x)^j=\boldsymbol{D}(x)^{j-1}+d\Delta\boldsymbol{D}(x) \tag{14}$$

$$d\Delta\boldsymbol{D}(x)=\boldsymbol{b}(x)\cdot d\Delta\boldsymbol{Q}(x) \tag{15}$$

Sada je moguće odrediti deformacije preseka prema:

Now, section deformations are possible to obtain by:

$$d\Delta\boldsymbol{d}(x)=\boldsymbol{r}(x)+\boldsymbol{f}(x)\cdot\Delta\boldsymbol{D}(x) \tag{16}$$

U ovom trenutku proračun se premešta na nivo vlakna, ali nakon završetka petlje po vlaknima, kriterijum konvergencije postavlja se za vektor sila u preseku.

At this point, computation is transferred to fibre level, but after the termination of fibre loop, convergence criterion on section force vector is imposed. It is done by

Time se primenjuju sukcesivne iteracije na nivou elementa dok vektor neuravnoteženih sila $\boldsymbol{D_U(x)}$ postane manji od date tolerancije. Da bi se odredio vektor neuravnoteženih sila u preseku $\boldsymbol{D_U(x)}$ pomoću (18), potrebne su presečne sile $\boldsymbol{D_R(x)}$ koje se dobijaju sumiranjem po površini poprečnog preseka:

enforcing successive iterations on element level until vector of unbalanced forces $\boldsymbol{D_U(x)}$ becomes less than a given tolerance. In order to determine $\boldsymbol{D_U(x)}$ using (18), resisting forces $\boldsymbol{D_R(x)}$ are required and computed by summation by cross section area:

$$\boldsymbol{D_R}(x) = \sum_{i=1}^{nfib} s_i A_i \boldsymbol{a}_i^T \tag{17}$$

$$\boldsymbol{D_U}(x) = \boldsymbol{D}(x) - \boldsymbol{D_R}(x) \tag{18}$$

Ako kriterijum konvergencije nije zadovoljen, vektor rezidualnih deformacija preseka korišćen u (16) se određuje prema:

If a convergence criterion is unsatisfied, sectional residual deformation vector used in (16) is determined as:

$$\boldsymbol{r}(x) = \boldsymbol{f}(x)\,\boldsymbol{D_U}(x) \tag{19}$$

Na nivou vlakna pretpostavlja se jednoaksijalno stanje napona i dilatacije vlakna $\boldsymbol{e_{fib}}$ se računaju iz vektora deformacija preseka $\boldsymbol{d}(x)$ sa:

At the fibre level, uniaxial state is assumed, and fibre strain $\boldsymbol{e_{fib}}$ is calculated from section deformation vector $\boldsymbol{d}(x)$ by:

$$d\Delta \boldsymbol{e}_{fib} = \boldsymbol{a}_{fib}(x) \cdot d\Delta \boldsymbol{d}(x), \tag{20}$$

gde $\boldsymbol{a_{fib}(x)}$ je linearna geometrijska matrica veličine *nfib* x *3*, sa *i*-tim redom (tj za *i*-to vlakno) datim sa:

where $\boldsymbol{a_{fib}(x)}$ is linear geometric matrix of size *nfib* x *3*, with *i*-th row (that is for the fibre *i*) given by:

$$\boldsymbol{a}_i = \{1 \quad z_i \quad -y_i\}, \tag{21}$$

Tangentni modul materijala je uopšteno izražen kao:

Tangent modulus of material is generally expressed by

$$E_{fib} = \Delta s_{fib} / \Delta e_{fib} \tag{22}$$

Vrednost E_{fib} predstavlja tangentni modul za vlakno pod brojem *fib*. Ove vrednosti su za jedan presek smeštene u kolonu matrice koja ima kolona koliko element ima Gausovih tačaka integracije.

Koristeći odabranu zavisnost napon-deformacija, pronalaze se naponi za svako vlakno, nakon čega je moguće izračunavanje vektora unutrašnjih sila u preseku $\boldsymbol{D_R}$ (17). Kao što je već rečeno, određivanje stanja elementa (*j* petlja) ovde se završava, i vektor $\boldsymbol{P_R}$ sila koje su prihvaćene elementom može se dobiti u globalnim koordinatama, prema:

E_{fib} represents the tangent modulus of the fiber number *fib*. These values for one section are stored in the column of the matrix, that has number of columns which coresponds to number of Gaussian integration points.

By using selected stress-strain relation, stresses of each fibre are found, after which the calculation of section resisting forces $\boldsymbol{D_R}$ is possible (17). As said before, element state determination (*j* loop) is completed, and global residual forces $\boldsymbol{P_R}$ are determined by:

$$\boldsymbol{P_R} = \boldsymbol{L_{ele}}^T \boldsymbol{Q} \tag{23}$$

Vektor neuravnoteženih sila u štapu $\boldsymbol{P_U}$ računa se kao:

Structure unbalanced forces can be determined as:

$$\boldsymbol{P_U} = \boldsymbol{P} - \boldsymbol{P_R} \tag{24}$$

Rezidualne sile elementa se koriste u samouravnotežujućem mehanizmu (7) kroz rezidualne deformacije elementa $\boldsymbol{s}$ (25), koje se dobijaju primenom principa virtuelnih sila.

Residual forces in the element are used for self-balance mechanism (7) through residual deformation of element $\boldsymbol{s}$ (25), which are obtained by the principle of virtual forces:

$$\boldsymbol{s} = \frac{L}{2} \sum_{\text{sec}=1}^{n\text{sec}} \left[w_{sec} \boldsymbol{b}(sec)^T \boldsymbol{r}(sec) \right] \tag{25}$$

Vektori označeni sa δ računaju se u svakoj iteraciji određivanja stanja elementa, dok se vektori označeni sa Δ računaju jednom za svaku Newton-Raphson iteraciju.

Vectors denoted with δ are calculated in every iteration of element state determination, while vectors denoted only with Δ are calculated once per NR iteration.

Tako se algoritam proračuna sastoji iz tri petlje: petlja inkremenata opterećenja, NR petlja za konstrukciju, i petlja određivanja stanja elementa. Unutar poslednje, postoje petlje po presecima i vlaknima, ali one ne unose neuravnotežene veličine, već su te veličine njima predate od strane tri glavne petlje.

Jedan od najvažnijih aspekata implementacije prezentovane formulacije KE jeste kriterijum konvergencije koji je nametnut, kako na nivou elementa, tako i na nivou cele konstrukcije. Petlja na nivou elementa se prekida kada svi preseci konvergiraju, ili kada se izvede propisan maksimalni broj iteracija (u Matrix 3D [28,29] usvojeno je 25 iteracija). Ako se ne dostigne konvergencija u pomenutom broju iteracija, prekida se i spoljna petlja, i nanosi manji inkrement opterećenja. Unutar petlje na nivou konstrukcije izvode se NR iteracije dok se ne postigne zadata tolerancija. Kriterijum konvergencije na ovom nivou može biti baziran na pomeranjima, silama ili kao energetski kriterijum. Criesfield u [7] objašnjava kako energetski kriterijum može biti varljiv, dok Fillipou u [22] predlaže upravo ovaj kriterijum. U Matrix 3D, za unutrašnju petlju je definisan samo kriterijum po silama, dok je za celu konstrukciju potrebno da budu zadovoljeni i energetski i kriterijum po silama da bi se nastavio proračun. Usvojene tolerancije su 10^{-6} za kriterijum po silama i 10^{-12} za energetski kriterijum.

2.1 Numerička integracija

Pošto je cilj korišćenja jednog KE za ceo štap precizno predstavljanje pravog ponašanja elementa, dva numerička izbora su od suštinske važnosti. Prvi je izbor tipa numeričke integracije, a drugi broj integracionih stanica (broj posmatranih poprečnih preseka) duž elementa. Očigledno je da što je veći broj preseka usvojen, veća je preciznost, ali uz cenu skuplje (duže) analize. Uobičajeno se koristi tri do pet preseka po elementu, dajući zadovoljavajuću tačnost. Međutim, važniji izbor je tip numeričke analize koji diktira pozicije posmatranih preseka, kao što je prikazano na slici 2. Kod ovog izbora, prednost ima Gauss-Lobattova numerička integracija (26) u odnosu na Gausovu integraciju. Iako je druga izvedena optimizujući paralelno težinske koeficijente i integracione stanice, prva ima fiksirane stanice (tačke integracije) na krajevima štapa gde se očekuju najveći momenti/krivine. Stoga, postoji minumum tri tačke, dve krajnje koje su fiksirane i proizvoljan broj slobodnih tačaka između, koje su postavljene simetrično u odnosu na sredinu elementa. Težinski koeficijenti slobodnih apscisa su dati u (27), a krajnjih u (28).

Hence, algorithm consists of three loops: load increment loop (*k* loop), NR structure (*i*) loop, and element state determination one (*j*). Inside the last one there are section and fibre loops, but they are unlikely to bring unbalanced quantities since they depend on values passed by the main 3 loops.

One of the most important aspects of implementation of presented FE is convergence criterion enforced on both the element and structure loop. Element loop is terminated when all of the sections achieve convergence, or when prescribed number of iterations is performed (in Matrix 3D [28,29] it is adopted as 25). If latter is the case, outer (structure) loop is also aborted, and smaller load increment is applied. Structure loop continues NR iterations until the tolerance is achieved. Convergence criteria may be displacement-based, force-based or energy-based. Cries field in [7] explains that energy criterion can be misleading, while Fillipou in [22] proposes this type of criterion. In Matrix3D, for inner loop*j*, force criterion is defined, while for structure loop, both energy and force criterion have to be satisfied to proceed. Adopted tolerances are 10^{-6} for force, and 10^{-12} for energy criterion.

2.1 Numerical integration

Since the goal of using one fibre FE per member is to accurately represent true behaviour of a member, two numerical choices are crucial. First one is type of numerical integration, and second one is number of sections per element. Obviously, the greater number of sections, greater is the accuracy, but this leads to greater cost of analysis. Usually, three to five sections per element are used, giving more than satisfactory accuracy. Even more important is the proper type of integration. This choice dictates positions of the considered sections, as shown in Figure 2. Regarding this particular issue, advantages of Gauss-Lobatto integration rule (26) surpasses the ones of Gauss integration. Even though the latter is derived optimising both the weights and the integration points (stations), former has fixed stations at the ends of interval where the highest bending moments/curvatures are expected. Hence, there are minimum three stations, two endpoints being fixed and arbitrary number of free stations in the middle, symmetrical about the midpoint of the element. The weights of free abscissas are given in (27),and of the endpoints in (28).

$$\int_{-1}^{1} f(x)\,dx = w_1 f(1) + w_n f(n) + \sum_{i=2}^{n-1} w_i f(x_i) \tag{26}$$

$$w_i = \frac{2}{n(n-1)\left[P_{n-1}(x_i)\right]^2} \tag{27}$$

$$w_1 = w_n = \frac{2}{n(n-1)} \tag{28}$$

gde je *n* ukupan broj tačaka integracije, a *P(x)* Legendreov polinom.

where *n* is number of total integration points (stations), and *P(x)* is a Legendre polynomial.

2.2 Materijalna nelinearnost – materijalni modeli

Postoji nekoliko materijalnih modela čelika koji su široko korišćeni u numeričkim studijama posledjih godina. Da bi dinamičke ili ciklične analize bile moguće, neophodno je specificirati histerezisne osobine materijala. Uobičajeno je korišćeno izotropno, kinematičko ili mešovito ojačanje. Svi navedeni histerezisni modeli implementirani su u pomenuti softver. Pored toga, moguće je nelinearnu vezu napona i deformacija zadati bilo kojim višelinijskim pravilom (multilinear). Ipak, multilinearni tipovi opisa ove zavisnosti mogu dovesti do numeričkih poteškoća. Pošto izraz za k_{sec} uključuje tangentni modul svakog vlakna pojedinačno, tokom analize kolapsa (kao što je *pushover* analiza, posebno ako se javlja izvijanje nekih elemenata), ako je razlika između dva susedna nagiba značajna, konvergencija će biti teško dostižna. Stoga se preferiraju materijalni modeli opisani glatkim krivama. Ovo je ispunjeno s bilo kojim od Ramberg-Osgood, Monti-Nutti ili Menegotto-Pinto modelom. Među ovim modelima, često korišćen Ramberg-Osgood ima jednu veliku nepogodnost iz aspekta prezentovane formulacije. Pošto prikazani algoritam zahteva izračunavanje napona iz dilatacija, a ovaj model nije opisan bijektivnom funkcijom napona, neophodno je rešiti jednačinu Ramber-Osgooda svaki put kada se traži napon u vlaknu. S obzirom na to što ima mnogo vlakana, preseka, iteracija i inkremenata, ovakav proračun postaje vremenski zahtevan. S druge strane, Menegotto-Pinto model je unapređen od strane Fillipou et al [12] da bi se uključilo izotropno ojačanje materijala. Za prikazane analize u ovom radu, korišćen je standardni Menegotto-Pinto model sa sledećim vrednostima parametara:

2.2 Material nonlinearity - material models

There are few material models extensively used in numerical researches of steel structures lately. To perform dynamic, or cyclic analysis, hysteretic properties need to be specified. Usually isotropic, kinematic or mixed strain hardening is chosen. All of them are implemented in aforementioned software. Besides, any multi linear material rule can be specified. Special advantage of the flexibility approach is that negative slopes (material failure) can be specified stresses are obtained from strains and not the other way around. However, multi linear type of stress-strain relation may lead to numerical obstacles. Since k_{sec} is calculated with tangent stiffness of each fibre, during collapse analysis (such as pushover, especially close to buckling), if the difference between two adjoining slopes is considerable, convergence will be difficult to achieve. Thus, material models described with smooth curves are preferred. This condition is fulfilled with either of Ramberg-Osgood, Monti-Nuti or Menegotto-Pinto model. Among these models Ramberg-Osgood has an important disadvantage. Since described algorithm requires calculation of stresses from strains, and this model is described with objective function of stress, it means that equation of material law must be solved for each strain. Because there are many fibres, sections, iteration and increments, it becomes vastly time-consuming. Menegotto-Pinto model is improved by Fillipou et al [12] to include isotropic strain hardening. For the analysis performed in this paper, regular model is used with the following values:

R_0=20, a_1=18.5, a_2=0.15, b=0.01.

$$s^* = b \cdot e^* + \frac{(1-b)\cdot e^*}{\left(1+e^{*R}\right)^{1/R}} \tag{29}$$

$$e^* = \frac{e-e_r}{e_0-e_r}\ , \qquad s^* = \frac{s-s_r}{s_0-s_r} \tag{30}$$

Normalizovani napon σ^* dobija se jednačinom (29) u odnosu na normalizovanu dilataciju ε^* (30). Oblik krive zavisi od odnosa ojačanja b i od parametra R, koji simulira *Baushinger*-ov efekat, i dat je u (31). Efekat ova dva parametra na oblik krive napon/dilatacija tokom neizmeničnog opterećenja prikazan je na slici 3. Parametar R kontroliše radijus prelaza između dve grane na slici 3, dok ξ menja R nakon promene smera opterećenja.

Normalised stress σ^* is found by equation (29) in relation to normalised strain ε^* (30). The curve is controlled by hardening ratio b and a parameter R, which simulates Baushinger effect, given in (31). The effect of those parameters to stress strain curve during load reversals is shown in Figure 3. Parameter R controls smoothness of transition between two branches on Figure 3, while ξ changes R throughout load reversals.

$$R = R_0 - \frac{a_1 x}{a_2 + x} \tag{31}$$

gde su a_1 i a_2 konstante materijala, a ξ je apsolutna vrednost plastične dilatacije tokom prethodne plastifikacije, normalizovana dilatacijom na granici tečenja ε_y, kao što pokazuje slika 3.

where a_1 and a_2 are material constants and ξ is the absolute value of the plastic strain of the last excursion, normalised with plastic strain ε_y, as shown in Figure 3.

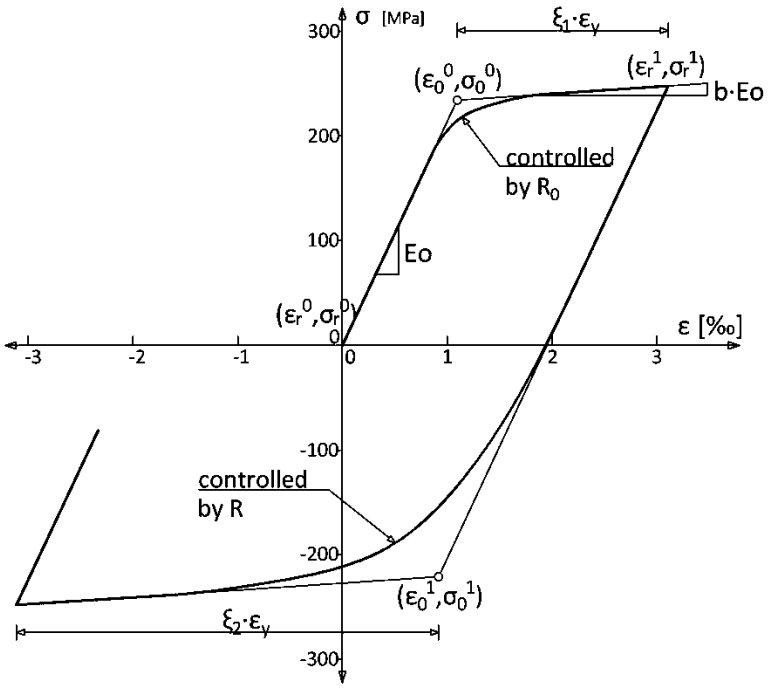

Slika 3. Guiffre-Mennegotto-Pinto materijalni model
Figure 3. Guiffre-Mennegotto-Pinto material model

Pored određivanja napona za datu dilataciju vlakna, potrebno je odrediti i tangentni modul E_i (25) koji je za Menegotto-Pinto model dat sa:

Besides determination of stress for a given strain of fibre, tangent modulus (25) ought to be calculated, and for Menegotto-Pinto model, E_i is given by:

$$E_i = \frac{s_0 - s_r}{e_0 - e_r} \cdot \left[b + \frac{1-b}{\left(1+e^{*R}\right)^{1/R}} \cdot \frac{1-e^{*R}}{1+e^{*R}} \right] \tag{32}$$

Tokom *j* petlje u procesu određivanja stanja elementa nailazi se na promenu znaka inkrementalne dilatacije, posebno u blizini izvijanja. U takvim situacijama, vrednosti $\boldsymbol{\varepsilon_0}$ i $\boldsymbol{\varepsilon_r}$ menjaju vrednost. Ali, da bi se sačuvala glatka kriva istorije napona/dilatacija jednog vlakna, prethodne vrednosti ($\boldsymbol{\varepsilon_0}$,$\boldsymbol{\varepsilon_r}$) čuvaju se u memoriji, u slučaju da se znak dva puta promeni tokom iteriranja.

It is encountered during *j* loop in the element state determination process that sign of incremental strain is reversed, especially near instability. In such situation, quantities $\boldsymbol{\varepsilon_0}$ and $\boldsymbol{\varepsilon_r}$ change values. But in order to preserve smooth stress-strain history curve of a fibre, previous values ($\boldsymbol{\varepsilon_0}$,$\boldsymbol{\varepsilon_r}$) are kept in memory in case two changes during *j* loop are experienced.

2.3 Geometrijska nelinearnost

Dva efekta geometrijske nelinearnosti uvrštena su u implementiranu FB formulaciju: P-Δ i P-δ. P-Δ, poznat još i kao geometrijska nelinearnost, jeste nelinearni efekat koji se javlja u svakoj konstrukciji u kojoj su elementi izloženi aksijalnim silama. Ovaj efekat uvodi u analizu sekundarne uticaje koji nastaju usled relativnog pomeranja krajeva štapa, Δ. P-δ je efekat kojim se modeliraju sekundarni uticaji koji nastaju usled lokalne deformacije štapa, to jest odstupanja elastične linije od tetive štapa. Prvi od pomenutih efekata (P-Δ) uveden je dodavanjem geometrijske matrice $\boldsymbol{K_g}$ matrici krutosti elementa u globalnim stepenima slobode (34). Matrica koja se dodaje obeležena je sa $\boldsymbol{K_g}$ i računa se prema (33), gde je $\boldsymbol{Z_0}$ nula matrica veličine 3x3. Ovakav način uključivanja *P*-Δ efekata u analizu precizniji je i takođe prikladniji za prikazanu formulaciju u odnosu na izrače-

2.3 Geometrical nonlinearity

Two effects regarding geometrical nonlinearity are represented through implemented FB formulation: *P*-Δ and *P-δ*. *P-Δ*, also known as geometric nonlinearity, is the nonlinear effect that occurs in each structure with elements subjected to axial forces. This effect introduces secondary forces as a result of the relative displacement of the member ends, Δ. *P-δ* is the effect that models the secondary forces caused by a local deformation of the member, i.e. elastic line deviation of the chord of the member. Former (*P-Δ*) is introduced complementing geometric matrix $\boldsymbol{K_g}$ to the element stiffness matrix in global degrees of freedom (34).It is denoted by $\boldsymbol{K_g}$, and calculated by (8), where $\boldsymbol{Z_0}$ is zero matrix 3x3. This way of including *P*-Δ effect in analysis is more accurate, and also more suitable for presented formulation in comparison with calculating only shear due to second

navanje samo transverzalnih sila usled efekata drugog reda, i potom ponavljanje proračuna sa ovom silom kao čvornim opterećenjem (kao što je npr. slučaj u programu *SAP2000*).

order effects, and then reiterate with this force as node load (as is used in SAP2000 e.g.).

$$\left[\boldsymbol{K_g}\right]_{12x12} = \begin{bmatrix} \left[\boldsymbol{K_s}\right] & -\left[\boldsymbol{K_s}\right] \\ -\left[\boldsymbol{K_s}\right] & \left[\boldsymbol{K_s}\right] \end{bmatrix} \quad , \tag{33a}$$

$$\left[\boldsymbol{K_s}\right]_{6x6} = \begin{bmatrix} \left[\boldsymbol{K_g}\right] & \boldsymbol{Z_0} \\ \boldsymbol{Z_0} & \boldsymbol{Z_0} \end{bmatrix}, \left[\boldsymbol{K_g}\right]_{3x3} = \begin{bmatrix} 0 & a & -b \\ a & c & 0 \\ -b & 0 & c \end{bmatrix} \tag{33b}$$

$$a = \frac{M_{zA} + M_{zB}}{L^2} \ , \quad b = \frac{M_{yA} + M_{yB}}{L^2} \ , \quad c = \frac{P}{L} \tag{33c}$$

gde je *P* negativno za silu pritiska. Konačno, matrica elementa je u globalnim stepenima slobode:

where *P* is considered negative for compression. Finally, element matrix in global degrees of freedom is:

$$[\boldsymbol{K_{ele}}] = \left[\boldsymbol{L}\right]^T_{5x12} \left[\boldsymbol{K_e}\right]_{5x5} \left[\boldsymbol{L}\right]_{5x12} + \left[\boldsymbol{K_g}\right]_{12x12} \tag{34}$$

Efekat sile koja deluje u pravcu tetive štapa (P-δ) predstavljen je korišćenjem funkcija stabilnosti u matrici krutosti elementa (5x5 - u prirodnim stepenima slobode). Izvođenje ovih funkcija (12) može se naći u [4,5], a prvi ih je uveo James još 1935. godine u radu koji se bavio metodom distribucije momenta. One su izvedene za moment savijanja na jednom kraju poluukliještene grede, uvodeći poprečna pomeranja usled rotacije jednog kraja stuba-grede, i stoga se mogu koristiti samo za kruto vezane elemente. Za proste štapove (npr. elemente sprega), potrebno je koristiti drugačiji set funkcija. Ove funkcije su prikazane u [4].

Effect of axial force acting through the lateral displacement of the beam-columns element (usually called P-small delta), is captured using stability functions in the element stiffness matrix (5x5 - natural degrees of freedom). Derivation of these functions (36) can be found in [4,5] and they were introduced by James in 1935 in a work dealing with moment-distribution method. They are derived for a propped cantilever, introducing lateral displacement due to rotation on one side of beam-column, and hence can be used only for continuous beam-columns. For different boundary conditions (i.e. brace member) different set of functions should be used. These functions are shown in [4].

$$\begin{bmatrix} \Delta P \\ \Delta M_{yA} \\ \Delta M_{yB} \\ \Delta M_{zA} \\ \Delta M_{zB} \end{bmatrix} = \begin{bmatrix} K_{e\,1,1} & 0 & 0 & 0 & 0 \\ 0 & S_{1y}/4 \cdot K_{e\,2,2} & S_{2y}/2 \cdot K_{e\,2,3} & 0 & 0 \\ 0 & S_{2y}/2 \cdot K_{e\,3,2} & S_{1y}/4 \cdot K_{e\,3,3} & 0 & 0 \\ 0 & 0 & 0 & S_{1z}/4 \cdot K_{e\,4,4} & S_{2z}/2 \cdot K_{e\,4,5} \\ 0 & 0 & 0 & S_{2z}/2 \cdot K_{e\,5,4} & S_{1z}/4 \cdot K_{e\,5,5} \end{bmatrix} \cdot \begin{bmatrix} \Delta d \\ \Delta q_{yA} \\ \Delta q_{yB} \\ \Delta q_{zA} \\ \Delta q_{zB} \end{bmatrix} \tag{35}$$

$$S_{1n} = \begin{cases} \dfrac{k_n L sin(k_n L) - (k_n L)^2 \cos(k_n L)}{2 - 2\cos(k_n L) - k_n L sin(k_n L)} \\ \dfrac{(k_n L)^2 \cosh(k_n L) - k_n L sinh(k_n L)}{2 - 2cosh(k_n L) + k_n L sinh(k_n L)} \end{cases}, S_{2n} = \begin{cases} \dfrac{(k_n L)^2 - k_n L sin(k_n L)}{2 - 2\cos(k_n L) - k_n L sin(k_n L)} \\ \dfrac{k_n L sinh(k_n L) - (k_n L)^2}{2 - 2cosh(k_n L) + k_n L sinh(k_n L)} \end{cases} \tag{36}$$

gde

where

$$k_n{}^2 = |P| / EI_n = |P| / \sum_{j=1}^{nsec} w_j (\sum_{i=1}^{nifb} E_i A_i z_i{}^2)_j$$

Gornji set jednačina (36) sa trigonometrijskim funkcijama se koristi kada je štap pritisnut, dok se donji red sa hiperboličkim funkcijama koristi ako je normalna sila *P* zatežuća. Funkcije S_1 se obično nazivaju ***s*** funkcije, dok su funkcije S_2 dobijene množenjem ***s***

Upper set of equations with trigonometric functions in (36) is used when axial force is compressive, while bottom set with hyperbolical functions is used if *P* is tensile. Functions S_1 are usually called *s* functions, and functions S_2 are derived by multiplying ***s*** with ***c***

funkcija sa ***c***, i stoga se obeležavaju sa ***sc***. Parametar ***c*** se naziva faktor prenosa, isto kao u približnoj metodi deformacija. Dijagrami ***s***, ***c*** i ***sc*** su prikazani na slici 4, kao funkcije promenjive $\rho=P/P_E$, gde je P_E Ojlerova kritična sila za zglobno oslonjen štap dužine *L*. S povećanjem aksijalnog pritiska, ***s*** opada dok faktor prenosa raste. Za $\rho=2.046$, ***s*** postaje *0*, a $\boldsymbol{c}\rightarrow\infty$, ali ***sc*** ima konačnu vrednost. Nulta vrednost ***s*** predstavlja beskonačnu fleksibilnost pri $P=2.046P_E$, vrednosti koja je poznata kao prva kritična sila poluukliještene grede. Pri vrednostima $\rho>2.046$ moment na neukliještenom kraju postaje ograničavajući i ovo objašnjava zašto krutost postaje negativna.

functions, and hence denoted as ***sc***. Parameter ***c*** is termed the carry-over factor, same as in slope-deflection method. The diagrams of ***s***, ***c*** and ***sc*** are shown in Figure 4, as functions of $\rho=P/P_E$, where P_E is Euler's critical force for a simple supported column with length *L*. With increase of axial compression, ***s*** decreases and carry-over factor increases. For $\rho=2.046$, ***s*** becomes *0*, and $\boldsymbol{c}\rightarrow\infty$, with ***sc*** finite. The zero value of ***s*** represents infinite flexibility at $P=2.046P_E$, a value already recognized to be the first buckling load for a fixed-hinged beam. At values $\rho>2.046$ moment at hinged end becomes restraining moment, and this explains why the stiffness becomes negative.

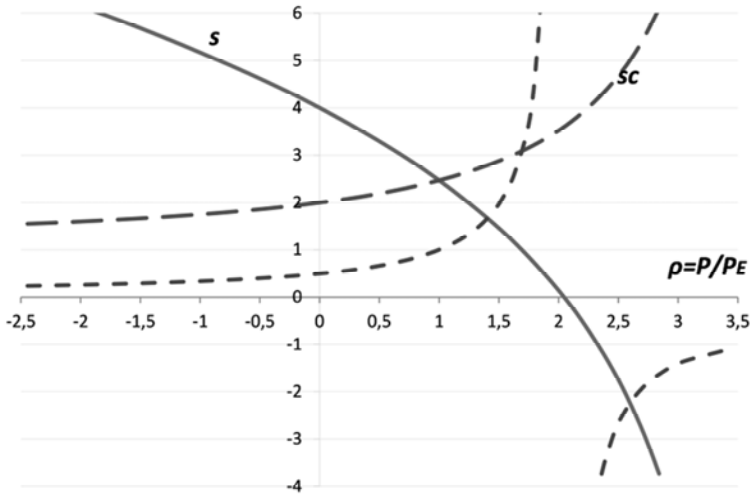

Slika 4. Dijagrami funkcija stabilnosti kao funkcije parametra ***ρ***
Figure 4. Diagrams of stability functions as a functions of ***ρ***

Dodatno, poprečne deformacije duž štapa su uključene u proračun inkrementalnih sila u preseku, (18). Matrica interpolacije sila (15) promenjena je tako da $\boldsymbol{b}_{2,1}$ postaje ***–δy(x)*** umesto *0*, i $\boldsymbol{b}_{3,1}$ postaje ***–δz(x)*** [11,20], gde je *x* prostorna koordinata duž elementa.

Additionally, lateral displacements are included in calculation of incremental section forces (18). Force interpolation matrix (15) is altered so $\boldsymbol{b}_{2,1}$ becomes ***–δy(x)*** instead of *0*, and $\boldsymbol{b}_{3,1}$becomes ***–δz(x)***[5,25], where *x* is a spatial coordinate throughout the element.

$$d_y(x)=d_{y,0}(x)-\frac{M_{zA}}{EI_z k_z^{\,2}}\left[\frac{\sin(k_z x)}{\tan(k_z L)}-\cos(k_z x)-\frac{x}{L}+1\right]-\frac{M_{zB}}{EI_z k_z^{\,2}}\left[\frac{\sin(k_z x)}{\sin(k_z L)}-\frac{x}{L}+1\right] \tag{37}$$

$$d_z(x)=d_{z,0}(x)+\frac{M_{nA}}{EI_n k_n^{\,2}}\left[\frac{\sin(k_y x)}{\tan(k_y L)}-\cos(k_y x)-\frac{x}{L}+1\right]+\frac{M_{yB}}{EI_y k_y^{\,2}}\left[\frac{\sin(k_y x)}{\sin(k_y L)}-\frac{x}{L}+1\right] \tag{38}$$

gde je $d_{i,0}(x)=L/1000\cdot\sin(p\,x/L)$, što predstavlja početnu imperfekciju elementa u obliku luka.

where $d_{i,0}(x)=L/1000\cdot\sin(p\,x/L)$, which represents initial bow-type imperfection of member.

2.4 Numeričke tehnike za nelinearne analize

Među nekoliko numeričkih metoda korišćenih za rešavanje sistema nelinearnih jednačina, ne postoji jedna značajno pogodnija od drugih. Više metoda su zadovoljavajuće za analize u kojima se ne javlja kolaps konstrukcije, i to su NR metoda, metoda sečice ili

2.4 Numerical techniques for nonlinear solution procedures

Among several numerical methods used for solving systems of nonlinear equation, there is no one exceptionally more suitable than the others. Several methods are sufficient for analysis in which limit point is

kombinacija sa NR, i tako dalje. U Matrix-u 3D koristi se klasična NR metoda, umesto modifikovane, s obzirom na to što je najveća teškoća ove metode izračunavanje tangentne krutosti pri svakoj iteraciji. Međutim, pošto se matrice krutosti elemenata računaju svakako, samo sastavljanje globalne matrice krutosti nije vremenski zahtevno, i komparativno je efikasnije u odnosu na korišćenje modifikovane NR metode. U prikazanom algoritmu, granica od 20 NR iteracija je nametnuta kao maksimum za dostizanje konvergencije, pre nego što se pribegne smanjivanju inkrementa opterećenja.

not reached, such as full or modified Newton-Raphson (NR), bisection method or combination with NR, etc. In Matrix 3D, full NR is used since the biggest difficulty of the method is calculation of tangent stiffness in each iteration. But since the element stiffness matrices are calculated either way, pure assembling of global matrix is much more beneficial than using modified NR method. In explained algorithm, limit of 20 iterations is imposed as maximum, before load increment is decreased.

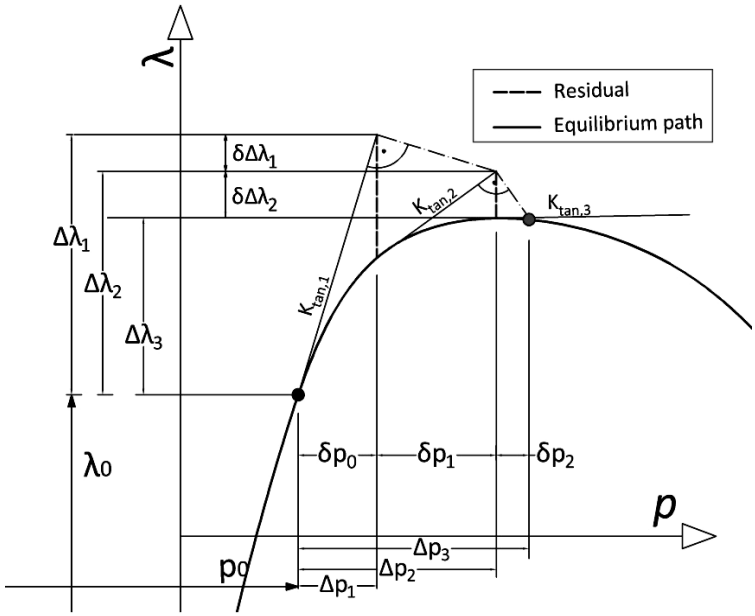

Slika 5. Grafička interpretacija tri iteracije Ramm-ove varijacije metode dužine luka
Figure 5. Graphically presented three iterations of Ramm's arc-length method

Iako su pomenute numeričke metode veoma efikasne, u blizini granične nosivosti ili sloma konstrukcije, one postaju nedovoljne. NR metoda nije u stanju da konvergira i neće dati traženo rešenje, kao što to neće moći ni u slučaju proloma unapred. U ovim situacijama, koje se javljaju kod problema izvijanja ili degradacije materijala (kod betona), potrebne su numeričke tehnike kontinuacije. Najpopularnija i verovatno najsveobuhvatnija jeste metoda dužine luka [7, 10]. Nekolike varijacije ove tehnike su najčešće: Criesfield-ova (cilindrična ili sferična metoda), Ramm-ova i Riks-Wemper-ova. Criesfield-ova metoda dužine luka je verovatno najkorišćenija i priprada grupi varijacija s konstantom dužinom luka. Za sve pomenute metode dužine luka, inkrement opterećenja Δl postaje nova promenjiva (umesto konstante, kao u NR metodi), povećavajući *n*-dimenzionalni prostor nepoznatih pomeranja, sakupljen u vektoru ***p***, na *n+1*-dimenzionalni prostor nepoznatih. Sistem je sa *n* jednačina neodređen, i stoga je neophodno formulisati dodatnu jednačinu. Ova jednačina je funkcija ograničenja koja se nameće rešenju. Osnovne razlike pomenutih metoda su upravo u toj jednačini.

Problem Criesfield-ove metode, čija funkcija ograničenja predstavlja konstantnu dužinu luka i opisana je kvadratnom jednačinom, jeste činjenica da postoje

Although aforementioned numerical methods are very efficient, in the proximity of limit point they become insufficient. NR method will not be able to surpass limit point, and also is unable to handle snap-through behaviour. For these situations, which are experienced with buckling or with material softening (concrete), continuation techniques are needed. The most popular, and very possibly the most robust one is the arc length method [7, 10]. Few variations are most often: Criesfield's (cylindrical or spherical), Ramm's or Riks-Wemper. Criesfield's arc length method is probably the most used one, and it belongs to the group of variation with constant arc length. For all of above-mentioned arc length methods, load increment Δl is considered as an additional unknown (instead of a constant, as in NR method), thereby augmenting the *n*-dimensional space of unknown displacements, collected in the array ***p***, to an *n+1*-dimensional space of unknowns. The system, with *n* equations, is indeterminate and an additional equation must be supplied. This equation is path-following restraint. Basic differences between above-mentioned methods are exactly in this equation.

Problem with Criesfield's method, where constraint equation is quadratic and represents constant arc length, is that there are two solutions of described problem, hence it needs predictor and corrector phase of solution,

dva rešenja tako definisanog problema, pa je neophodna prediktorska i nešto problematičnija korektorska faza rešenja. Drugim rečima, hiper-sfera s centrom u rešenju prethodnog inkrementa preseca funkciju odgovora u dve tačke, od kojih je jedna željeno rešenje, a druga se nalazi na već utvrđenom delu krive odgovora. Ramm-ov metod je zasnovan na pronalaženju preseka traženog polja otpornosti konstrukcije sa iterativno obnavljanom hiperpločom. Ramm-ova i Criesfield-ova metoda su implementirane u Matrix 3D u spoju s klasičnom NR metodom, ali samo će Ramm-ova jednačina (13) biti prikazana pošto nijedna prednost Criesfield-ove metode nije otkrivena dosadašnjom upotrebom i testiranjem od strane autora. Takođe, ipak treba napomenuti da je iskustvo autora nastalo upotrebom ove metode dovelo do zaključka da je parametar β, koji meri komparativni značaj pomeranja i sila, efikasnije usvojiti različitim od nule, suprotno mišljenju nekih autora.

latter being more problematic. Namely, the hyper-sphere with its centre in the last converged solution intersects equilibrium path in two points, one being the desired solution, and the other on the equilibrium path portion already determined. Ramm's method is based on finding intersection between desired field of resistance with updated hyper plane. For all mentioned methods load increment is variable, which requires another equation to be solved. Their main differences are in that equation. Both Ramm's and Criesfield methods are implemented in Matrix 3D in conjunction with full NR method, but only Ramm's equation (39) will be shown, since none of the advantages of Criesfield's method is uncovered in present use by the authors. It however should be noted that authors' experience with its use led to conclusion that β factor, which is a value that weights the importance of the contribution of displacements and loads, preferably be taken nonzero, contrary to what many authors suggests.

$$dl = \frac{\Delta \boldsymbol{p_0}^T d\,\bar{\boldsymbol{p}}}{\Delta \boldsymbol{p_0}^T d\,\boldsymbol{p_t} + \Delta l_0 b^2 \boldsymbol{P_{ef}}^T \boldsymbol{P_{ef}}} \tag{39}$$

gde je:

- dl iterativna promena parametra λ (nivoa opterećenja – videti sliku 5),
- Δl_0 inkrementalni parametar opterećenja izmenjen u svakoj iteraciji (*0* znači prethodni, I kroz iteracije uzima vrednosti $\Delta\lambda_1$, $\Delta\lambda_2$ itd.),
- $\Delta \boldsymbol{p_0}$ kumulativni vektor pomeranja po iteracijama (*0* označava prethodnu iteraciju),
- $d\,\boldsymbol{p_t}$ iterativna promena vektora pomeranja koja nastaje usled neuravnoteženih sila iz NR metode (pomeranja usled rezidualnih sila),
- $d\,\bar{\boldsymbol{p}}$ je vektor pomeranja koji odgovara opterećenju $\Delta\lambda_1 \boldsymbol{P_{ef}}$.

where:

- dl iterative change of load-level parameter (see Figure 5),
- Δl_0 incremental load parameter changed in every iteration (*0* meaning the last, and it takes values $\Delta\lambda_1$, $\Delta\lambda_2$ *etc.)*,
- $\Delta \boldsymbol{p_0}$ cumulative vector of displacement by iterations (*0* meaning the last iteration)
- $d\,\boldsymbol{p_t}$ iterative change of the displacement vector that stem from unbalanced forces in NR method
- $d\,\bar{\boldsymbol{p}}$ displacement vector corresponding to fixed load $\Delta\lambda_1 \boldsymbol{P_{ef}}$.

3 VERIFIKACIJA FORMULACIJE

Implementacija gorepomenute formulacije je verifikovana u pogledu tačnosti i efikasnosti poređenjem s dostupnim rezultatima i rezultatima dobijenim analizom komercijalnim softverima baziranim na metodi konačnih elemenata putem dva primera. Prvi primer predstavlja stub sa svim krajnjim stepenima slobode fiksiranim, osim podužnog pomeranja na gornjem kraju, kako je prikazano na slici 6, s ciljem da se verifikuje predloženi element u pogledu tačnosti i efikasnosti pri proračunu kritične sile stuba sa imperfekcijama. Drugi primer je Vogelov portalni ram, koji se uobičajeno koristi pri kalibrisanju naprednih neelastičnih analiza sa uključenom teorijom drugog reda. Kako je nosivost rama određena neelastičnim izvijanjem stuba, ovaj primer je dobar uporedni test za bilo koju neelastičnu formulaciju [6].

3 VERIFICATION OF FOMULATION

Implementation of above-mentioned formulation is verified for accuracy and efficiency by the comparison of predictions with accessible results and those generated by commercial finite element packages through two examples. First one investigates a column with all end restrains fixed except for longitudinal displacement at the upper end, as shown in Figure 6, with the aim to verify the accuracy and efficiency of the proposed element in capturing the buckling loads of columns with imperfections. Second example is the Vogel's portal frame, which is usually adopted for calibrating advanced second-order inelastic analysis. Since the frame collapse is determined by the column's inelastic buckling, this example is a good benchmark test for any inelastic formulation [6].

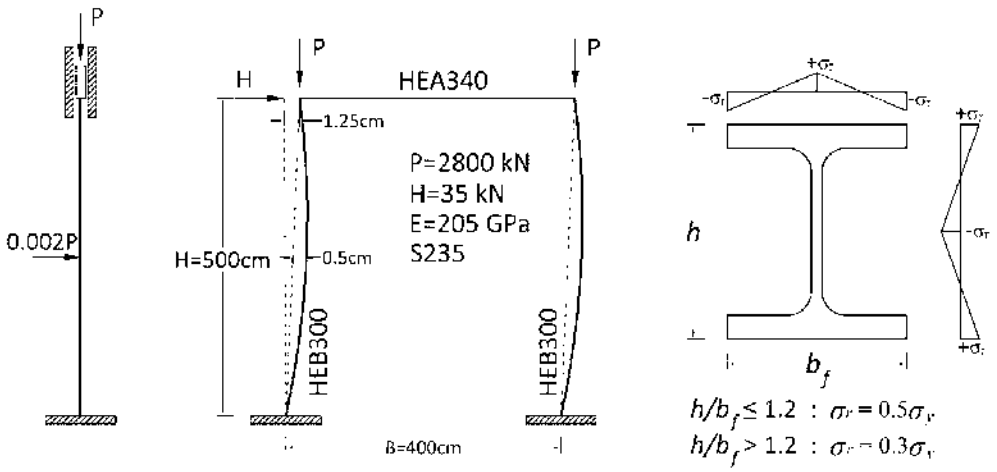

Slika 6. Stub uklješten na oba kraja (levo), Vogelov ram (sredina), raspored zaostalih napona (desno)
Figure 6. Column clamped on both ends (left), Vogel's frame (centre), residual stress pattern (right)

U oba modela je uključena početna imperfekcija, modelirana preko ekvivalentnih sila u prvom primeru i pomeranjem čvorova u drugom. Oba modela obuhvataju već pomenute inicijalne imperfekcije odstupanja od pravca ose duž elementa. Iako obuhvatanje zaostalih napona nije pogodno u formulaciji baziranoj na fleksibilnosti i pri korišćenju Manegoto-Pinto modela, moguće je prevazići probleme uz nekoliko improvizacija pri kodiranju. Raspored zaostalih napona u poprečnom preseku koji je korišćen u ovom radu je predložen od strane Evropskog kongresa za konstrukcijski čelik – ECCS, prikazan je na slici 6. Naponi su pri prvom inkrementu aplicirani direktno na vlakna preseka kao početni naponi.

Krive sila-pomeranje stuba dobijene korišćenjem predloženog elementa (Slika 7) poređene su sa onima koje su dobijene iz programa *SAP2000* i *SeismoStruct*. Materijalni model korišćen u programu Matrix 3D (PW) i *SeismoStruct* (SS) jeste Manegoto-Pinto sa inicijalnim modulom 210 GPa i post-elastičnim ojačanjem od 1%, dok je bilinearni materijal sa identičnim ojačanjem korišćen u modelu iz programa *SAP2000*. Vlaknasti model iz programa *SAP2000* precenjuje kritičnu silu za oko 18% pri korišćenju dva elementa i 6% pri korišćenju četiri elementa. Kritična sila dobijena prema programu *SeismoStruct* i prema predloženom modelu gotovo su identične, dok razlike u pomeranjima mogu biti objašnjene neobuhvatanjem zaostalih napona u SS modelu. Valja napomenuti i to da *SeismoStruct* ima implementirane vlaknaste elemente bazirane na sili dok su u *SAP2000* modelu korišćeni elementi bazirani na pomeranju. Projektna otpornost stuba na izvijanje određena prema pravilima EC3 (označena sa $N_{b,Rd}$) takođe je označena na grafiku radi poređenja. Povećanje broja elemenata zasnovanih na metodi deformacija u paketu *SAP2000* dovelo bi do boljeg slaganja s rezultatima dobijenim u SS i PW modelima. Podaci o tačnosti u zavisnosti od broja elemenata mogu se pronaći u [25], ali treba naglasiti da povećanje broja elemenata čini analizu vremenski zahtevnijom.

Both models include initial out-of-plumbness imperfections, modelled by equivalent load in first example, and rearrangement of nodes in the second. Both models include already mentioned out-of-straightness initial imperfection throughout their length. Even though residual stresses incorporation is not so convenient for both flexibility approach and Menegotto-Pinto model, it may be overcome with few coding improvisations. Residual stress pattern of cross section used for this research is proposed by European Convention for Constructional Steelwork – ECCS as illustrated in Figure 6. Residual stresses are assigned directly to fibres as initial stresses at first increment.

The load-deflection curves of the column obtained by the proposed element (Figure 7) are compared with those generated by *SAP2000* and *SeismoStruct*. Material model used in Matrix 3D (PW) and *SeismoStruct* (SS)is Menegotto-Pinto with initial modulus of 210GPa and post-elastic hardening of 1%, while bilinear material with the same hardening is used for *SAP2000* model. Fibre element of *SAP2000* overpredicts buckling load by about 18% if two elements are used, and 6% if 4 elements per member are used. Critical force obtained by *Seismo Struct* and proposed element are almost identical, while the difference in displacement can be partly explained by the absence of residual stresses in SS model. It should be noted that *Seismo Struct* has FB element implemented while for *SAP2000* model, displacement-based fibre element is used. Design buckling resistance of a column determined by EC3 rules of design (labelled as $N_{b,Rd}$) is marked on the graph for comparison. Increasing the number of displacement-based elements in *SAP2000* package would lead to better agreement with the results obtained in the SS and PW models. Accuracy depending on the number of elements can be found in [25], but it should be noted that the increase of the element number makes analysis more time-consuming.

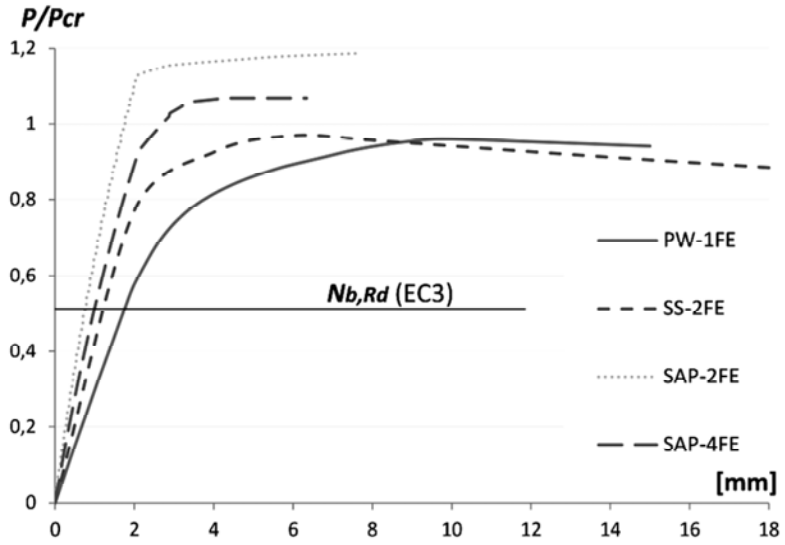

Slika 7. Krive sila-pomeranje stuba
Figure 7. Load-displacement curve of column

Na slici 7 su prikazana poređenja krivih sila-pomeranje za Vogelov ram, dobijenih predloženim elementom s rezultatima nekoliko autora. Prvo ga je analizirao Vogel 1985. [27], čiji je model plastične zone (PZ) nepoznat autorima, a kasnije Klark 1994. [6], koji je koristio 50 PZ elemenata po stubu i 20 za gredu. Kim i Li [14] korišćenjem komercijalnog softvera Abaqus, modelirali su ram sa 8952 2D-shell elementa. Alvarenga i Silveira [1] 2009. godine koristili su vlaknasti model sa osam elemenata po stubu i šest u gredi. Poređenje sile nosivosti (granične tačke) i maksimalnih horizontalnih pomeranja gornjeg desnog čvora prezentovano je u Tabeli 1.

Figure 7 (right) shows the comparison of the load-deflection curves for Vogel's frame predicted by the proposed element with results of several researchers. It was first analysed by Vogel in 1985. [27], whose plastic-zone (PZ) model is unknown to authors, and later by Clarke in 1994. [6], who used 50 PZ elements per column and 20 for the beam. Kim and Lee [14], using the Abaqus commercial software, modelled the frame with 8952 2D-shell elements. Alvarenga and Silveira [1] in 2009. used fibre model with 8 elements per column and 6 for the beam. Comparison of ultimate load (limit point) and maximum horizontal displacement of upper right joint is presented in Table 1.

Tabela 1. Vogelov ram: opterećenje loma i pomeranje
Table 1. Vogel's frame: collapse load and drift

Tačka otkaza ***Collapse point***	Vogel [27]	Clarke [6]	Kim&Lee [14]	Alvarenga [1]	**Predloženi element** ***Present work***
λ [%]	102,2	102,3	102,9	100,7	102,8
u_{Ah} [mm]	17,3	17,1	18,9	17	14,3

Kao što se može videti iz Tabele 1, predloženom FB modelu je potreban samo jedan element po štapu kako bi postigao rezultate koji su dobijeni programom *Abaqus* sa dvodimenzionalnim konačnim elementima korišćenim u [14] ili osam vlaknastih elemenata kao u [1]. Ipak, preciznost u određivanju granične sile je značajno veća nego u određivanju pomeranja. U određenoj meri razlike mogu biti uslovljene različitim post-elastičnim modulom. U svim citiranim radovima korišćen je bilinearni model elastično-savršeno plastično, dok je u ovom radu usvojeno post-elastično ojačanje od 2.05 GPa kako bi se izbegle numeričke poteškoće i zbog čega se javlja donekle kruće ponašanje. Konačno, prezentovani podaci prikazuju zadovoljavajuće poklapanje rezultata dobijenih korišćenjem samo jednog predloženog FB elementa po štapu sa analizama s većim nivoom diskretizacije.

As it can be recognized from Table 1, proposed FB need only one element per member to match the results generated by Abaqus with two-dimensional finite elements used in [14] or 8 fibre elements as in [1]. Again, precision in determination of limit load is considerably greater than for a displacement. Some divergence of results can be attributed to different post-elastic modulus. In all cited analyses elastic-perfectly plastic bilinear model was used, while in present study post-elastic hardening of *2.05* GPa is adopted in order to avoid numerical difficulties and hence somewhat stiffer behaviour. Altogether, presented data illustrate considerable agreement between results obtained using only 1 proposed FB element per member and analyses with higher order of discretization.

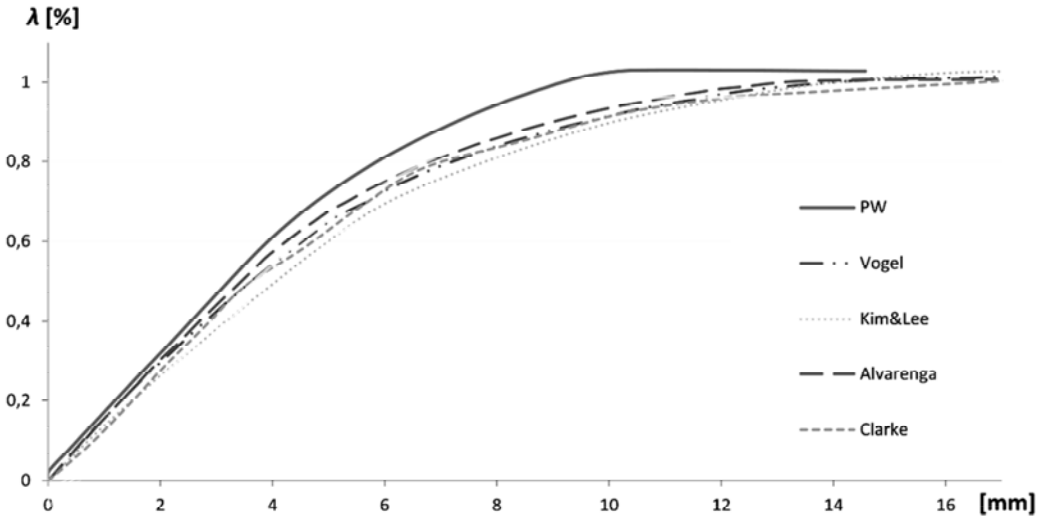

Slika 8. Odnos parametra opterećenja i pomeranja vrha Vogelovog rama
Figure 8. Load level parameter-top displacement of Vogel's frame

3.1 Prikaz rezultata u matrix 3D

Pored pomenutih komercijalnih softvera (*SAP2000* i *SeismoStruct*) postoji nekoliko akademskih koji koriste sličnu ili napredniju (korotacionu) formulaciju vlaknastog elementa u odnosu na prikazanu u ovom radu. Dva najčešće korišćena takva softvera su *OpenSees*, nastao na *Berkley*-u, koji je *open-source* softver, i *Engineer's Studio*, nastao na Univerzitetu u Tokiju. Ovi programi se uglavnom koriste za svrhe akademskih istraživanja, a ređe pri projektovanju objekata, zato što ne poseduju grafički interfejs. Matrix 3D, iako primarno koncipiran kao akademski softver za analizu konstrukcija, osmišljen je i kao praktičan alat za naprednije analize inženjerima. Stoga je prezentacija rezultata dostupna u različitim oblicima. Na Slici 9 nalaze se različiti prikazi napona u celoj konstrukciji za odabrani nivo opterećenja: kompletan dijapazon napona u konstrukciji (levo), samo naponi u posmatranim presecima (sredina) i distribucija plastičnih deformacija u konstrukciji (desno). Poslednji prikaz je zapravo interpolirana (između preseka) prezentacija napona većih i manjih od dve zadate granice napona, ali ako se ove granice postave kao +/- granica tečenja, prikaz odgovara distribuciji plastičnih dilatacija.

3.1 Result presentation in matrix 3D

Beside mentioned commercial software (*SAP2000* and *SiesmoStruct*) there are several academic packages that use similar or more advanced (corotational) formulation of fibre element, than the one presented in this paper. Two most widely used are *Open Sees*, developed on Berkley, which is open source software, and *Engineer's Studio*, made in Tokyo University. These programs are mainly used for research purposes and rarely for design, since they do not possess graphical interface. Matrix 3D, even though primarily made as academic software, is meant to be practical engineers tool for more refined analyses. Therefore, presentation of results is possible in various manners. Figure 9 depicts displays of stresses in whole structure for a selected load step: full range of stresses in a structure (left), only stresses in observed sections (middle) and spread of plastic strains through the structure (right). The last one is actually a smoothened presentation (between sections) of a stresses higher and lower than two set stress limits, but if the limit is set to yield stress, the output corresponds to plastic strain distribution.

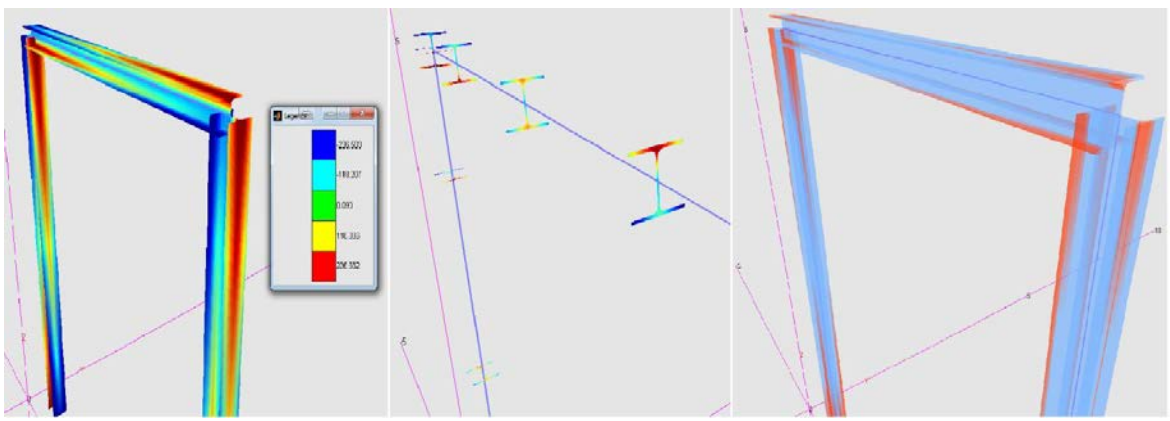

Slika 9. Različiti tipovi prikaza rezultata
Figure 9. Various displays of results

Pored globalnog pregleda rezultata, naponi i dilatacije, kao i radni dijagrami, mogu se sagledati za svako pojedinačno vlakno bilo kog preseka. Ovo je predstavljeno na slici 10 za HEA profil sa usvojenim početnim naponima kao u prikazanom primeru.

Besides the overall inspection of results, stresses and strains, along with stress strain curve, can be acquired for each fibre in any section. This is shown in Figure 10 for a HEA profile with initial stresses distribution as used in aforementioned examples.

Slika 10. Rezultati za pojedinačno vlakno
Figure 10. Results for a single fibre

4 ZAKLJUČCI I DISKUSIJA

Vlaknasti modeli imaju ključnu prednost pri preciznom predstavljanju ponašanja konstrukcija, s jednostavnom pripremom modela i u mogućnosti su da prikažu rezultate koji su uobičajeni za inženjere, to jest dijagrame presečnih sila. To znači da nije potrebno dodatno vreme za modeliranje konstrukcija s vlaknastim elementima, u poređenju s klasičnim linijskim elementima. Pored toga, mnoge prednosti sofisticiranih i preciznih analiza su omogućene upotrebom vlaknastih elemenata. To su, na primer: uvođenje realnog ponašanja materijala, pronalaženje graničnog opterećenja i kritičnih konfiguracija, ili čak ponašanje konstrukcije posle tačke loma. U slučaju nelinearne dinamičke analize, elementima s raspodeljenom plastičnosti nije potrebna pretpostavka pozicije zglobova, jer su oni u mogućnosti da prikažu „stvarno" rasprostiranje plastičnosti. Uz pomoć predstavljene formulacije, postoji mogućnost analiziranja ponašanja konstrukcija uz upotrebu veoma sofisticiranih materijalnih modela, i moguće je istraživati kolaps konstrukcije, ili pravu otpornost konstrukcije, pošto modeliranje destrukcije materijala ne unosi posebne numeričke teškoće.

Uzimajući u obzir čelične konstrukcije, kompletna geometrijski-materijalno nelinearna analiza s početnim imperfekcijama (GMNIA) može biti izvršena sa ovim tipom elemenata i podešavanja u programu Matrix 3D. Uz dodatak naprednog heurističkog algoritma koji se koristi u programu Matrix 3D za odabir koraka opterećenja, granično opterećenje može biti određeno veoma precizno. Ovoj činjenici teže novi koncepti koeficijenata sigurnosti. U Evrokodu 3, dimenzionisanje pritisnutih elemenata uključuje mnoge aproksimacije koje su morale biti uvedene u prošlosti. Uzimajući u obzir trenutni koncept kombinovanja dejstava i koeficijente sigurnosti, nepristrasno je reći da je pomoć kompjutera neizbežna. Ovakvom analizom, koja je prezentovana, mogu se preciznije odrediti koeficijenti sigurnosti, što je i sam cilj dimenzionisanja.

Formulacija i numeričke procedure, koje su prezentovane ovde, samo su mali deo akademskog CAD programa Matrix 3D. To je veoma razvijen, višenamenski program, koji obuhvata različite tipove nelinearnih

4 CONCLUSION AND DISSCUSION

Fibre elements have the essential advantage of representing very accurate behaviour of structures, while requiring simple pre-processing and is capable of delivering results common for engineers, i.e. internal force diagrams. This actually means that no extra time is needed for structural modelling with fibre elements than with commonly used line elements. Beside this, many advantages of more sophisticated and accurate analysis are on the reach with introduction of fibre elements. Such as, for example, introducing real material behaviour, finding a limit load and critical configuration, or even exploring the structural behaviour beyond limit point. And in the case of nonlinear dynamic analysis, elements with distributed plasticity need no presumptive positioning of hinges, and are able to show „true" spreading of plasticity. With the use of proposed formulation, there is a possibility to analyse structure behaviour through the use of a very sophisticated material models, and especially investigate collapse of structure, or real strength of a structure, since material damage fail to induce any numerical problems.

Considering steel structures, complete geometrically and materially nonlinear analysis with initial imperfection (GMNIA) can be performed with this type of element and setting in Matrix 3D. Including advanced heuristic algorithm Matrix 3D uses for load stepping, limit load of the structure can be very precisely determined. This fact aspire the new concept of safety coefficients. In Eurocode 3, design of compressed elements includes many approximations that had to be done in the past. Considering present concept of combining loads and safety coefficients, it is unbiased to say that computer aid is unavoidable. When such, analysis presented can determine safety coefficients more accurately which is the aim of design in general.

Formulation and numerical procedures presented here are just a small part of academic CAD software Matrix 3D. It is highly developed multipurpose software capable of different types of nonlinear analysis, including 2D and 3D finite elements, nonlinear dynamic analysis, impact loads, accelerogram inputs etc. On top of that, it is user friendly as everything can be set and viewed from

analiza, uključujući 2D i 3D konačne elemente, nelinearne dinamičke analize, udarna opterećenja, ulaz akcelerogramima i tako dalje. Pored toga, program je prilagođen korisniku, jer sve može biti podešeno i pregledano iz korisničkog interfejsa. Ovo predstavlja osnovnu prednost prezentovanog akademskog softvera u odnosu na *OpenSees* koji se smatra jednim od vodećih paketa za naučna numerička istraživanja. Dalje istraživanje, koje je već u toku, obuhvatiće uvođenje modela proklizavanja veza (za armaturu i kompozitne preseke), uključenje smicanja u FB formulaciji, vitoperenje, adaptivnu *pushover* analizu i tako dalje. Prezentovani rad je drugi u nizu radova kojima će se potvrditi i verifikovati tačnost i mogućnosti novonastalog akademskog softvera za ispitivanje konstrukcija.

Zahvalnost

Ovaj rad je proistekao iz dela istraživačkog projekta TR 36043, koji je podržalo Ministarstvo prosvete i nauke Republike Srbije.

user interface. This is the basic advantage of the presented academic software compared to *OpenSees*, which is considered one of the leading packages for numerical scientific research. Future work that is already in progress will include introducing bond-slip model (for reinforcement and composite sections), including shear in FB formulation, warping, adaptive pushover etc. The present work is the second in a series of papers that will confirm and verify the accuracy and possibilities of newly academic software for testing of structures.

Acknowledgments

The work reported in this paper is a part of the investigation within the research project TR 36043 supported by the Ministry for Education and Science Republic of Serbia.

5 LITERATURA
LITERATURE

[1] Alvarenga A. R, Silveira R. A. M: Second-order plastic-zone analysis of steel frames Part I: Numerical formulation and examples of validation, Latin Amer J of Solids and Struct, Vol. 6, No.2, pp. 131-152, 2009.
[2] Ayoub A, Filippou F. C: Mixed formulation of bond-slip problems under cyclic loads, J of Struct Eng,Vol. 125,No. 6, pp. 661-671, 1999.
[3] Ayoub A, Filippou F. C: Mixed formulation of nonlinear steel-concrete composite beam-element, J of Struct Eng,Vol. 126, No. 3, pp. 371-381, 2000.
[4] Bažant Z, Cedolin L: Stability of structures, World Scientific, Singapore, 2010.
[5] Chen W, Lui E:Structural Stability: Theory and Implementation, Elsevier, Amsterdam, 1987.
[6] Clarke M. J: Plastic zone analysis of frames. In W.F. Chen and S. Toma, editors, Advanced analysis of steel frames: theory, software and applications. CRC Press, Boca Raton, 1994.
[7] Criesfield M.A: Non-linear Finite Element Analysis of Solids and Structures, Vol.1, John Wiley & Sons, New York,USA, 2000.
[8] D'Ambrisi A, Filippou F. C: Modeling of cyclic shear behaviour in RC members, J of Struct Eng,Vol. 125, No.10, pp. 1143-1150, 1999.
[9] De Souza R.M: Force-based finite element for large displacement inelastic analysis of frames, PhD Thesis - Univ. Of California, Berkley, USA, 2000.
[10] De Souza Neto E.A, Peric D, Owen D.R.J: Computational methods for plasticity, Wiley, UK, 2008.
[11] Filippou F.C, D'Ambrisi A, Issa A: Nonlinear static and dynamic analysis of reinforced concrete subassemblages, Rep 92/08 EERC, Univ. Of California, Berkley, USA, 1992.
[12] Filippou F.C, Popov E.P, Bertero V.V:Effects of bond deterioration on hysteretic behavior of reinforced concrete joints, Report UCB/EERC 83/19, Univ. Of California, Berkley, USA, 1983.
[13] Hajjar J.F, Molodan A, Schiller P.H:A distributed plasticity model for cyclic analysis of concrete-filled steel tube beam-columns and composite frames. Engineering Structures, Vol. 20, No. 6, pp. 398-412, 1998.
[14] Kim S.E, Lee D.H: Second-order distributed plasticity analysis of space steel frames, Engineering Structures,Vol. 24, No.6, pp. 735–744, 2002.
[15] Kostić S, Deretić-Stojanović B: Formulacija fiber elementa prilikom nelinearne analize ramova, Građevinski materijali i konstrukcije,Vol. 59, No. 2, pp. 3-13, 2016.
[16] Mazars J. et al: Using multifiber beams to account for shear and torsion: applications to concrete structural elements, Comput Methods Appl Mech Eng, Vol.195, No. 52, pp. 7264–7281, 2006.
[17] Mullapudi R, Ayoub A: Modeling of the seismic behavior of shear-critical reinforced concrete columns, Engineering Structures,Vol. 32, No.11, pp. 3601-3615, 2010.
[18] Neuenhofer A, Fillipou F. C: Evaluation of nonlinear frame finite-element models, J of Struct. Eng,Vol. 123, No. 7, pp. 958-965, 1997.
[19] Neuenhofer A, Filippou F. C: Geometrically nonlinear flexibility-based frame finite element, J. Struct. Engrg., ASCE, Vol. 124, No. 7, pp. 704-711, 1998.
[20] Nguyen Q.H. et al:Analysis of composite beams in the hogging moment regions using a mixed finite element formulation, J of Constr Steel Resarch, Vol. 65, No. 3, pp. 737-748, 2009.

[21] Prestandardand Commentary for the Rehabilitation of Building (FEMA-356), Washington, DC: Federal Emergency Management Agency, 2000.
[22] Spacone E, Ciampi V, Filippou F.C: Mixed formulation of nonlinear beam finite element, Comput Struct, Vol. 58, No.1, pp. 71-83, 1996.
[23] Spacone E., Ciampi V., Filippou F. C.: A beam element for seismic damage analysis, Rep 92/07 EERC, Univ. Of California, Berkley, USA, 1992.
[24] Taucer F, Spacone E, Filippou F.C: A fiber beam-column element for seismic response analysis of reinforced concrete structures, Rep 91/17 EERC, Univ. Of California, Berkley, USA, 1991.
[25] Thai H.T, Kim S.E: Second-order inelastic analysis of cable-stayed bridges, Finite Elements in Analysis and Design, Vol. 53, pp. 48–55, 2012.
[26] Thai H.T, Kim S.E: Practical advanced analysis software for nonlinear inelastic analysis of space steel structures, Advances in Engineering Software, Vol. 40, No. 9, pp. 786–797, 2009.
[27] Vogel U: Calibrating frames. Stahlbau,Vol. 54, pp. 295–311, 1985.
[28] Žarković D: Computer software for structural analysis and design of reinforced concrete structures, Zbornik radova Fakulteta tehničkih nauka, Novi Sad,Vol. 24, No. 5, pp. 1587-1590, 2009.
[29] Žarković D, Brujić Z, Lađinović Đ: Application of Ottosen's model to flexural failure of RC beams, E-GTZ, Tuzla, BiH, 2016.

REZIME

IMPLEMENTACIJA VLAKNASTOG "STUB-GREDA" ELEMENTA U AKADEMSKI *CAD* SOFTVER - *MATRIX 3D*

Đorđe JOVANOVIĆ
Drago ŽARKOVIĆ
Zoran BRUJIĆ
Đorđe LAĐINOVIĆ

U radu su prikazane teoretske osnove linijskog konačnog elementa koji je implementiran i testiran u okviru akademskog softvera za analizu konstrukcija razvijenog na Fakultetu tehničkih nauka. Sam element je formulisan na osnovu interpolacije unutrašnjih sila i baziran na diskretizaciji poprečnog preseka na vlakna, kao i podeli štapa na proizvoljan broj preseka. Pored materijalne obuhvaćena je i geometrijska nelinearnost. Razmatrana su ineka numerička pitanja neophodna za izvođenje opisanog inkrementalno-iterativnog proračuna. Konačno, prikazani su rezultati proračuna i upoređeni sa dostupnim rezultatima.

Ključne reči: vlaknasti model, stub-greda, akademski softver, nelinearne analize

SUMMARY

FIBER BEAM-COLUMN ELEMENT IMPLEMENTATION IN ACADEMIC CAD SOFTWARE *MATRIX 3D*

Djordje JOVANOVIC
Drago ZARKOVIC
Zoran BRUJIC
Djordje LADJINOVIC

Theoretical foundations of beam-column finite element implemented (and tested) within academic CAD software developed on FTN (Department of civil engineering) are presented in this paper. Afore-mentioned FE is force-based fibre element, divided into a discrete number of monitored sections. Besides of material nonlinearity, finite-element is capable of capturing geometrical nonlinearity. Some of numerical issues needed for performing incremental-iterative solution procedures with those elements are addressed in the paper. Finally, results and comparison with available data are shown.

Key words: fibre element, beam-column, academic software, nonlinear analysis

Spisak simbola / *Notation*

Skalarne veličine / *Scalar values:*

w_i Gausovi težinski koeficijenti / *Gauss weight coefficients*

E_i Jangov modul elastičnosti vlakna *i* / *Young modulus of fiber i*

A_i površina vlakna *i / area of fiber i*

z_i, y_i koordinate vlakna *i* u odnosu na težište preseka / *coordinates of fiber i with respect to centroid of section*

N normalna sila u štapu / *axial force in element*

P normalna sila u štapu / *axial force in element*

M_{iK} moment savijanja oko ose i na kraju K štapa / *bending moment around axis i, at the end K of element*

R radijus prelaza na radnom dijagramu Menegotto-Pinto modela / *parameter of transistion curve in Menegotto-Pinto material model*

L dužina štapa / *element lenght*

l parametar nivoa opterećenja / *load level parameter*

dl promena parametra nivoa opterećenja unutar jedne iteracije / *change in load level parameter inside one iteration*

x prostorna koordinata duž elementa / *space coordinate along the element*

Vektori i matrice / *Vectors and matrices:*

$\boldsymbol{K}_{sys}$ matrica krutosti sistema ***I*** *system stiffness matrix*

$\boldsymbol{P}_{ef}$ ukupno opterećenje konstrukcije ***I*** *total load of structure*

$\boldsymbol{p}$ vektor pomeranja krajeva štapa / *vector of structure deformations*

$\boldsymbol{Q}$ vektor presečnih sila štapa / *vector of element end forces*

$\boldsymbol{q}$ vektor deformacija štapa / *vektor of element deformations*

$\boldsymbol{L}_{ele}$ matrica transformacije štapa / *element transformation matrix*

$\boldsymbol{s}$ vektor rezidualnih deformacija štapa / *vector of residual element deformations*

$\boldsymbol{b}(x)$ interpolaciona funkcija presečnih sila u štapu / *force interpolation matrix*

$\boldsymbol{F}$ matrica fleksibilnosti štapa / *element flexibility matrix*

$\boldsymbol{f}(x)$ matrica fleksibilnosti preseka / *sectional flexibility matrix*

$\boldsymbol{k}_{sec}(x)$ matrica krutosti preseka / *sectional stiffness matrix*

$\boldsymbol{D}(x)$ vektor presečnih sila u preseku *x / vector of section forces in section x*

$\boldsymbol{D}_U(x)$ vektor neuravnoteženih sila u preseku *x / vector of unballanced forces in section x*

$\boldsymbol{D}_R(x)$ vektor unutrašnjih sila u preseku *x* koje su posledica izračunatih napona u preseku / *vector of residual section forcesin section x as a result of calculated stresses*

$\boldsymbol{P}_R$ vektor unutrašnjih sila u štapu / *vector of residual element forces*

$\boldsymbol{P}_U$ vektor neuravnoteženih sila u štapu / *vector of unballanced element forces*

$\boldsymbol{r}(x)$ vektor rezidualnih deformacija preseka / *vector of residual sectional deformations*

$\boldsymbol{e}_{fib}$ dilatacija vlakna pod brojem *fib* / *dilatation of fiber numberfib*

$\boldsymbol{a}_{fib}(x)$ linearna geometrijska matrica vlakana u preseku *x / linear geometric matrix of fibers in sectionx*

$\boldsymbol{d}(x)$ vektor deformacije preseka / *vector of sectional deformations*

Predznaci veličina / *Symbols:*

Δ označava promenu veličine usled datog inkrementa opterećenja $\Delta\boldsymbol{P}$ / *represent change of variable due to structure load increment* $\Delta\boldsymbol{P}$

d označava promenu veličine između *Newton-Raphson*-ovih (NR) iteracija ***I*** *represents change of variable between Newton-Raphson (NR) iterations*

IN MEMORIAM

dr **PETAR MITROVIĆ**, dipl.inž.građ.
(1935-2016)

U Beogradu, 10. avgusta 2016. godine, u 82. godini, preminuo je dr Petar Mitrović, dugogodišnji direktor Instituta za puteve AD Beograd, redovni član Inženjerske akademije Srbije, istaknuti stručnjak iz oblasti putarstva i građevinskih – geotehničkih konstrukcija.

Rođen je 2. januara 1935. u Prokuplju, od oca Predraga i majke Olge. Osnovnu i srednju školu završio u Kragujevcu, a Građevinski fakultet u Beogradu 1961. Na Rudarsko-geološkom fakultetu u Beogradu, na Katedri za geotehniku, magistrirao je 1979, a doktorirao 1992. godine.

Petar je ceo svoj radni vek proveo u Institutu za puteve, gde se posvetio stručnom radu i obrazovanju, kako svom ličnom, tako i obrazovanju mlađih kolega. Od 1967. do 1981. godine bio je više puta u Francuskoj (Pariz, Bordo i Monpelje), gde je specijalizirao: tehnologiju betona, zemljane radove i armiranje tla, sanacije klizišta, projektovanje i građenje kolovoza.

U periodu od 1961. do 1984. godine, u pomenutom institutu postigao je vrhunske rezultate kao inženjer i rukovodilac:

- bio je u nadzoru na izgradnji auto-puta "Bratstvo–jedinstvo", deonice: Umčari–Kolari, Predejane–V. Han i Bujanovac–Preševo, zatim puta kroz Đerdapsku klisuru, magistrale Priština–Rožaje i Kuršumlija–Priština–Peć (1961–1974);
- rukovodilac betonske laboratorije (1966–1969);
- šef sektora za geotehniku (1975–1978);
- direktor OOUR-a "Istraživanja i ispitivanja" (1979–1984).

U periodu od 1984. do 1986. godine, odlazi u Afriku gde radi kao šef misije Ujedinjenih nacija, na izgradnji Pan-afričke putne magistrale Dakar – Port Said, na deonici kroz Burkinu Faso. Po povratku, bio je na najvažnijim funkcijama u Institutu za puteve:

- tehnički direktor (1986–1989);
- naučni direktor (1990–1992);
- generalni direktor (1992–1999);
- savetnik generalnog direktora (2000–2003).

Početkom 2004. godine odlazi u penziju, ali nastavlja da radi do sredine 2012, kao savetnik u Zavodu za geotehniku.

Petar je dao veliki doprinos u stručnim organizacijama i časopisima gde je bio:

- potpredsednik i generalni sekretar Društva za puteve Srbije (1982–1991);
- predsednik Društva za puteve Srbije (1992–1999);
- glavni urednik časopisa "Institut za puteve" (1970–2012);
- glavni urednik časopisa "Put i saobraćaj" (2003–2012);
- član Nacionalnog komiteta Svetske putarske organizacije IRF-a (1990–2006);
- član Inženjerske akademije Srbije (IAS), redovni od 2008. godine.

Bez obzira na obaveze rukovođenja, sve vreme bavio se istraživanjima i projektovanjem. Uradio je preko pet stotina projekata sanacija klizišta, puteva, mostova, tunela i građevinskih objekata u Srbiji i republikama bivše Jugoslavije. Najveća i najsloženija klizišta jesu: "Umka i Duboko" na putu Beograd–Obrenovac, brojne sanacije na obilaznici Beograda, "Lapišnica" kod Sarajeva, "Ražanj" i "Bračin" na auto-putu E-75, "Studenica" na putu Ušće–Ivanjica, sanacija kosine na graničnom prelazu "Mehov krš" na putu Rožaje – K. Mitrovica i brojni drugi.

Objavio je 140 stručnih i naučnih radova u zemlji i inostranstvu, iz oblasti geotehnike, građenja i održavanja puteva i građevinskih materijala.

Napisao je sedam stručnih knjiga iz oblasti geotehnike:

1) Optimizacija plitko fundiranih potpornih konstrukcija (1995);
2) Teren kao sredina za gradnju objekata (1997);
3) Dreniranje u cilju melioracije i sanacije terena (1999);
4) Duboko fundirane potporne konstrukcije (2002);
5) Primena plastičnih materijala pri izgradnji i održavanju puteva i objekata (2005);
6) Primena plastičnih materijala pri izgradnji i održavanju puteva i objekata, dopunjeno izdanje (2007);
7) Sanacije klizišta i nedovoljno nosivih tla (2013).

Dr Petar Mitrović radio je na desetak naučnoistraživačkih i razvojnih projekata iz oblasti saobraćaja, putarstva i građevinskih konstrukcija.

Za svoj rad odlikovan je ordenom Rada prvog reda (1971) i ordenom Zasluga za narod sa crvenom zastavom (1977).

Dr Petar Mitović je publikovao veći broj radova u našem Časopisu.

Dragi Petre, u tvom Institutu za puteve, stručnoj javnosti i putnoj privredi Srbije i regiona, ostavio si neizbrisive tragove, kao sjajan ČOVEK i INŽENJER.

U ime tvojih saradnika, poštovalaca i prijatelja,

Branko Jelisavac

UPUTSTVO AUTORIMA*

Prihvatanje radova i vrste priloga

U časopisu Materijli i konstrukcije štampaće se neobjavljeni radovi ili članci i konferencijska saopštenja sa određenim dopunama, iz oblasti građevinarstva I srodnih disciolina (geodezija I arhitektura). Vrste priloga autora i saradnika koji će se štampati su: originalni naučni radovi, prethodna saopštenja, pregledni radovi, stručni radovi, prikazi objekata i iskustava (studija slučaja), kao i diskusije povodom objavljenih radova.

Originalni naučni rad je primarni izvor naučnih informacija i novih ideja i saznanja kao rezultat izvornih istraživanja uz primenu adekvatnih naučnih metoda. Dobijeni rezultati se izlažu sažeto, ali tako da poznavalac problema može proceniti rezultate eksperimentalnih ili teorijsko numeričkih analiza, tako da se istraživanje može ponoviti i pri tome dobiti iste ili rezultate u okvirima dopuštenih odstupanja, kako se to u radu navodi.

Prethodno saopštenje sadrži prva kratka obaveštenja o rezultatima istraživanja ali bez podrobnih objašnjenja, tj. kraće je od originalnog naučnog rada.

Pregledni rad je naučni rad koji prikazuje stanje nauke u određenoj oblasti kao plod analize, kritike i komentara i zaključaka publikovanih radova o kojima se daju svi neophodni podaci pregledno i kritički uključujući i sopstvene radove. Navode se sve bibliografske jedinice korišćene u obradi tematike, kao i radovi koji mogu doprineti rezultatima daljih istraživanja. Ukoliko su bibliografski podaci metodski sistematizovani, ali ne i analizirani i raspravljeni, takvi pregledni radovi se klasifikuju kao stručni radovi.

Stručni rad predstavlja koristan prilog u kome se iznose poznate spoznaje koje doprinose širenju znanja i prilagođavanja rezultata izvornih istraživanja potrebama teorije i prakse.

Ostali prilozi su prikazi objekata, tj. njihove konstrukcije i iskustava-primeri u građenju i primeni različitih materijala (studije slučaja).

Da bi se ubrzao postupak prihvatanja radova za publikovanje, potrebno je da autori uvažavaju Uputstva za pripremu radova koja su navedena u daljem tekstu.

Uputstva za pripremu rukopisa

Rukopis otkucati jednostrano na listovima A-4 sa marginama od 31 mm (gore i dole) a 20 mm (levo i desno), u Wordu fontom Arial sa 12 pt. Potrebno je uz jednu kopiju svih delova rada i priloga, dostaviti i elektronsku verziju na navedene E-mail adrese, ili na CD-u. Autor je obavezan da čuva jednu kopiju rukopisa kod sebe.

Od broja 1/2010, prema odluci Upravnog odbora Društva i Redakcionog odbora, radovi sa pozitivnim recenzijama i prihvaćeni za štampu, publikovaće se na srpskom i engleskom jeziku, a za inostrane autore na engleskom (izuzev autora sa govornog područja srpskog I hrvatskog jezika).

Svaka stranica treba da bude numerisana, a optimalni obim članka na jednom jeziku, je oko 16 stranica (30000 slovnih mesta) uključujući slike, fotografije, tabele i popis literature. Za radove većeg obima potrebna je saglasnost Redakcionog odbora.

* **Uputstvo autorima je modifikovano i treba ga, u pripremi radova, slediti.**

GUIDELINES TO AUTHORS

Acceptance and types of contributions

The Building Materials and Structures journal will publish unpublished papers, articles and conference reports with modifications in the field of Civil Engineering and similar areas (Geodesy and Architecture).The following types of contributions will be published: original scientific papers, preliminary reports, review papers, professional papers, objects describe / presentations and experiences (case studies), as well as discussions on published papers.

Original scientific paper is the primary source of scientific information and new ideas and insights as a result of original research using appropriate scientific methods. The achieved results are presented briefly, but in a way to enable proficient readers to assess the results of experimental or theoretical numerical analyses, so that the research can be repeated and yield with the same or results within the limits of tolerable deviations, as stated in the paper.

Preliminary report contains the first short notifications on the results of research but without detailed explanation, i.e. it is shorter than the original scientific paper.

Review paper is a scientific work that presents the state of science in a particular area as a result of analysis, review and comments, and conclusions of published papers, on which the necessary data are presented clearly and critically, including the own papers. Any reference units used in the analysis of the topic are indicated, as well as papers that may contribute to the results of further research. If the reference data are methodically systematized, but not analyzed and discussed, such review papers are classified as technical papers.

Technical paper is a useful contribution which outlines the known insights that contribute to the dissemination of knowledge and adaptation of the results of original research to the needs of theory and practice.

Other contributions are presentations of objects, i.e. their structures and experiences (examples) in the construction and application of various materials (case studies).

In order to speed up the acceptance of papers for publication, authors need to take into account the Instructions for the preparation of papers which can be found in the text below.

Instructions for writing manuscripts

The manuscript should be typed one-sided on A-4 sheets with margins of 31 mm (top and bottom) and 20 mm (left and right) in Word, font Arial 12 pt. The entire paper should be submitted also in electronic format to e-mail address provided here, or on CD. The author is obliged to keep one copy of the manuscript.

As of issue 1/2010, in line with the decision of the Management Board of the Society and the Board of Editors, papers with positive reviews, accepted for publication, will be published in Serbian and English, and in English for foreign authors (except for authors coming from the Serbian and Croatian speaking area).

Each page should be numbered, and the optimal length of the paper in one language is about 16 pages (30.000 characters) including pictures, images, tables and references. Larger scale works require the approval of the Board of Editors.

Naslov rada treba sa što manje reči (poželjno osam, a najviše do jedanaeset) da opiše sadržaj članka. U naslovu ne koristiti skraćenice ni formule. U radu se iza naslova daju ime i prezime autora, a titule i zvanja, kao i ime institucije u podnožnoj napomeni. Autor za kontakt daje telephon, adresu elektronske pošte I poštansku adresu.

Uz sažetak (rezime) od oko 150-250 na srpskom i engleskom jeziku daju se ključne reči (do sedam). To je jezgrovit prikaz celog članka i čitaocima omogućuje uvid u njegove bitne elemente.

Rukopis se deli na poglavlja i potpoglovlja uz numeraciju, po hijerarhiji, arapskim brojevima. Svaki rad ima uvod, sadržinu rada sa rezultatima, analizom i zaključcima. Na kraju rada se daje popis literature.

Kod svih dimenzionalnih veličina obavezna je primena međunarodnih SI mernih jedinica.

Formule i jednačine treba pisati pažljivo vodeći računa o indeksima i eksponentima. Autori uz izraze u tekstu definšu simbole redom kako se pojavljuju, ali se može dati i posebna lista simbola u prilogu.

Prilozi (tabele, grafikoni, sheme i fotografije) rade se u crno-beloj tehnici, u formatu koji obezbeđuje da pri smanjenju na razmere za štampu, po širini jedan do dva stupca (8 cm ili 16,5 cm), a po visini najviše 24,5 cm, ostanu jasni i čitljivi, tj. da veličine slova i brojeva budu najmanje 1,5 mm. Originalni crteži treba da budu kvalitetni i u potpunosti pripremljeni za presnimavanje. Mogu biti i dobre, oštre i kontrastne fotokopije. Koristiti fotogrfije, u crno-beloj tehnici, na kvalitetnoj hartiji sa oštrim konturama, koje omogućuju jasnu reprodukciju.

U popisu literature na kraju rada daju se samo oni radovi koji se pominju u tekstu. Citirane radove treba prikazati po abecednom redu prezimena prvog autora. Literaturu u tekstu označiti arapskim brojevima u uglastim zagradama, kako se navodi i u Popisu citirane literature, napr [1]. Svaki citat u tekstu mora se naći u Popisu citirane literature i obrnuto svaki podatak iz Popisa se mora citirati u tekstu.

U Popisu literature se navode prezime i inicijali imena autora, zatim potpuni naslov citiranog članka, iza toga sledi ime časopisa, godina izdavanja i početna i završna stranica (od - do). Za knjige iza naslova upisuje se ime urednika (ako ih ima), broj izdanja, prva i poslednja stranica poglavlja ili dela knjige, ime izdavača i mesto objavljivanja, ako je navedeno više gradova navodi se samo prvi po redu. Kada autor citirane podatke ne uzima iz izvornog rada, već ih je pronašao u drugom delu, uz citat se dodaje «citirano prema...».

Autori su odgovorni za izneseni sadržaj i moraju sami obezbediti eventualno potrebne saglasnosti za objavljivanje nekih podataka i priloga koji se koriste u radu.

Ukoliko rad bude prihvaćen za štampu, autori su dužni da, po uputstvu Redakcije, unesu sve ispravke i dopune u tekstu i prilozima.

Rukopisi i prilozi objavljenih radova se ne vraćaju. Sva eventualna objašnjenja i uputstva mogu se dobiti od Redakcionog odbora.

Radovi se mogu slati i na e-mail: folic@uns.ac.rs ili miram@uns.ac.rs

Veb sajt Društva I časopisa: www.dimk.rs

The title should describe the content of the paper using a few words (preferably eight, and up to eleven). Abbreviations and formulas should be omitted in the title. The name and surname of the author should be provided after the title of the paper, while authors' title and position, as well as affiliation in the footnote. The author should provide his/her phone number, e-mail address and mailing address.

The abstract (summary) of about 150-250 words in Serbian and English should be followed by key words (up to seven). This is a concise presentation of the entire article and provides the readers with insight into the essential elements of the paper.

The manuscript is divided into chapters and subchapters, which are hierarchically numbered with Arabic numerals. The paper consists of introduction and content with results, analysis and conclusions. The paper ends with the list of references. All dimensional units must be presented in international SI measurement units. The formulas and equations should be written carefully taking into account the indexes and exponents. Symbols in formulas should be defined in the order they appear, or alternatively, symbols may be explained in a specific list in the appendix. Illustrations (tables, charts, diagrams and photos) should be in black and white, in a format that enables them to remain clear and legible when downscaled for printing: one to two columns (8 cm or 16.5 cm) in height, and maximum of 24.5 cm high, i.e. the size of the letters and numbers should be at least 1.5 mm. Original drawings should be of high quality and fully prepared for copying. They also can be high-quality, sharp and contrasting photocopies. Photos should be in black and white, on quality paper with sharp contours, which enable clear reproduction.

The list of references provided at the end of the paper should contain only papers mentioned in the text. The cited papers should be presented in alphabetical order of the authors' first name. References in the text should be numbered with Arabic numerals in square brackets, as provided in the list of references, e.g. [1]. Each citation in the text must be contained in the list of references and vice versa, each entry from the list of references must be cited in the text.

Entries in the list of references contain the author's last name and initials of his first name, followed by the full title of the cited article, the name of the journal, year of publication and the initial and final pages cited (from - to). If the doi code exists it is necessary to enter it in the references. For books, the title should be followed by the name of the editor (if any), the number of issue, the first and last pages of the book's chapter or part, the name of the publisher and the place of publication, if there are several cities, only the first in the order should be provided. When the cited information is not taken from the original work, but found in some other source, the citation should be added, "cited after ..."

Authors are responsible for the content presented and must themselves provide any necessary consent for specific information and illustrations used in the work to be published.

If the manuscript is accepted for publication, the authors shall implement all the corrections and improvements to the text and illustrations as instructed by the Editor.

Writings and illustrations contained in published papers will not be returned. All explanations and instructions can be obtained from the Board of Editors.

Contributions can be submitted to the following e-mails: folic@uns.ac.rs or miram@uns.ac.rs

Website of the Society and the journal: www.dimk.rs

Izdavanje časopisa "Građevinski materijali i konstrukcije" finansijski su pomogli:

INŽENJERSKA KOMORA SRBIJE

REPUBLIKA SRBIJA
MINISTARSTVO PROSVETE, NAUKE I TEHNOLOŠKOG RAZVOJA

UNIVERZITET U BEOGRADU
GRAĐEVINSKI FAKULTET

DEPARTMAN ZA GRAĐEVINARSTVO I GEODEZIJU
FAKULTET TEHNIČKIH NAUKA NOVI SAD

INSTITUT IMS AD, BEOGRAD

UNIVERZITET CRNE GORE
GRAĐEVINSKI FAKULTET - PODGORICA

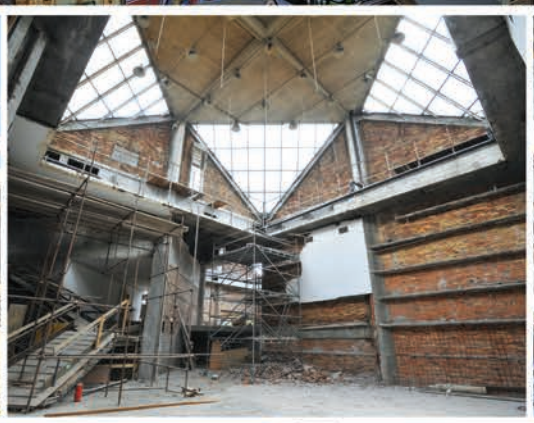

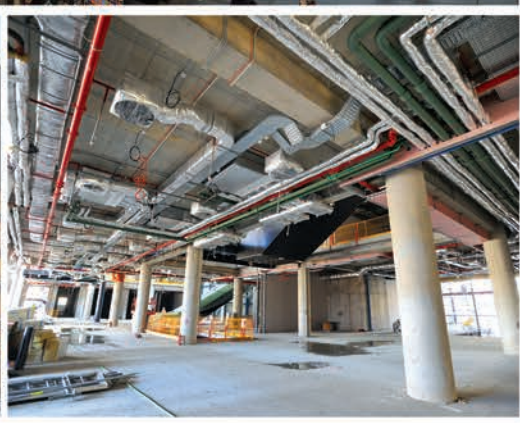

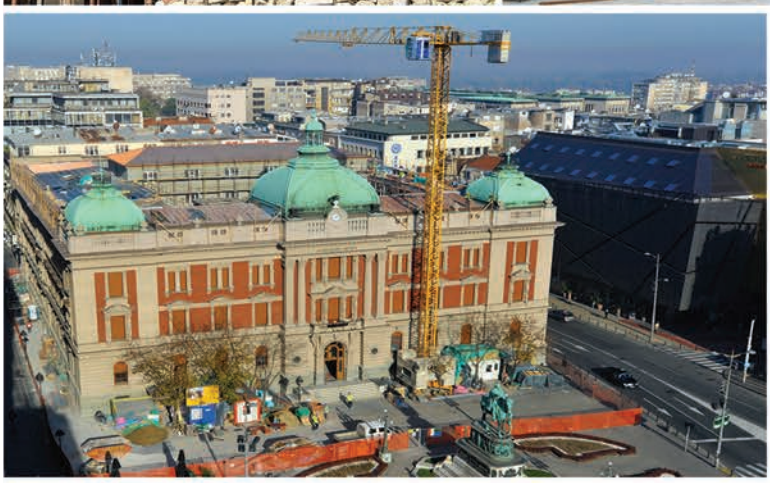

KOTO

www.koto.rs | office@koto.rs | +381 11 394 51 24 | Vojvode Stepe 466 | Beograd

IZOMONT®
BEOGRAD

IZOMONT d.o.o. BEOGRAD Preduzeće za završne radove u gradjevinarstvu inženjering i konsalting

KVALITET POD NOGAMA

Kompanija IZOMONT D.O.O. iz Beograda bavi se izvođenjem završnih radova u građevinarstvu. Prvenstveno smo specijalizovani za betoniranja, izradu industrijskih podova i hidroizolacija.

HODROIZOLACIJA

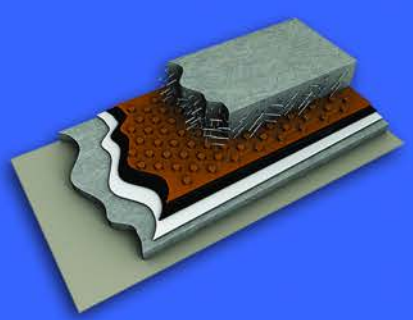

BETONIRANJE

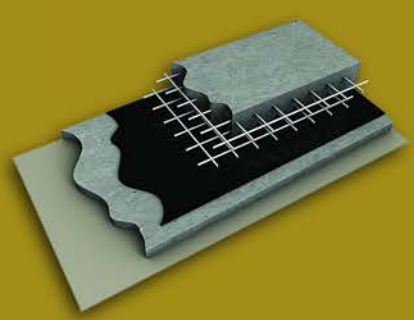

INDUSTRIJSKI PODOVI

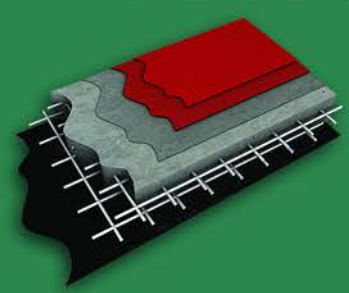

IZOMONT d.o.o.
Bulevar Patrijarha Germana 202
11226 Beograd
Republika Srbija

Telefon:
Tel: +381 11 3907 923
Fax: +381 11 3907 921

Web:
izomont@gmail.com
www.izomont.co.rs

CEMENT. AGREGATI. BETON.

Kompanija CRH je vodeći diversifikovani proizvođač građevinskih materijala na svetu. CRH u Srbiji proizvodi cement, agregate i beton. CRH je posvećen unapređivanju građevinske delatnosti kroz isporuku vrhunskih materijala i proizvoda za sprovođenje i održavanje infrastrukturnih, stambenih i komercijalnih projekata. Naša kompanija za ekološka rešenja Ecorec nudi usluge odgovornog upravljanja otpadom.

www.crhserbia.com

25 YEARS OF EXPERIENCE
IS SOMETHING THAT YOU CAN'T BUY

INELAS ERECO D.O.O

Inelas Ereco d.o.o. se bavi prodajom i servisiranjem laboratorijske opreme u domenu ispitivanja građevinskih materijala kao što su
- Agregati - Asfalt, bitumen i putevi - Beton - Cement i malter - Čelik - Zemljište
- Opšta laboratorijska oprema

Inelas Ereco d.o.o. Tošin bunar 274a, Novi Beograd
tel +381 11 2284 574, info@inelasereco.rs

Učestvuj u stvaranju arhitekture budućnosti

LafargeHolcimAwards

5. Međunarodna LafargeHolcim Nagrada za projekte održive gradnje

- Ukupni nagradni fond: 2.000.000 USD
- Posebna kategorija **Nova generacija** za mlade profesionalce i studente
- Prijave do 21. marta 2017. na www.lafargeholcim-awards.org/enter

A member of LafargeHolcim

LAFARGE

Korak po korak vodič za prijavu možeš pronaći na www.lafargeholcim-awards.org/guide

BUILDING TRUST

NAPREDNA SIKA REŠENJA U OBLASTI STRUKTURALNIH OJAČANJA

Kompanija Sika pruža trajnu dodatnu vrednost vlasnicima građevinskih objekata, njihovim konsultantima i izvođačima, kao i tehničku podršku tokom svih faza projekta, od ispitivanja uslova i razvoja inicijalnog koncepta ojačanja pa sve do uspešnog završetka i primopredaje projekta

SIKA – VAŠ PARTNER NA GRADILIŠTU

- Globalni lider na tržištu građevine i građevinske hemije
- Najbolja tehnička ekspertiza i praksa za sanaciju betona i strukturalna ojačanja
- Odlična reputacija kod vodećih izvođača i ugovarača posla

SIKA VREDNOSTI I INOVACIJE U GRAĐEVINI

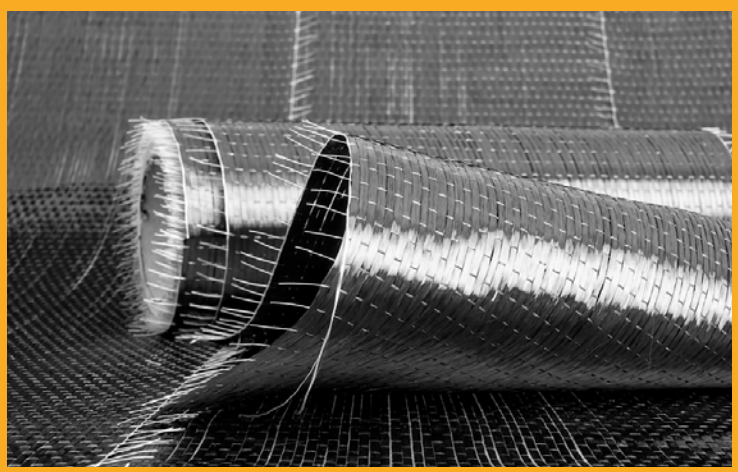

- Integrisani proizvodi i sistemi visokih performansi koji mogu da povećaju i poboljšaju kapacitet, efikasnost, trajnost i estetiku zgrada i drugih objekata – u korist naših klijenata i boljeg održivog razvoja
- Sika mreža obučenih i iskusnih građevinskih stručnjaka

JEDINSTVENA SIKA REŠENJA U ZAHTEVNIM USLOVIMA

- Rešenja za gotovo sve uslove apliciranja
- Kontrolisano vreme rada, vreme sazrevanja i očvršćavanja za različite vremenske uslove
- Posebna rešenja završnih ojačanja za korišćenje kod betona slabije jačine i drugih podloga

POTVRĐENI SIKA SISTEMI I TEHNIKE APLICIRANJA

- Preko 40 godina iskustva u strukturalnim ojačanjima, sistemima i tehnikama
- Proizvodi i sistemi sa brojnim testovima i procenama kako internim tako i eksternim
- Najviši međunarodni standardi proizvodnje i kontrole kvaliteta

doka

Oplatna tehnika.

Vaš pouzdan partner

za brzu, bezbednu i ekonomičnu gradnju!

Doka Serb je srpski ogranak austrijske kompanije **Doka GmbH**, jednog od svetskih lidera na polju inovacija, proizvodnje i distribucije oplatnih sistema za sve oblasti građevinarstva. Delatnost kompanije Doka Serb jeste isporuka oplatnih sistema i komponetni za primenu u visokogradnji i niskogradnji, pružanje usluga konsaltinga, izrade tehničkih planova i asistenicije na gradilištu.

Panelna oplata za ploče Dokadek 30 – Evolucija u sistemima oplate za ploče

Dokadek 30 je ručna oplata lake čelične konstrukcije, bez nosača sa plastificiranim ramovima, koji su prekriveni kompozitnim drveno-plastičnim panelom površine do 3 m^2.

Izuzetno brzo, bezbedno i lako postavljanje oplata

- Mali broj delova sistema i pregledna logistika uz samo dve veličine panela (2,44 x 1,22 m i 2,44 x 0,81 m)
- Dovoljan 2-člani tim za jednostavnu i brzu montažu elemenata sa tla bez merdevina i bez krana
- Sistemski određen položaj i broj podupirača i panela, unapred definisan redosled postupaka
- Prilagođavanje svim osnovama zahvaljujući optimalnom uklapanju sa Dokaflex-om
- Specijalni dizajn sprečava odizanje panela pod uticajem vetra
- Horizontalno premeštanje do 12 m^2 Dokadek 30 pomoću DekDrive

Više informacija o sistemu naći ćete na našem sajtu **www.doka.rs**

Doka Serb d.o.o. I Svetogorska 4, 22310 Šimanovci I Srbija I **T** +381 22 400 100
F +381 22 400 124 I serb@doka.com I **www.doka.rs**

Zajedno gradimo održive veze

TITAN Cementara Kosjerić deo je TITAN Grupe, multiregionalnog, vertikalno integrisanog proizvođača cementa i građevinskih materijala, sa preko 115 godina poslovnog iskustva. Grupa, čije je sedište u Grčkoj, posluje u 10 zemalja i zapošljava više od 5.500 ljudi širom sveta. Kroz svoju istoriju, TITAN je uvek kombinovao vrhunsku operativnost sa poštovanjem ljudi, društva i životne sredine.

Naš uspeh zasnovan je na korišćenju najboljih dostupnih tehnologija, sistematičnom istraživanju, stalnom unapređenju znanja i vrhunskoj stručnosti naših zaposlenih. Održivi razvoj je integralni deo našeg poslovanja, a negovanje i jačanje saradnje sa svim stejkholderima od vitalnog značaja za postavljanje čvrste osnove za održivu i bolju budućnost za sve.

Titan Cementara Kosjerić d.o.o.
Živojina Mišića b.b.
31260 Kosjerić, Srbija

www.titan.rs

TITAN
CEMENTARA KOSJERIĆ